AN ABSTRACT OF THE THESIS OF Allison Kathryn Miller for the Master of Science in Biology presented October 10, 2014.

Title: The Higher-Level Systematics of the Class Holothuroidea (Phylum Echinodermata): A Six-Gene Molecular Phylogenetic Approach

Approved:

_____

Alexander M. Kerr, Chairperson, Thesis Committee

Sea cucumbers (Holothuroidea) are some of the most morphologically diverse, ecologically important, and economically valued echinoderms; however, the higher-level systematics of the class remains controversial. Here, I present a phylogeny of the extant Holothuroidea estimated with maximum parsimony, maximum-likelihood, and Bayesian approaches using approximately 5.1 kb of mitochondrial (COI, 16S, 12S) and nuclear DNA (H3, 18S, 28S) sequences from 50 holothuroid terminals representing 17 of the 25 families. I found that at least three of the six orders are non-monophyletic. Apodida is sister to the rest of Holothuroidea. Apodida and Elasipodida lack respiratory trees and are positioned paraphyletic and sister to a clade with respiratory trees. Elasipodida is polyphyletic. Aspidochirotida is paraphyletic with representatives from four orders (Molpadida, Dendrochirotida, Dactylochirotida, and Elasipodida) nested within it. Dendrochirotida is paraphyletic with Dactylochirotida situated well within.

Molpadida's position was least certain; it unstably groups with Dendrochirotida and two other mixed clades that are dominated by members of Aspidochirotida. These results indicate that there has been rampant homoplasy in the anatomical features used as traditional taxonomic characters, necessitating a major systematic revision of Holothuroidea and a new perspective on the evolution of the class.

TO THE OFFICE OF GRADUATE STUDIES

The members of the committee approve the thesis of Allison Kathryn Miller presented October 10, 2014.

_____
Alexander M. Kerr, Chairman

_____
Daniel P. Lindstrom, Member

_____
Maria Celia Malay, Member

ACCEPTED:

_____ _____
John A. Peterson, Ph.D. Date
Assistant Vice President,
Graduate Studies,
Research and Sponsored Programs

THE HIGHER-LEVEL SYSTEMATICS OF THE CLASS HOLOTHUROIDEA (PHYLUM ECHINODERMATA): A SIX-GENE MOLECULAR PHYLOGENETIC APPROACH

BY

ALLISON KATHRYN MILLER

A thesis submitted in partial fulfillment of the

requirements for the degree of

MASTER OF SCIENCE

IN

BIOLOGY

UNIVERSITY OF GUAM

October 2014

ACKNOWLEDGEMENTS

I would like to express my gratitude to my adviser, Dr. Alexander Kerr, for his support, patience, and encouragement throughout my master's studies. He motivated me to challenge myself and offered priceless learning opportunities that allowed me to grow as a research scientist. I would also like to thank my committee members, Drs. Daniel Lindstrom and Maria Celia Malay for their time and valuable advice. My sincere appreciation goes to Dr. Greg Rouse for his kind hospitality while I was at Scripps Institution of Oceanography, for the specimens he contributed, and for his continuous guidance throughout my project. Without his collaboration this study would not have existed. I would also like to thank Jose Carvajal for his time and laboratory advice. Also, my humble appreciation goes to Drs. Mark O'Loughlin and Dave Pawson for their holothuroid identification help. I would also like to thank Niki Davey and the National Institute of Water and Atmospheric Research for their kind donations, and Sun Kim and the Korean Ocean Research Development Institute for their generosity and amenities while I was visiting Chuuk. I would also like to give my appreciation to the University of Guam Marine Laboratory staff and students. Finally, I will forever be in debt to James Collins and my family for their love and encouragement during this period of my life. This study was funded by the National Science Foundation Echinoderm Tree of Life grant (DEB 1036219) and the National Oceanic and Atmospheric Administration Western Pacific Coral Reef Institute fund.

TABLE OF CONTENTS

PAGE

LIST OF TABLES

PAGE

LIST OF FIGURES

PAGE

CHAPTER 1: INTRODUCTION

1.1 Biology, Ecology, and Biodiversity of Holothuroids

Holothuroids (sea cucumbers) are a diverse group of marine invertebrates in the phylum Echinodermata. Having evolved in the Upper Ordovician (beginning ca. 466 mya) (Reich, 2010b), before the appearance of the first amphibians, dinosaurs, or vascular plants, holothuroids have had ample time to develop many unique forms and adaptations. For example, holothuroids are some of the only echinoderms to develop non-pentaradial forms, and are probably the only echinoderms to evolve radial symmetry more than once (Kerr and Kim, 1999). Holothuroid forms vary greatly in diversity (Figure 1); holothuroids have "L"-shaped, "U"-shaped, flask-shaped, web-like, tailed and – even – "pig"-shaped forms. The group is also well known for their unusual defensive adaptations. Some holothuroids have white, sticky, anally-discharged filaments called Cuvierian tubules that can entangle a predator. Other species, such as *Stichopus horrens* Selenka, 1867, can shed large pieces of their body wall to escape predators. "Anal teeth" are another unique defensive adaptation that some species have developed; the small hard "teeth" which line the cloacal opening are believed to have evolved as a response to certain parasitic carapid fish, known

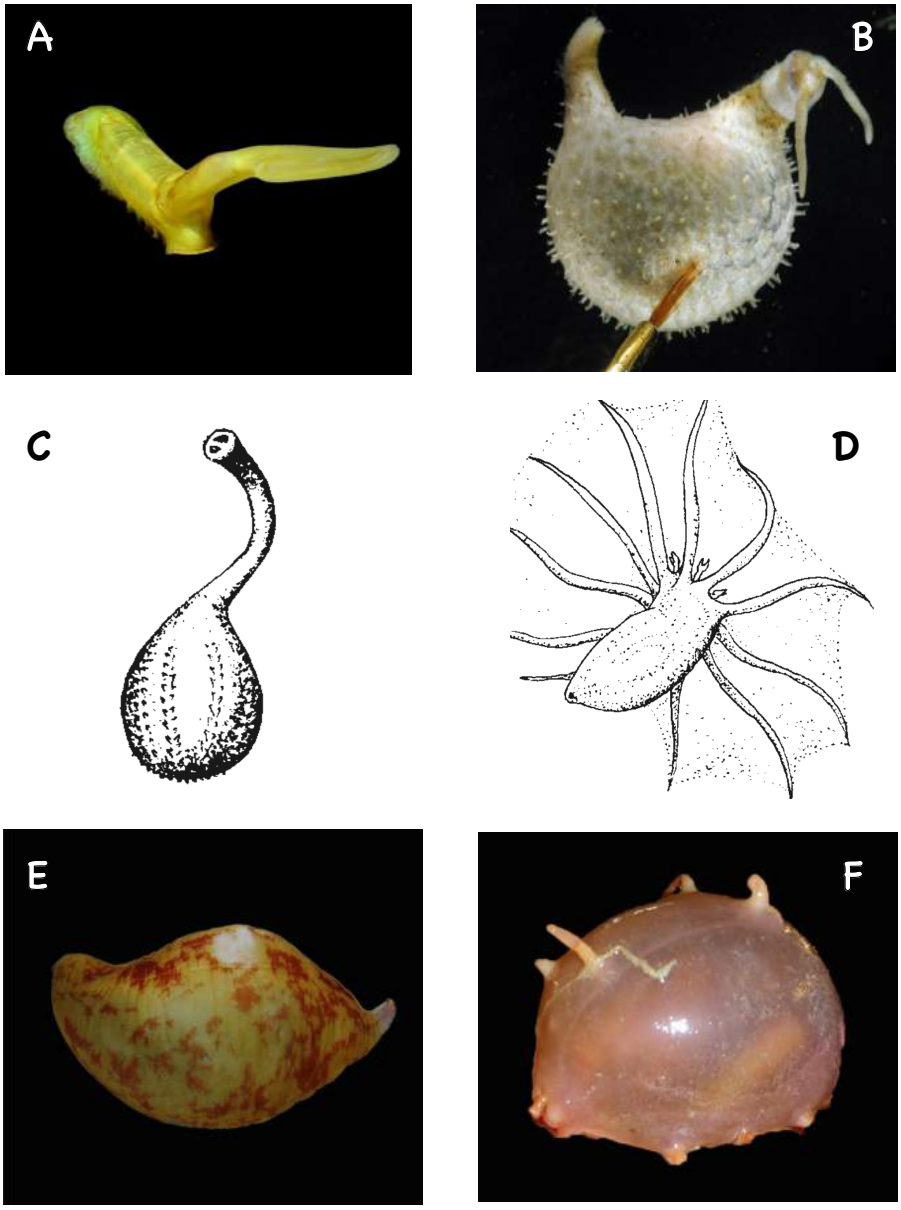

Figure 1. Example holothuroid body forms. **A:** "L"-shaped form, *Psychropotes*, Psychropotidae, Elasipodida; **B:** "U"-shaped form, *Ypsilothuria,* Ypsilothuridae, Dactylochirotida (Image: Dr. Greg Rouse); **C:** Flask-shaped form, *Rhopalodina*, Rhopalodinidae, Dactylochirotida (Image: Kerr and Kim, 1999); **D:** Web-shaped form, *Pelagothuria*, Pelagothuriidae, Elasipodida (Image: Kerr and Kim, 1999); **E:** Tailed form, *Paracaudina*, Caudinidae, Molpadida; **F:** Pig-shaped form, *Scotoplanes*, Elpidiidae, Elasipodida.

as pearlfish (Parmentier and Vandewalle, 2005).[1] The success of holothuroid adaptation is demonstrated by the class's presence in nearly every marine habitat from shallow-water reef flats to deep-sea ocean trenches. Holothuroids are even known to reside in the deepest part of the world's seabed hydrosphere, Challenger Deep (approximately 10.9 km below sea level), where they are the largest metazoans (Gallo, 2015, unpubl.).

Multiform as they may be, most holothuroids share a relatively standard set of anatomical structures (Figure 2). All echinoderms have a tough calcareous endoskeleton, a water vascular system and pentamerous (or radial) body symmetry. In addition to these common characteristics, holothuroids have an oral ring of modified tubefeet (called tentacles) and specific types of endoskeleton structures: a calcareous pharyngeal ring and (in 90% of extant species) an endoskeleton that is calcareous, but is reduced to isolated microscopic "ossicles" (Kerr, 2000). The holothuroid calcareous ring is typically composed of 10 plates which alternate in size: the radials are the largest (lying within the radii or ambulacra), while the interradials are the smallest. The calcareous ring acts as an anchor for muscles that contract the body longitudinally and operate the oral tentacles. These oral tentacles come in several taxonomic-specific forms, simple

[1] Pearlfish (family Carapidae, genus *Encheliophis* Müller, 1842), are long and slender fish that may parasitize a holothuroid host by entering through its anal opening. Once inside, the fish will reside in the host's coelomic cavity and feed on its gonads.

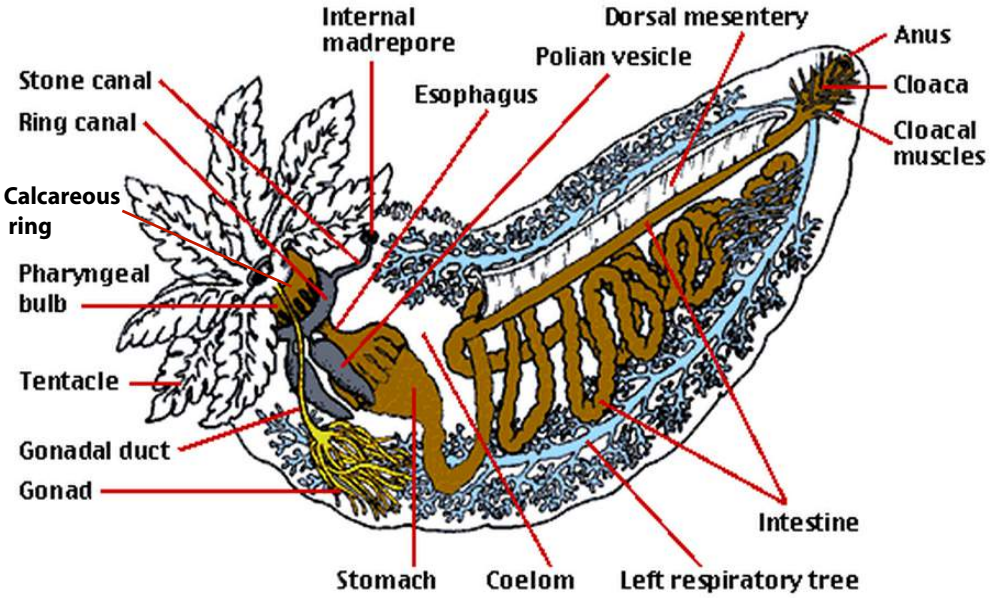

Figure 2. Typical anatomy of dendrochirote holothuroids (after Ivy Livingstone).

(tentacles that lack secondary appendages, no figure), dendritic (Figure 3A), peltate (Figure 3B), digitate (Figure 3C), and pinnate (Figure 3D). Holothuroid tentacles are used primarily for feeding – simple and peltate tentacles are used by infaunal- and surficial-feeding species, respectively, while digitate and pinnate forms are used by suspension-feeding species. Lastly, holothuroids, with the exception of a few members,[2] are unique in that 90% of species have microscopic calcareous bodies, called ossicles, imbedded in their tissue. These ossicles come in a variety of shapes (Figure 4) and taxonomists often use them to identify holothuroid species, genera, and, occasionally, families and orders. However, because ossicle forms differ between holothuroid members of the same species depending on size and age (Hansen, 1975; Massin, 1994; Cutress, 1996; Massin et al., 2000), their use as a diagnostic morphological character has increasingly been questioned (e.g., Samyn, 2003).

Holothuroid diversity is greatest in the tropics; however, biodiversity hotspots also occur in other geographical locations. Of the approximately 2,120 recorded species, the highest species diversity occurs in the Indo-west Pacific eulittoral, where over 250 species (Clark and Rowe, 1971) have been described. Surprisingly, the high-latitude Antarctic region, an area thought to be physically challenging to many marine species, also harbors a large number of holothuroid

[2] Some species of dendrochirotes, dactylochirotes, and elasipodans appear to have extremely large externally-encompassing body-wall plates.

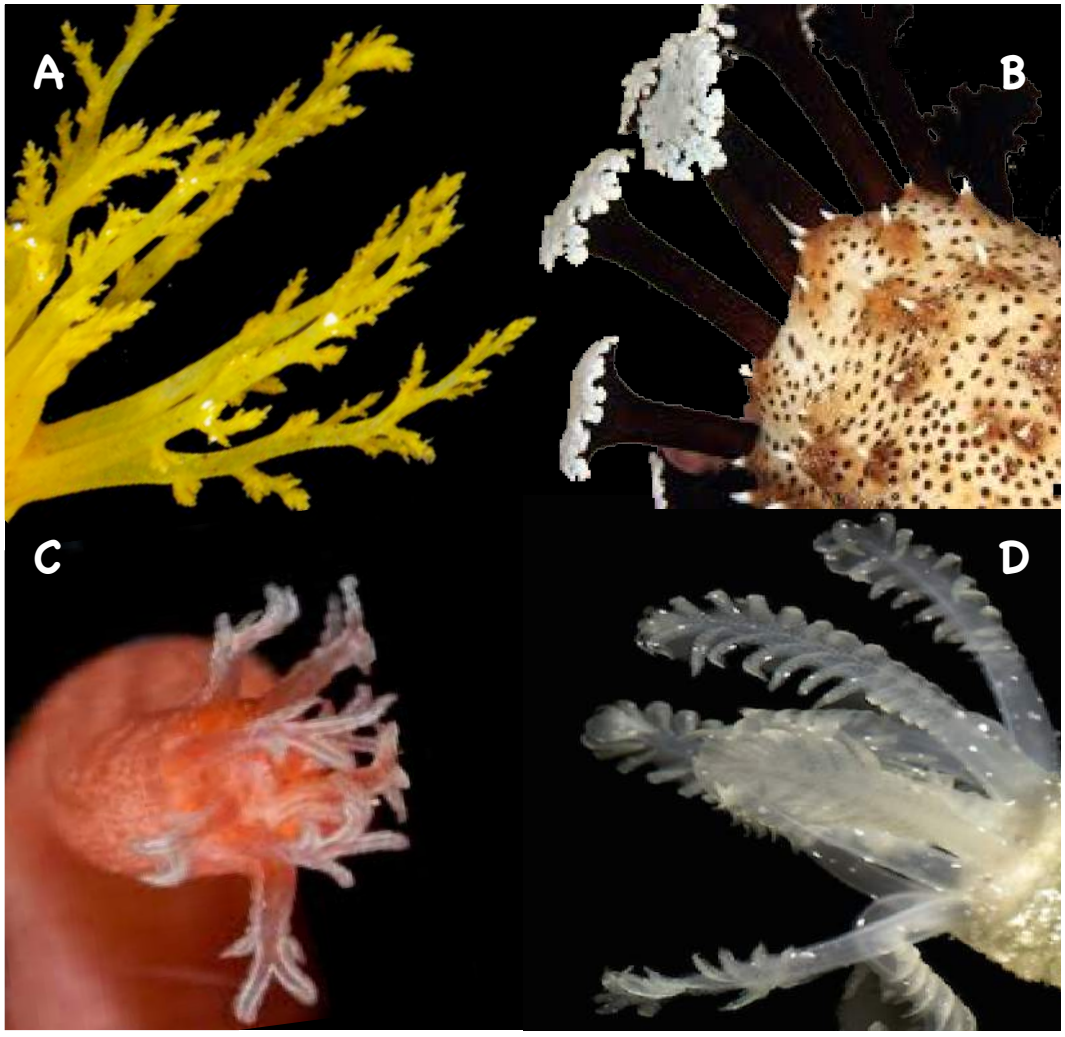

Figure 3. Holothuroid oral tentacle forms. **A:** dendritic; **B:** peltate; **C:** digitate; **D:** pinnate.

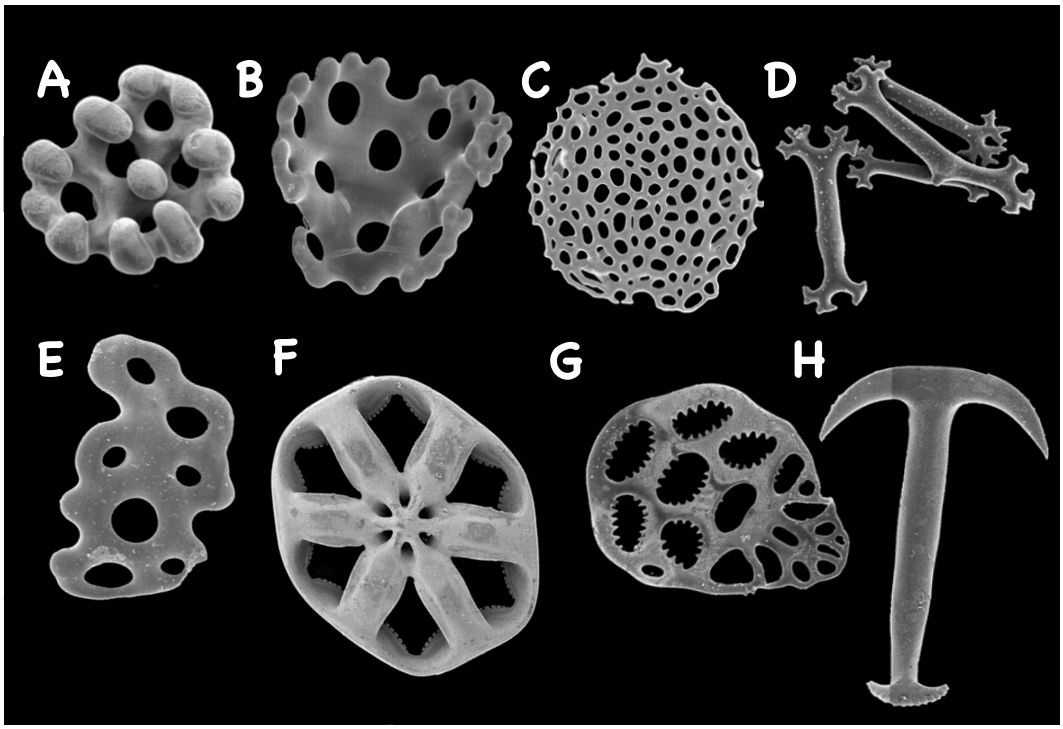

Figure 4. Examples of several common holothuroid ossicles. **A:** knobbed button; **B:** cup; **C:** plate; **D:** rods; **E:** smooth button; **F:** wheel; **G:** anchor plate of Apodida and Synaptidae; **H:** anchor of Apodida and Synaptidae.

species. O'Loughlin et al. (2010a) reported that up to 187 holothuroid species (representing all of the currently accepted holothuroid orders) have been recorded south of the Antarctic Convergence.

In addition to this geographic diversity, holothuroids are also abundant in many marine habitats. On certain Indo-west Pacific reefs, *Holothuria* (*Halodeima*) *atra* Jaeger, 1833, numbers from 1 to over 30 individuals per m^2 (Bakus, 1973; Conand, 1996; Uthicke, 1994). The red *Squamocnus brevidentis* Hutton, 1872 on some 'forsterian' rocky walls is found in such high densities (up to 1000 individuals per m^2) that one area has informally been dubbed the "Strawberry Fields" (Figure 5) (Alcock, 2013). Holothuroids are also abundant in the deep ocean, where they comprise a majority (often over 80%) of the mobile epibenthic megafauna (>20cm in length) on the deep sea floor (Hansen, 1975; Christiansen and Thiel, 1992; Ruhl, 2007). This high abundance gives tenability to Kerr and Kim's (2001) conclusion that "the ubiquity of holothuroids in the largest ecosystem, the abyssal plain, ostensibly renders them one of the dominant large animals on earth."

Ecologically, holothuroids are essential members of many marine ecosystems. On Indo-Pacific coral reefs, two abundant holothuroid species (*Holothuria atra* and *Stichopus chloronotus* Brandt, 1835) produce significant amounts of recycled ammonium and phosphate through excretion and

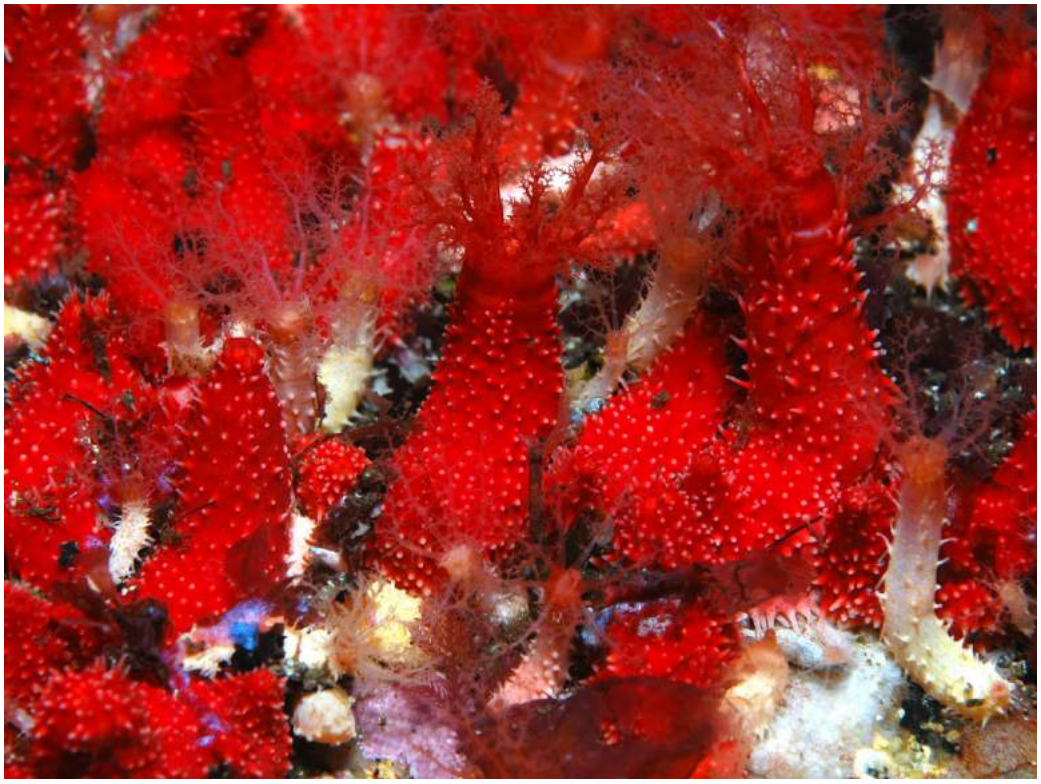

Figure 5. *Squamocnus brevidentis* population in New Zealand. Numbers at the entrance of Long Sound (Preservation Inlet, New Zealand) are so large that the holothuroid communities are often referred to as "the strawberry fields" (Image: Pete S, Shaun C, Matthew D, © 2007 ianskipworth.com).

respiration (Uthicke, 2001a). Once expelled into the water column or nearby sediments, these combined nutrients benefit the benthic microalgae community (Uthicke, 2001b), which provides sustenance for holothuroids and other reef consumers. This tightknit "benthic recycling system" is thought to maintain stable productivity levels within oligotrophic coral reef ecosystems (Uthicke, 2001a). Holothuroids also act as $CaCO_3$ dissolvers in the Great Barrier Reef (Schneider et al., 2011). By digesting and dissolving carbonate elements (sand and broken coral) *Stichopus hermanni* Semper, 1886, and *Holothuria (Mertensiothuria) leucospilota* Brandt, 1835, directly increase the alkalinity of surrounding waters at One Tree Reef (Capricorn Group of the Great Barrier Reef). This increased alkalinity, could act as a buffer to environmental pH changes caused by ocean acidification, which some scholars predict will reach a critical level by the end of this century (Caldeira and Wickett, 2003; Solomon et al., 2007). Holothuroids are also keystone species of seagrass ecosystems. The exclusion of *Holothuria (metriatyla) scabra* Jaeger, 1833 from a seagrass habitat resulted in an increase of benthic microalgae and a corresponding decrease in seagrass growth (Wolkenhauer et al., 2009). Beyond the tropics, holothuroids and other echinoderms are important carbon cyclers in the deep sea (Hughes et al., 2011) and elsewhere. In the temperate waters of Cape Cod Bay, for example, the fecal cones produced by *Molpadia oolitica* Pourtalès, 1851, provide habitat for polychaete (*Euchone incolor* Hartman, 1965), amphipod (*Aeginina longicornis*

Krøyer, 1843), and bivalve (*Thyasira gouldi Philippi*, 1845) suspension feeders (Rhoads and Young, 1971).

Holothuroids are also economically important. For centuries in Southeast Asia more than 47 species of holothuroids (Máñez and Ferse, 2010; Uthicke et al., 2010; Purcell et al., 2012) have been collected and processed into 'trepang' or 'bêche-de-mer' (Conand & Byrne, 1993) which is then exported to northern Asian countries where these products are often consumed as culinary delicacies (Conand, 1989). Lately, the growing demand for these edible species, along with overexploitation in traditionally fished areas, has led harvesters to expand globally into areas with virgin stocks, such as the Caribbean Sea (Hasbún and Lawrence, 2002), the Mozambique Channel (Conand et al., 1997), the Gulf of Alaska (Alaska Department of Fish and Game, 2012), the North Atlantic Ocean (Bruckner, 2005), the South Pacific Ocean (Toral-Granda, 2008), the eastern Pacific (Martinez, 2001; Pérezrul and Chávez, 2005), and the Red Sea (Ahmed and Lawrence, 2007). This high demand has also led to skyrocketing prices. For example, high-valued species, such as *Apostichopus japonicus*, Selenka, 1867, sell from US$970 to US$2,950 per kg in Hong Kong retail markets (Purcell et al., 2012).

Despite their economic value, ecological importance, and astonishing diversity, the relationships between many holothuroid families, orders, and suborders remain unresolved or controversial. As a result, many questions

regarding holothuroid evolution remain unanswered. Holothuroids have some of the most diverse larval and adult forms of all the echinoderms (Kerr and Kim, 1999), yet how these forms evolved and what factors influenced their evolution remains largely unknown. The question of how often the holothuroid plated skeleton (large, often imbricating, ossicles seen in extant elasipodans (Deimatidae), dactylochirotes, and dendrochirotes) arose and whether this trait's evolution is synapomorphic (shared by two or more sister taxa and their most recent ancestor who is preceded by ancestors who did not possess the trait) or plesiomorphic (retained from its ancestors) is undetermined. The answer to this question, and others, could be addressed through a phylogenetic analysis of the class.

A higher-level phylogenetic analysis of the holothuroid class could also provide insight on the rates of evolution and conservatism of characters. For example, if a plated skeleton is a retained ancestral feature of holothuroids, as predicted by Pawson and Fell (1965), then it would appear that all of the now plate-less holothuroids (about 90% of extant holothuroids) lost the trait at a high rate. Phylogenetic analyses of the class could help resolve other questions such as how, or in what manner, holothuroids re-evolved bilateral symmetry.[3] Or how and why some holothuroids took this one step further and regained radial symmetry (secondary radial symmetry), such as that of the family Rhopalodinidae (body

[3] All echinoderms evolved from a bilateral ancestor, but holothuroids, unlike the rest of the echinoderms, re-evolved a secondary bilateral symmetry.

shape portrayed in Figure 1C). Understanding these processes will be an important first step towards understanding the evolution of the echinoderm body plan and the loss or gain of body symmetry in general.

An analysis of holothuroid phylogenetics could also answer questions concerning the state of evolution in the deep ocean. It is theorized, that key groups of present deep-sea fauna (echinoids and octopods) are very old (possibly early to late Triassic in origin), and that the deep sea is an evolutionary more stable environment (i.e., deep-sea species are less susceptible to extinction events than are shallow-water forms) (Thuy et al., 2012). Since many extant groups of holothuroid are restricted to the deep sea, understanding their intra- and inter-relationships with shallow-water holothuroids, while also comparing their evolutionary history to the fossil record and to major geological events (e.g., ocean anoxic events), could support or refute this hypothesis. In the next introductory sections I outline the current taxonomic status of the class, provide a review of the taxonomic history of the class, and propose a method to achieve the most complete and up-to-date phylogeny of Holothuroidea.

1.2 Review of the Class Holothuroidea

In this section, I review the systematic history of Holothuroidea. I first briefly define Pawson and Fell's (1965) six widely used holothuroid orders:

Apodida, Elasipodida, Aspidochirotida, Molpadida, Dendrochirotida, Dactylochirotida (a more detailed morphological analysis of each order and their corresponding families is given by Kerr and Kim (2001)). I chose Pawson and Fell's interpretation of the class because of its relative stability; there have been few changes to the interpretation's orders and families over the last fifty years. Then I will present the history of the taxonomy of the Class in chronological order, beginning with Semper (1868), who was the first to provide a holothuroid phylogeny, to the most recently published higher-level systematic interpretation by Smirnov (2012).

1.2.1 The Six Currently Accepted Holothuroidea Orders: A brief Introduction

The order Apodida contains approximately 314 species in 47 genera arranged in three families: Chiridotidae, Myriotrochidae, and Synaptidae. Apodans have digitate, pinnate or, in some small species, simple tentacles, lack respiratory trees and tubefeet, and have a calcareous ring that lacks posterior projections. The group lacks radial canals, radial hemal vessels, tentacle ampullae, and anal papillae. Apodans have complete circular body wall muscles and possess longitudinal muscles. In some species, statocysts (organs used for balance) are present. Ossicles of apodans primarily consist of "wheels" and "anchor plates."

Wheels (circular ossicles with six or more spokes) are found in adult members of the families Chiridotidae and Myriotrochidae and in the auricularia larvae of some synaptids. Anchor plates (plates that attach to anchor-shaped ossicles) are found in Synaptidae. Table ossicles are not present. The overall body shape of apodans is vermiform with a very thin and often transparent body wall through which respiration occurs (Lambert, 1997). They include the longest echinoderms, with lengths ranging from one to two millimeters to over three meters (Kerr, 2001). Apodans are often infaunal, burrowing in sediments of both shallow and deep waters.

The order Molpadida contains approximately 103 species in 12 genera within four families: Caudinidae, Eupyrgidae, Gephyrothuriidae, and Molpadiidae. Molpadidans have simple or digitate tentacles, respiratory trees, lack tubefeet, and have a calcareous ring that lacks posterior projections. Members of the order generally have radial canals, radial hemal vessels, tentacle ampullae, and some molpadidans are equipped with retractor muscles and anal papillae. Molpadidans have pairs of radial muscle bands and, with the exception of Molpadiidae, lack statocysts. Some species possess phosphate bodies in their body walls which give them a brown or chestnut appearance (Pawson, 1977; Smirnov, 2012). Molpadidan ossicle forms include two- or three-pillared tables, “caudinid” cups, and perforated plates. Most species have elongated, or “rat-

tailed," posteriors (Figure 1E) and reside in both shallow and deep infaunal habitats.

The order Aspidochirotida contains approximately 373 species in 34 genera within three families: Stichopodidae, Holothuriidae, and Synallactidae. Aspidochirotans have distinctive shield-shaped tentacles, respiratory trees, tubefeet, and a calcareous ring that lacks posterior projections. They have radial canals, radial hemal vessels, tentacle ampullae (in two families), and some members have calcified anal papillae (anal teeth). The families Holothuriidae and Stichopodidae have pairs of radial muscle bands. Aspidochirotan ossicles consist of perforated plates, tube foot endplates, and three- to four- pillared tables. Their body shape varies from cylindrical to dorsally-flattened and their body walls are often soft and pliable. Aspidochirotans are the most abundant holothuroids on tropical reefs, and most stichopodids and holothuriids reside in shallow waters.

The order Elasipodida contains approximately 170 species in 29 genera within five families: Deimatidae, Elpidiidae, Laetmogonidae, Pelagothuriidae, and Psychropotidae. Elasipodans have shield-shaped and, in the case of the Pelagothuriidae, dendritic tentacles, a calcareous ring that lacks posterior projections, tentacle ampullae (limited to some), radial hemal vessels and anal papillae. Members of the order lack respiratory trees and, with the exception of Elpidiidae, lack statocysts. Hansen (1975) considered the order to be monophyletic based on multiple invariant characters: "the dorsal attachment of

the mesentery throughout its length" and, as mentioned, "the absence of respiratory trees." Hansen also believed that a third character, the switch from tubefeet ampullae to ambulacral cavities between dermal layers, separated the order from the rest of the class. Hansen, along with other authors (Mortensen, 1925; Smiley, 1994; Smirnov, 2012), primarily used ossicle types to link the order and distinguish families within the order. Laetmogonidae and Elpidiidae have wheels with cruciate primordia, while Elpidiidae and Psychropotidae have "psychropotid" rods (crosses usually comprised of four curved arms). Deimatidae alone has perforated plates, and in Pelagothuriidae no ossicles are present. Elasipodans, with the exception of Deimatidae, have gelatinous, often translucent, body walls and "are usually easy to recognize due to their conspicuous and often strangely shaped ambulacral appendages and broad ventral sole bordered by large tubefeet, or by a brim of fused tubefeet" (Hansen, 1975). Elasipodans primarily reside in deep-sea benthic environments; however, pelagothuriids and some members of Elpidiidae and Psychropotidae are facultative swimmers (Miller and Pawson, 1990) and can be found in mesopelagic, bathypelagic, and abyssopelagic pelagic zones (Hansen and Madsen, 1956; Pawson, 1982; Ohta, 1985; Solís-Marín et al., 2012).

Dendrochirotida contains approximately 680 species, in 114 genera within seven families: Cucumariidae, Heterothyonidae, Paracucumidae, Phyllophoridae, Sclerodactylidae, Placothuriidae, and Psolidae. Dendrochirotes have branched

tentacles, respiratory trees, and a calcareous ring comprised of many small components (or, in some species, long posterior projections). All families have radial canals, radial hemal vessels, and anal papillae. Most dendrochirotes lack tentacle ampullae, or if they have them they are reduced. Dendrochirotes possess singular radial muscle bands, longitudinal muscles, and muscles used to retract their anterior introverts (retractor muscles). Dendrochirote ossicles include perforated plates, baskets, tube foot endplates, two- to four-pillared tables, and "dendrochirote buttons". The family Paracucumidae is the only group to have spired plates (plates with an orthogonal protruding spire). Dendrochirotes body walls range from soft and pliable to rigid and packed with ossicles. Their body shapes, usually cylindrical or "U"-shaped, are only rarely flattened ventrally. Most dendrochirotes are found in shallow and deep waters, either attached to hard substrate or partially buried in fine sediment, where they use their highly-branched tentacles to suspension-feed. A few burrowing species possess simple tentacles for deposit feeding.

Lastly, the order Dactylochirotida contains approximately 76 species in nine genera within three families: Rhopalodinidae, Ypsilothuriidae, and Vaneyellidae. Dactylochirotes have tentacles with minimal digits, respiratory trees, tubefeet, and a calcareous ring that lacks posterior projections. All dactylochirote families have retractor muscles and radial hemal vessels; a few, such as the rhopalodinids, possess anal papillae and longitudinal muscles

(Thandar, 2001). Tentacle ampullae are absent. The ossicles of dactylochirotes consist of perforated plates and spired plates. Two- to four-pillared tables are specific to Rhopalodinidae. Dactylochirotes have a body that is often completely encased in enlarged flattened ossicles and are either "U" shaped (Figure 1B), fusiform, or pear shaped. Rhopalodinids are unique in that their mouth and anus are found together on the bottleneck portion of their pear-shaped body (Figure 1C). Dactylochirotes are often encountered buried in sediments in both shallow and deep waters.

1.2.2 Former Inferences of the Higher-Level Systematics of the Class

Like the rest of the animal classes, holothuroid phylogeny evolved through a series of systematic theories. The most influential and revolutionary theory to date was provided by C. Darwin in his 1859 book The Origin of Species, which, after its publication, was very quickly incorporated into the works of taxonomists in every field. The first holothuroid taxonomist to utilize Darwin's phylogenetic ideas, or rather, to classify organisms based on their evolutionary relationships, was Semper. In his 1868 work he attempted to configure the first phylogeny of the holothuroid class (Figure 6A). Semper, like Gray (1853) and Bronn (1860) before him, decided to separate the genus *Rhopalodina* Gray, 1853 into a separate class (Diplostomidea) and then continued to group the remaining holothuroids,

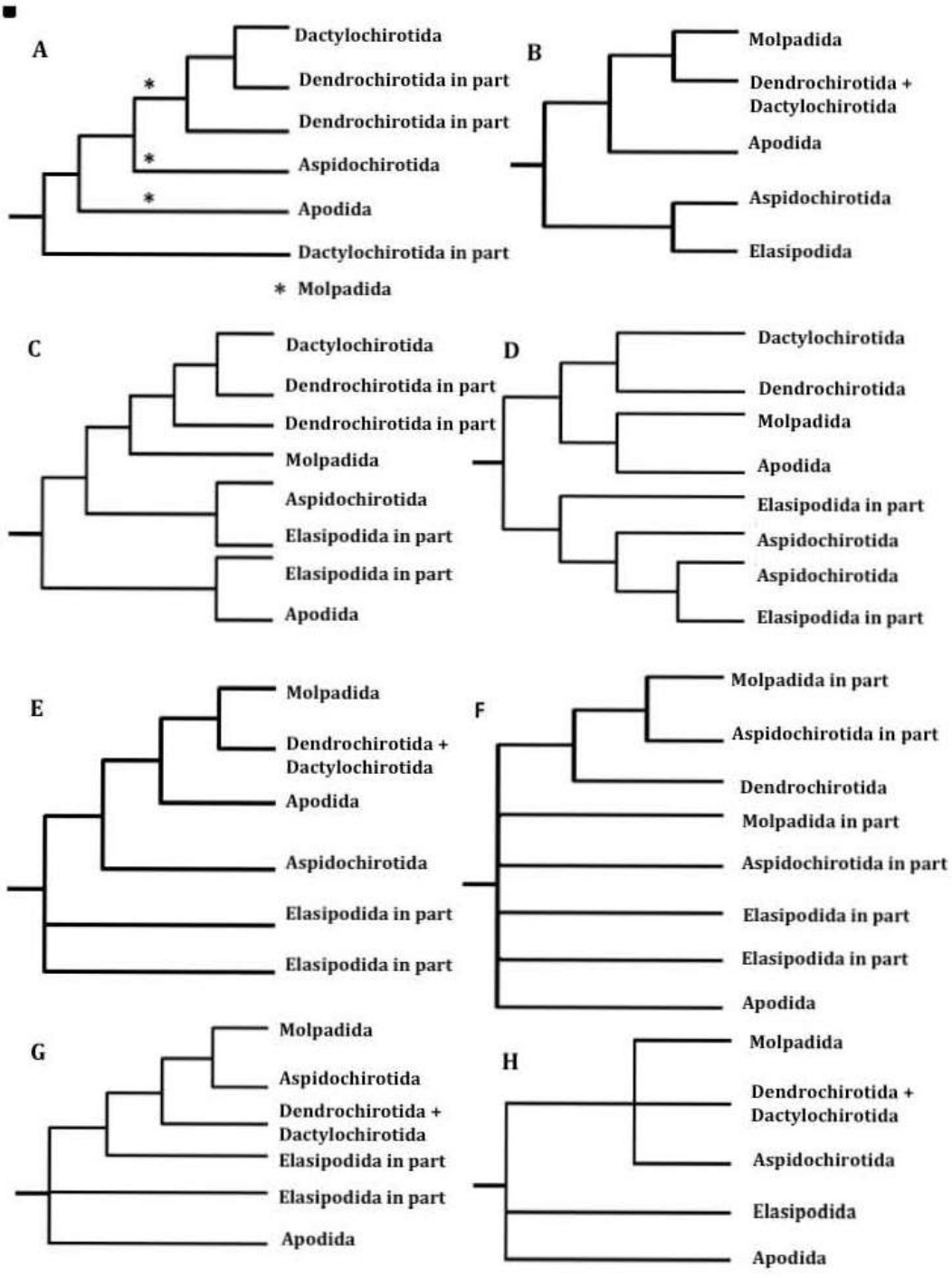
A
Dactylochirotida
Dendrochirotida in part
Dendrochirotida in part
Aspidochirotida
Apodida
Dactylochirotida in part
* Molpadida
B
Molpadida
Dendrochirotida + Dactylochirotida
Apodida
Aspidochirotida
Elasipodida
C
Dactylochirotida
Dendrochirotida in part
Dendrochirotida in part
Molpadida
Aspidochirotida
Elasipodida in part
Elasipodida in part
Apodida
D
Dactylochirotida
Dendrochirotida
Molpadida
Apodida
Elasipodida in part
Aspidochirotida
Aspidochirotida
Elasipodida in part
E
Molpadida
Dendrochirotida + Dactylochirotida
Apodida
Aspidochirotida
Elasipodida in part
Elasipodida in part
F
Molpadida in part
Aspidochirotida in part
Dendrochirotida
Molpadida in part
Aspidochirotida in part
Elasipodida in part
Elasipodida in part
Apodida
G
Molpadida
Aspidochirotida
Dendrochirotida + Dactylochirotida
Elasipodida in part
Elasipodida in part
Apodida
H
Molpadida
Dendrochirotida + Dactylochirotida
Aspidochirotida
Elasipodida
Apodida

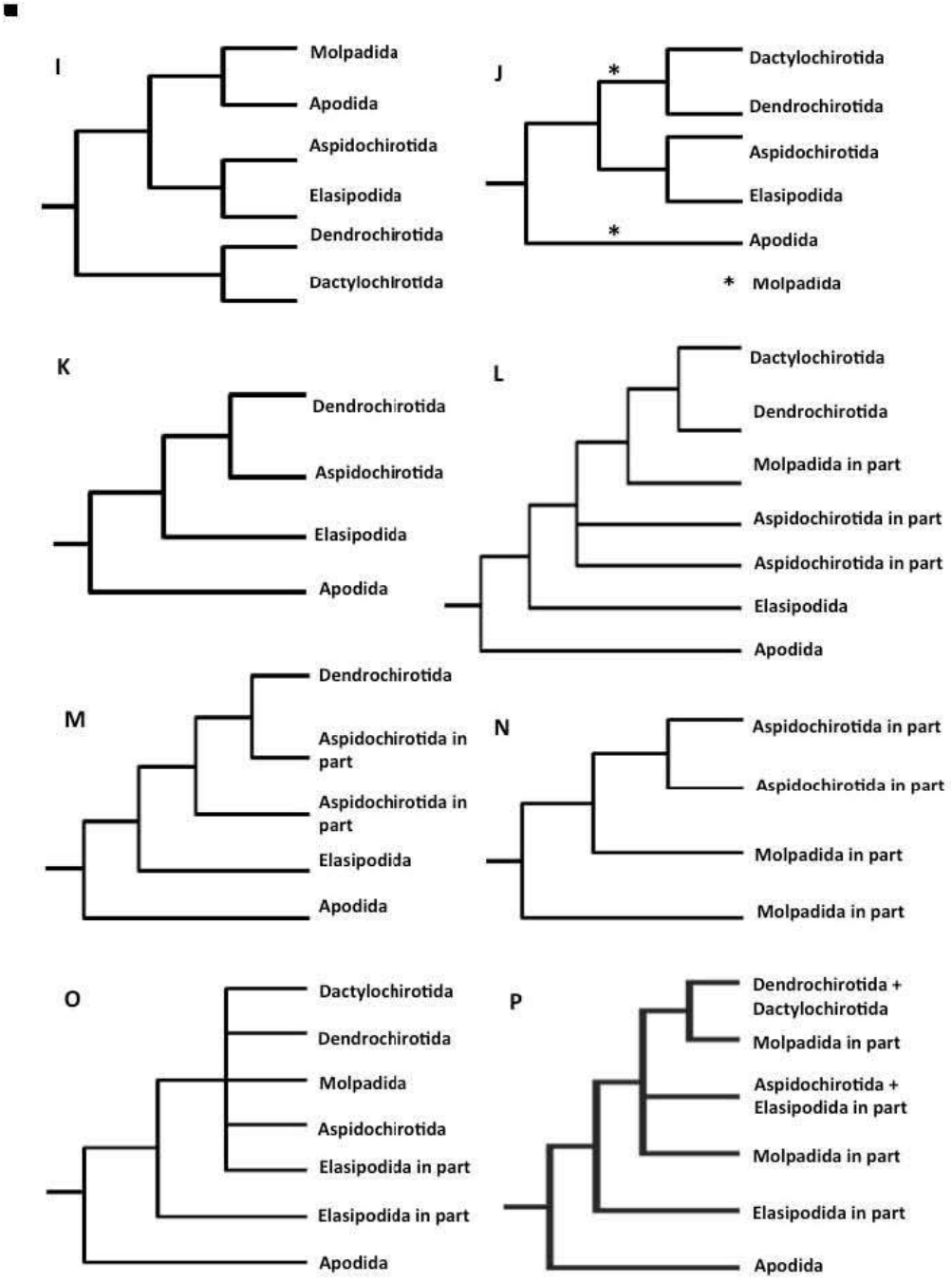
I
Molpadida
Apodida
Aspidochirotida
Elasipodida
Dendrochirotida
Dactylochirotida
J
*
*
Dactylochirotida
Dendrochirotida
Aspidochirotida
Elasipodida
Apodida
* Molpadida
K
Dendrochirotida
Aspidochirotida
Elasipodida
Apodida
L
Dactylochirotida
Dendrochirotida
Molpadida in part
Aspidochirotida in part
Aspidochirotida in part
Elasipodida
Apodida
M
Dendrochirotida
Aspidochirotida in part
Aspidochirotida in part
Elasipodida
Apodida
N
Aspidochirotida in part
Aspidochirotida in part
Molpadida in part
Molpadida in part
O
Dactylochirotida
Dendrochirotida
Molpadida
Aspidochirotida
Elasipodida in part
Elasipodida in part
Apodida
P
Dendrochirotida +
Dactylochirotida
Molpadida in part
Aspidochirotida +
Elasipodida in part
Molpadida in part
Elasipodida in part
Apodida

Figure 6. Previous hypotheses of extant holothuroid phylogenetic relationships. A, Semper (1868). B, Ludwig (1891). C, Haeckel (1896). D, Perrier (1902). E, MacBride (1906). F, Östergren (1907). G, Becher (1909). H, Cuénot (1948). I, Phylogenetic interpretation of Pawson and Fell's (1965) Linnaean classification. J, Haude (1992). K, Smith's (1997) interpretation of data from Littlewood et al. (1997). L, Kerr and Kim (2001). M, Lacey et al. (2005). N, Kamarudin et al. (2010). O, Reich (2010). P, Phylogenetic interpretation of Smirnov's (2012) system. Taxon designations are from Pawson and Fell (1965) and asterisks indicate alternative positions of Molpadida.

like Selenka (1867) before him, into those possessing respiratory trees (Pneumophora) and those without (Apneumona). Largely employing the recapitulation theory (the idea that during early ontogeny an animal's successive forms resemble those occurring through their species' evolution from a remote ancestor), Semper (1868) determined that the most ancient holothuroid forms possessed simple tentacles, yet lacked tubefeet. Therefore, he proposed Synaptidae (=Apodida) and Molpadidae (=Molpadida) to be the most "ancient," i.e., most representative of the "ancestral type". Those holothuroids possessing papillae and tubefeet Semper considered to be a more recent vintage, and those with only tubefeet he deemed the most recent. Lastly, Semper used ossicle and calcareous ring morphology to determine holothuroid relationships at the species level. This was based largely on his belief that these two characters held the lowest phylogenetic value because they were formed in the latest stages of holothuroid development.

Ludwig's (1889-1892) phylogenetic interpretation of the class (Figure 6B), though comprehensive, contradicted his taxonomic interpretation presented in the same monograph. After evaluating embryological and adult morphological characters, Ludwig decided to split the class into two orders, those with tubefeet (Actinopoda) and those without (Paractinopoda). He believed that the class was comprised of five families of which Dendrochirotae (=Dendrochirotida+Dactylochirotida *sensu* Pawson and Fell 1965), Molpadiidae

(=Molpadida), and Synaptidae (=Apodida) shared a common dendrochirote-like ancestor, just as the Aspidochirotae (=Aspidochirotida) and Elasipodida shared a common aspidochirotan-like ancestor. However, this phylogenetic belief was contrasting to Ludwig's (1889-1892) taxonomy of the class. For example, in his system, Ludwig described Synaptidae as the oldest family and separated it from the rest of the class, while in his phylogeny he grouped it within Paractinopoda and sister to Actinopoda.

Haeckel (1896), noting of Ludwig's (1891) phylogenetic error, re-evaluated the class using paleontological discoveries, anatomical evidence, and ontogeny. In his final interpretation of the class (Figure 6C), Haeckel (1896) raised Ludwig's (1889-1892) families to orders and included a new order Nectothuriae (which today comprises members of the elasipodan Pelagothuriidae). Otherwise, Haeckel's (1896) final phylogeny, which included the subclasses Actinopoda and Paractinota, largely resembled Ludwig's.

In 1902 Perrier created a class phylogeny (Figure 6D) that depicted two subclasses (Apoda and Pedata) and four orders: Paractinopoda (=Apodida), Anactinopoda (=Molpadida), Aspidochirota (=Aspidochirotida), and Dendrochirota (=Dendrochirotida). Like Ludwig (1889-1892) and Haeckel (1896) before him, Perrier (1902) divided his two subclasses by the absence (Apoda) or presence (Pedata) of tubefeet. Contrary to Semper's (1868) beliefs that ossicles were of little phylogenetic value, Perrier (1902) used ossicle morphology to

justify his subclass descriptions. He proposed that his orders Paractinopoda and Anactinopoda fell within the same subclass (Apoda) due to their shared anchor-shaped ossicles. Perrier (1902) defined the rest of his orders and families primarily by anatomy: Aspidochirotida members shared similarities in tentacle morphology and retractor muscles, and dendrochirotes shared similarities in tentacle morphology, retractor muscles, respiratory trees, and stone canals. Perrier did not include Ludwig's (1889-1892) and Haekel's (1896) order Elasipodida in his phylogeny because he believed the clade to be derived from the Synallactidae. Lastly, at the family level, Perrier (1902) included the family Rhopalodinidae (now within Dactylochirotida) in his Dendrochirotida order, and sister to the remaining dendrochirotes (Figure 6D).

In 1906, MacBride hypothesized six main groups as orders within his phylogenetic interpretation of the class (Figure 6E). He agreed with his predecessors about the monophyly of Aspidochirota (=Aspidochirotida), Elasipoda (=Elasipodida), Dendrochirota (=Dendrochirotida), Molpadonia (=Molpadida), and Synaptida (=Apodida), but proposed a sixth class, Pelagothuriida, to accommodate swimming holothuroids. MacBride further believed that his groups Elasipoda and Pelagothuriida (Pelagothuriidae) diverged first from a shield-shaped-tentacle and an external-madreporite bearing ancestor by "migrating into deeper water" and "taking to swimming." Along with tentacle morphology and the positioning of the madreporite opening, MacBride used the

presence of respiratory trees together with habitat type to classify the rest of his orders within the class.

Östergren (1907) did not agree with MacBride's (1906) six orders and instead included Ludwig's (1891) five orders in his phylogeny of the class. In his difficult-to-interpret reconstruction, Östergren (1907) posited that Elasipodans are the most ancient group, but appears to have placed Apodida as sister to the rest of the holothuroid group. Östergren's tree appears to have left many evolutionary possibilities open, e.g., his dotted and solid tree branches connect both his Deimatidae and Synallactidae to his more derived Psychropotidae, thus demonstrating his uncertainty whether respiratory trees were, secondarily lost in Psychropotidae. Finally, although it is clear that Östergren saw Aspidochirotida and Molpadonia (=Molpadida) as more derived groups, how exactly they split from their ancestor branch is unclear from his tree. Figure 6F is my best interpretation of Östergren's (1907) evolutionary tree.

Soon after Östergren (1907) published his work, Becher (1909) presented his holothuroid phylogeny (Figure 6G). Becher's work went largely unnoticed until Smirnov (2012) rediscovered and summarized its content. According to Smirnov (2012), Becher (1909) divided the class into two main groups: holothuroids with, or those presumed once possessing, respiratory trees and those primitively lacking the organs. He placed the latter "lungless" group, comprised of his synaptida (=Apodida), elpidiida (=Elasipodida) and deimatida (=

Elasipodida)), with their wheel-shaped ossicles and statocysts, as a paraphyletic group at the base of his tree, but did not clarify which of the three groups diverged first. Becher believed the next groups to diverge after the synaptids, elpidiids and the deimatids were the "lung" holothuroids which had respiratory trees and, in most members, table-like ossicles (Dendrochirotida, Aspidochirotida, and Molpadida). Becher's phylogenetic tree displays the close relationship of the orders Molpadiiden (= Molpadida) and the group Aspidochirotida (as it is currently known), but his placement of Synallactidae is less precise. Smirnov (2012) understood Becher's (1909) description to mean that Synallactidae "was a primitive group of 'lung' holothurians, which gave rise to numerous other taxa." I illustrate a single aspidochirotan branch in Becher's tree because Becher listed all but one questionable synallactid member ("Synallactes wood-masoni") within the order Aspidochirotida.

Closely resembling Becher's (1909) phylogeny, Cuénot (1948) described his thoughts about the holothuroid class in one chapter of Traité de Zoologie. Cuénot agreed with Becher (1909) that Synaptides (=Apodida) was separate from the rest of the class (Smirnov, 2012). However, unlike Becher (1909) who divided his groups largely by the presence or absence of respiratory trees, Cuénot (1948) decided to divide his five orders largely by the presence or absence of tubefeet: Apodida (containing Synaptides and Actinopoda (containing Dendrochirotes (=Dendrochirotida)), Molpadides (=Molpadida), Aspidochirotes

(=Aspidochirotida), and Elasipodes (=Elasipodida). Cuénot's higher-order relationships are difficult to determine from his phylogenetic tree, but it appears that he thought the elasipodans diverged first (or possibly evolved from an aspidochirotan-like ancestor) followed by the dendrochirotes, molpadidans, and aspidochirotans. An interpretation of this tree is depicted in Figure 6H.

The current most widely used class interpretation was produced by Pawson and Fell in 1965 (Figure 6I). This classification, rendered as a phylogeny in Figure 6I, focuses primarily on differences in tentacle morphology, body morphology, and the shape of the calcareous ring. Like previous authors (Ludwig, 1889-1891; Haeckel, 1896; Deichmann, 1930), Pawson and Fell (1965) agreed on the five generally accepted orders of their time, but defined a sixth order (Dactylochirotida) based on the group's digitiform to digitate tentacles and plated (imbricate) body walls. Pawson and Fell incorporated this new group along with Dendrochirotida into a new subclass Dendrochirotacea and considered it sister to the clade Aspidochirotacea (containing Elasipodida and Aspidochirotida) + Apodacea (containing Molpadida and Apodida). Two of these subclasses may not be monophyletic (Kerr, 2000; Kerr and Kim, 2001, Lacey et al., 2005). Pawson and Fell also considered Aspidochirotida and Elasipodida to be closely related due to their similar characters: tubefeet, shield-shaped tentacles (10-30 in number), lack of oral introvert retractor muscles, and bilateral symmetry. Pawson and Fell tentatively hypothesized that the orders Apodida and Molpadida were of

close relation because they both lacked tubefeet. This last hypothesis, however, was later challenged by many authors on the basis of convergent evolution.

Haude's (1992) analysis of the class primarily matched that of Pawson and Fell (1965), but Haude (1992) questioned the placement of Molpadida with Apodida in the subclass Apodacea, and suggested that the order could also belong in Pawson and Fell's (1965) Dendrochirotacea subclass. Haude (1992) also, consistent with the findings of many other authors (Semper, 1886; Huxley, 1878; Semon, 1888; Cuénot, 1891; Östergren, 1907; Seilacher, 1961), did not agree with Pawson and Fell's (1965) view of a common dendrochirote-like ancestor and instead believed it to be an apodan-like ancestor (Figure 6J). Later, the molecular analyses of Smith (1997) and Littlewood et al. (1997) supported the idea of an early divergence of an apodan-like ancestor from the rest of the class. Using 28S- and 18S-like ribosomal gene sequences from four orders, their phylogeny suggested that elasipodans evolved secondarily and that aspidochirotans and dendrochirotes were the most derived orders (Figure 6K).

Like Smith (1997), Kerr (2000) also believed the order Apodida was sister to the rest of the class. In his analysis of four holothuroid orders (Apodida, Elasipodida, Aspidochirotida, Dendrochirotida) Kerr (2000) used published molecular sequences (Raff et al., 1988; Wada and Satoh, 1994; Littlewood et al., 1997) to demonstrate better-supported results of the Smith (1997) and Littlewood et al. (1997) phylogeny. Kerr (2000), like Hansen (1975) and Littlewood et al.

(1997) before him, dismissed Pawson and Fell's (1965) subclass Aspidochirotacea and later dismissed Apodacea, which was also found to be non-monophyletic (Kerr and Kim, 2001). Although Kerr and Kim (2001) opposed most of Pawson and Fell's (1965) subclasses, they did agree with the monophyly of four of their six holothuroid orders (Figure 6L). Lastly, Kerr and Kim (2001) characterized the monophyly of Molpadiida (= Molpadida) and Dendrochirotida as uncertain for two reasons. First, Molpadiida included two families that the authors thought should be more derived (i.e., Eupyrgidae and Gephyrothuriidae). Second, although Kerr and Kim found Dendrochirotida to be paraphyletic, the authors recognized that support for the clade was based on a successively weighted analysis and was defined by a single subset of characters.

Lacey et al. (2005) largely reiterated Kerr and Kim's (2001) morphological analysis of the Class using molecular data (Figure 6M). By analyzing 18S ribosomal RNA gene sequences of four holothuroid orders (Apodida, Elasipodida, Aspidochirotida, and Dendrochirotida), Lacey et al. concluded that the subclass Aspidochirotacea was paraphyletic: Aspidochirotida was more closely related to Dendrochirotida than to Elasipodida. Later, Kamarudin et al. (2010), realizing that Lacey et al.'s (2005) use of 18S rDNA limited their relationship clarity at the genus level, used 16S ribosomal RNA (16S rRNA) gene sequences to better define four genera in two holothuroid orders (Figure 6N).

In 2010 Reich added fossil evidence to the already existing morphological and molecular evidence supporting the belief that Apodida is sister to the rest of Holothuroidea. Reich postulated a close relationship of Elasipodida to Apodida, which he based on the similarities of Early/Middle Silurian and Middle and Late Devonian apodan wheels to elasipodan wheels. Although Reich was confident about the less-derived positions of Apodida and Elasipodida within the class, he was unsure of the positioning of the rest of the class (Figure 6O), primarily because of the incomplete holothuroid fossil record.

The latest class-level holothuroid taxonomic publication to date is a work that was published in 2012 by Smirnov. Primarily considering the views of Becher (1909) and Kerr and Kim (2001), along with the results from previously published molecular-phylogenetic (Smith (1997) and Lacey et al. (2005)) and paleontological findings (Reich (2010a) and Reich (2010b)), Smirnov (2012) proposes a system that is, as he says it, "based on the analysis of morphological, primarily anatomical characters and interpretation of their significance for the systematics that has been achieved after 180 years of holothurian study." As a result, he completely reevaluates and reconstructs Pawson and Fell's (1965) system (Figure 6I vs. Figure 6P). In his system, Smirnov (2012) proposes four subclasses: Arthrochirotacea, Synaptacea, Elpidiacea, and Holothuriacea. Arthrochirotacea includes the extinct order Arthrochirotida, Synaptacea includes one order Synaptida (=Apodida), Elpidiacea includes one order Elasipodida

(Elasipodida in part), and Holothuriacea includes four orders Aspidochirotida (Aspidochirotida + Elasipodida in part), Dendrochirotida (=Dendrochirotida + Dactylochirotida), Moladiida (=Molpadida in part), and Gephyrothuriida (re-established). Smirnov's system (Figure 6P) partially follows Becher's (1909) phylogeny which depicts a two-group division of the Class. Smirnov proposes that one group include holothuroids that have wheel-shaped ossicles and do not have respiratory trees, and that a second group include holothuroids that have both respiratory trees and secondarily-lost respiratory trees. Like Kerr and Kim (2001), Smirnov (2012) writes that most of Pawson and Fell's (1965) subclasses are polyphyletic. For example, Smirnov (2012) deems Aspidochirotacea to be polyphyletic because its members (aspidochirotans and elasipodans) convergently evolved similar morphologies (e.g., the modification of dorsal tubefeet into papillae, he argues, could have easily been independent). Smirnov further suggests that Dendrochirotacea (=Dendrochirotida and Dactylochirotida) be abolished and that all of its members should be synonymized into one dendrochirote-like clade. Lastly, Smirnov, like other authors before him (Haude, 1992; Smith, 1997; Pawson, 1982; Kerr and Kim, 2001), considers Apodacea to be polyphyletic because he concludes that tubefeet were convergently lost and that digitate tentacles were convergently gained in both apodans and molpadidans.

Many different taxonomists have analyzed multiple holothuroid characters over the years, yet a complete higher-level phylogeny of Holothuroidea has not

been agreed upon. Questions concerning the relationships of families within orders, of orders within subclasses, and of subclasses within the class persist. To date, there has been much work conducted on the holothuroid intra-family-level relationships. Solís-Marín (2003), Byrne et al. (2010), Honey-Escandón et al. (2012), and Kim et al. (2013) are examples of recent genera- and species-level phylogenetic analyses; however, fewer studies have been conducted on the family relationships within the currently accepted holothuroid orders. For example, a current hypothesis is that the family Phyllophoridae is sister to the rest of the dendrochirote families, yet tests for this relationship have not been conducted. Similarly, the position of the unusual family Pelagothuriidae within the Elasipodan order has long been questioned. Molecular analyses of members from this family have never been conducted and a thorough analysis might result in surprising outcomes, such as the division of an entire order. The positions of the orders within Pawson and Fell's (1965) holothuroid subclasses and class are also unclear: Is the order Dendrochirotida more closely related to Aspidochirotida or Molpadida? Or is Molpadida placed within Aspidochirotida? And where does Dactylochirotida sit within the class? – is it nestled within Dendrochirotida as suggested by Kerr and Kim (2001) and Smirnov (2012), or should it remain its own clade as suggested by Pawson and Fell (1965)? It is also largely agreed upon that the current holothuroid subclasses need renovation (Hansen, 1975; Smirnov, 1984; 2012; Kerr and Kim, 2001; Lacey et al., 2005); however, a complete

analysis has yet to be conducted. In addition to all these questions, the monophyly of all subclasses through most family-level relationships needs to be addressed.

Though numerous, many of these previously mentioned uncertainties have the potential to be, if not resolved, at least thoroughly investigated. Many questions regarding the holothuroid class remain unanswered due to poor fossil records, variability in the assessment of morphological characters, the amount of non-parallel/non-convergent morphological characters that can be assessed, and the lack of viable tissue material (for molecular analysis) from rare extant specimens. However, new holothuroid fossils are being discovered regularly, and with recent technological advances in deep-sea exploration rare specimens are becoming increasingly available for molecular research. In collaboration with morphological work, these recent advances will assist in the resolution of many of the class's current taxonomic uncertainties.

1.3 The Latest Approach: Molecular Phylogenetics

Although Smirnov (2012) and multiple taxonomists before him produced thorough and insightful hypotheses about the higher-level relationships of the class, the majority of these hypotheses were formulated from analyses of unstandardized sets of morphological characters. The incongruence of these characters has fueled ongoing debate among holothuroid morphologists; many

morphologists will argue that certain characters are more evolutionarily important or independent than others and will often criticize other studies for inclusion or exclusion of those characters from an analysis. In addition, the number of characters used in many holothuroid studies is low – numerous past studies included no more than 10 characters. Finally, even if characters are agreed upon and a large number of characters are used, they can still be innately variable and subject to observation bias. For example, the shape of an ossicle (commonly referred to as "ossicle form") is a character used to identify holothuroids on many taxonomic levels (species to families). However, as mentioned before, this form can change in number, size, and shape in different age groups of the same species (Hansen, 1975; Samyn, 2003).

Molecular phylogenetics has proven successful in numerous recent phylogenetic studies: Bernhard et al. (2001), class Spirotrichea; Fulton and Strobeck (2006), superfamily Arctoidea; Schoch et al. (2009), class Dothideomycetes; Rouse et al. (2013), class Crinoidea, are just a few examples. The success of molecular phylogenetics is largely due to its use of sequence data, which has three advantages over morphological characters: 1. There are a large number of potential characters available to infer relationships – entire genomes are now being assessed, 2. The capability to distinguish cryptic species, or the ability to detect substitutions within genes that are not represented morphologically, and 3. The ability to specify parameters, or the ability to

determine the likelihood of substitution events for particular sequences which can then be used to select the most appropriate evolution models (Nadler, 1995).

By aligning and comparing DNA, RNA, or protein sequences to identify molecular relationships, the molecular phylogenetic method uses data about an organism's gene regions and cellular biology to identify relationships at different evolutionary levels. For example, ribosomal genes, such as 16S ribosomal DNA (16S rDNA) and 18S ribosomal DNA (18S rDNA), are vitally important to prokaryotes and eukaryotes, respectively, and are therefore conserved (i.e., have slower mutation rates) (Hillis and Dixon, 1991). In contrast, other protein encoding genes, such as the mitochondrial gene cytochrome oxidase subunit 1 (COI), have faster mutation rates (largely due to the mtDNA maternal inheritance and haploid nature) and are therefore less conserved.

These gene observations have been documented in members of Holothuroidea and have been used to determine holothuroid phylogenetic relationships. In their 1996 publication, Arndt et al. noted that 'large ribosomal RNA (lrRNA) genes sequences' from members of two orders (Dendrochirotida and Aspidochirotida) "demonstrate a suitable level of variation for phylogenetic analysis, both among genera and among families." Arndt et al. (1996) also discussed how the COI gene, which becomes too saturated (i.e., what appears to be a decrease in sequence divergence rate is actually due to multiple mutations at the same sites) to accurately determine relationships above the family level, can

be used to determine holothuroid relationships at the species level. This last finding has been confirmed by recent studies (Solís-Marín et al., 2004; Uthicke et al., 2004; Byrne et al., 2010; Uthicke et al., 2010; Kim et al., 2013). Lastly, the partial class-wide analysis by Lacey et al. (2005) demonstrated the utility of the 18S rDNA gene to decipher holothuroid relationships at the ordinal level.

These studies prove that different mitochondrial and nuclear derived genes, with different rates of mutation or different degrees of conservancy, can offer information about specific taxonomic-level relationships within Holothuroidea. Therefore, to achieve a well-supported class phylogeny, wherein many of the taxonomic relationships (species through subordinal) are represented, multiple genes of different evolutionary rates should be combined. This "multi-gene" analysis, as it is called, is a conventional method for studying intra-class phylogenetic relationships in metazoans (Bernhard et al., 2001; Fulton and Strobeck, 2006; Schoch et al., 2009; Rouse et al., 2013).

1.4 Objectives

In this study, I use molecular phylogenetic methods to address current questions concerning the higher-level systematics of Holothuroidea. By sequencing six genes (16S ribosomal DNA (16S rDNA), 18S ribosomal DNA (18S rDNA), histone H3 (H3), 12S ribosomal DNA (12S rDNA), 28S ribosomal

DNA (28S rDNA) and cytochrome oxidase subunit I (COI)) from representatives from each of the currently recognized orders and incorporating them into multi-gene analyses, I investigate:

1. The monophyly of all subclass through most family-level relationships within Holothuroidea

2. The phylogenetic relationships of the orders within the holothuroid class

3. The phylogenetic relationships of the holothuroid families within their corresponding orders

CHAPTER 2: METHODS

2.1 Taxon sampling and collection

Echinoderm Tree of Life (EToL) associates and I collected targeted holothuroids using scuba, snorkel, and deep sea trawling methods (the exact method depended on the habitat depth), from the Philippine Sea, Weddell Sea, Tasman Sea, Baffin Bay, and the North Pacific Ocean. Of the 50 holothuroid exemplars that I sequenced, 38 were obtained during the NSF Echinoderm Tree of Life (EToL) (http://echinotol.org) and Western Pacific Coral Reef Institute (WPCRI) sponsored expeditions that were conducted in the waters of Guam (US territory), Chuuk (Federal States of Micronesia), and the Scotia Arc region. I acquired five other specimens from the Florida Museum of Natural History Invertebrate Zoology Collection (FMNH-IZC), Museum Victoria Marine Invertebrates Collection (MV-MIC), and the Scripps Institution of Oceanography Benthic Invertebrates Collection (SIO-BIC). The last seven species I used were collected by AM Kerr (unpublished) in the 1990's from various locations (Guam, California, Cook Islands, Great Barrier Reef, Florida, Pohnpei, and British Virgin Islands (BVI)). Altogether, I obtained exemplars from every extant Pawson and Fell (1965) order and approximately 17 of their 25 families. From GenBank I acquired sequences from two echinoderm species that I used as outgroup

sequences (Table 1). I chose an echinoid and an asteroid because of their class-level relationships to Holothuroidea; Echinoidea is sister to Holothuroidea, and Asteroidea is sister to the Holothuroidea+Echinoidea clade Echinozoa (Janies, 2001; Janies et al., 2011).

EToL colleagues and I used a standard three-step field-collection system to insure that every specimen we collected was documented and preserved correctly. First, we photographed the live holothuroid in situ and ex situ (deep sea specimens were only photographed in vitro). Second, we subsampled tentacles and tubefeet (1-mm pieces in 95% ethanol), after we blotted them with a paper towel to remove excess water and debris. Third, we placed the entire holothuroid in 95% ethanol (≈ 1:3 ratio of tissue to ethanol) where it was preserved as a voucher specimen. To ensure preservation, we stored the subsamples at 4^{o} C and performed a 95% ethanol change after approximately five days. I, with occasional help from other EToL colleagues, identified all the voucher specimens we collected and then deposited them in either the Scripps Institution of Oceanography Benthic Invertebrate Collection or in the Florida Museum of Natural History Invertebrate Zoology Collection. See section 2.7 for more information regarding vouchers and catalog numbers.

I identified families and genera, primarily according to Smiley 1994; however, I used more detailed and recently published literature to identify the difficult taxa. I assessed each specimen's general anatomy (e.g., body length,

Table 1. GenBank accession numbers for outgroup taxa. GenBank (GB) accession numbers are given for all six genes (H3, COI, 16S, 12S, 18S, and 28S) used in the current study.

Taxon as Listed On Trees	Source	18S	16S	H3	12S	28S
Patiria miniata	GB	DQ060777.1	DQ297074.1	DQ676897.1	AY370695.1	DQ060004.1
Strongylocentrotus purpuratus	GB	L28056.1	X12631.1	NM_214544.1	X12631.1	XM_790710.3

body shape, tentacle number, and tentacle structure) and ossicle morphology; I analyzed general anatomy through dissection, and documented ossicle morphology via light-emitting diode (LED) microscopy. I believe my colleagues and I collected several new species during this study, and I will describe them more thoroughly in future publications. For now, however, I identified them to the genus or family level.

2.2 DNA extraction, amplification, and sequencing

I compiled data from six gene regions: 16S ribosomal DNA (16S rDNA) (partial), 18S ribosomal DNA (18S rDNA), histone H3 (H3) DNA (partial), 12S ribosomal DNA (12S rDNA) (partial), 28S ribosomal DNA (28S rDNA) (partial), and cytochrome oxidase subunit 1 (COI) DNA. I extracted the total genomic DNA (gDNA) from subsampled tissue (95% ethanol solution) following the Qiagen DNeasy protocol for animal tissues: samples were incubated (~55°C) in a proteinase K solution for 1.5 to 3 hours (depending on the subsample), isolated via spin filter and ethanol precipitation, and then stored at 4°C. I used polymerase chain reaction (PCR) with 5′ and 3′ primers (Table 2) to amplify three mitochondrial genes and gene fragments (COI, ~ 690 bp; 16S, ~ 671 bp; 12S, ~ 474 bp) and three nuclear genes and gene fragments (18S, ~ 1860 bp; H3, ~ 335

Table 2. Primers for the six genes (H3, COI, 16S, 12S, 18S, and 28S) used in the current study. Corresponding PCR conditions are described below.

Primer	Sequence 5' → 3'	Source
Histone H3[a]		
H3af	ATG GCT CGT ACC AAG CAG ACV GC	(Colgan et al., 1998)
H3ar	ATA TCC TTR GGC ATR ATR GTG AC	(Colgan et al., 1998)
COI[b]		
CO1ef	ATA ATG ATA GGA GGR TTT GG	(Arndt et al., 1996)
CO1er	GCT CGT GTR TCT ACR TCC AT	(Arndt et al., 1996)
16S[c]		
16S-arL	CGC CG TTT ATC AAA AAC AT	(Palumbi, 1996)
16S-brH	CCG GTC TGA ACT CAG ATC ACG	(Palumbi, 1996)
12S[d]		
12S A	CTG GGA TTA GAT ACC CCA CTA	(Janies, 2011)
12S B	TGA GGA GGG TGA CGG GCG GT	(Janies, 2011)
18S[e]&*f*		
18S-1F	TAC CTG GTT GAT CCTG CCA GTA G	(Janies, 2011)
18S-5R	CTT GGC AAA TGC TTT CGC	(Giribet et al., 1996)
18S-3F	GTTCGATTCCGGAGAGGGA	(Giribet et al., 1996)
18S-bi	GAG TCT CGT TCG TTA TCG GA	(Janies, 2011)
18S-a2.0	ATG GTT GCA AAG CTG AAA C	(Janies, 2011)
18S-9R	GAT CCT TCC GCA GGT TCA CCT AC	(Janies, 2011)
28S[g]		
F3935ASTERIASIT28	CTG CCC AGT GCT CTG AAT GTC	(Janies, 2011)
R4795ASTERIASIT28	ATC TGC GGT TCC TCT CGT ACT	(Janies, 2011)

[a] Denaturation at 95°C for 3min followed by 40 cycles of: 95°C for 30 s 53°C for 45 s, 72°C for 45 s, and a final annealing at 72°C for 5 min.
[b] Denaturation at 95°C for 3min followed by 40 cycles of: 95°C for 40 s 45°C for 40 s, 72°C for 50 s, and a final annealing at 72°C for 5 min.
[c] Denaturation at 95°C for 3min followed by 35 cycles of: 95°C for 40 s 50°C for 40 s, 68°C for 50 s, and a final annealing at 68°C for 5 min.
[d] Denaturation at 95°C for 3min followed by 35 cycles of: 94°C for 30 s 50-55°C for 60 s, 72°C for 90 s, and a final annealing at 72°C for 5 min.
[e] Primers 1F/5R: Denaturation at 95°C for 3min followed by 40 cycles of: 95°C for 30 s 49°C for 30 s, 72°C for 90 s, and a final annealing at 72°C for 8 min.
[f] Primers 3F/bi and 9R/a 2.0: Denaturation at 95°C for 3min followed by 40 cycles of: 95°C for 30 s 52°C for 30 s, 72°C for 90 s, and a final annealing at 72°C for 8 min.
[g] Denaturation at 95°C for 3min followed by 38 cycles of: 94°C for 30 s 53°C for 30 s, 68°C for 60 s, and a final annealing at 68°C for 5 min.

bp; 28S, ~ 995 bp). I performed the PCR reactions using two different reagent mixes; either 12.5 µl GoTaq Green Master Mix (Promega, Inc), 1.0 µl primer, 1.0 µl template DNA, and 9.5 µl H_20; or Illustra puReTaq Ready-To-Go PCR Beads (GE Healthcare, Inc), 1.0 µl primer, 1.0 µl template DNA, and 22.0 µl H_20. The PCR conditions generally followed a constant program: denaturation at 95°C for 30s, annealing at 45°C to 55°C for 40s, and extension at 72°C for 1 min; this was repeated for 40 cycles. After PCR, I used agarose gel (1.5%) electrophoresis to confirm that my desired PCR length was obtained; if it was, I purified the PCR product. I did this by adding 2.0 µl ExoSAP-it PCR Product Clean-up to each PCR product and then ran them through a thermocycler using the ExoSAP-it thermocycler protocol (i.e., incubation at 37°C for 15 min followed by inactivation heating at 80°C for 15 min). I then loaded the purified PCR product (5.0 µl) along with 1.0 µl of the appropriate primer (one well with the forward primer and another well with the reverse), and 9.0 µl H_20 into 96-well plates and sent them to the Europhins sequencing facility (http://www.operon.com/services/dna-sequencing/sample-prep.aspx) where they were sequenced using cycle sequencing technology (dideoxy chain termination/cycle sequencing) on ABI 3730XL sequencing machines. I edited the sequenced data with the Geneious (R6.1.6) (Kearse et al., 2012) program and I will deposit these edited sequences into GenBank before my colleagues and I publish.

2.3 Alignment, saturation evaluation, highly-variable section removal, and model selection

I aligned all of the sequences by gene partition (18S rDNA, 16S rDNA, 12S rDNA, 28S rDNA, H3, COI) using MAFFT 7 (Katoh and Standley, 2013) with the E-INS-i strategy in place. I then used Geneious (R6.1.6) (Kearse et al., 2012) and Mesquite 2.75 (Maddison and Maddison, 2011) to manually review each alignment for obvious mis-alignments and for gaps in the protein coding gene alignments. I also checked the entirety of the protein coding genes (COI and histone H3) with Mesquite 2.75: First, I set the codon position and the genetic code (as "Echinoderm mitochondrial" for CO1 and "Standard" for H3), and then I colored the nucleotides by amino acid. I considered the protein coding alignments to be complete if the amino acids of each taxon flowed continuously from beginning to end. Upon submission of the final ms to a journal, I will submit the cropped (overhangs and primer sequences) master alignments to Treebase (www.treebase.org/).

To ensure that the most robust phylogenetic inferences were made, I first performed several tests on the aligned partitions. The ability to 1. Identify homologous sites by sequence alignment, and 2. Identify areas of an alignment that display substantial substitution saturation, is key to achieving an accurate phylogenetic reconstruction (Xia, 2009). Therefore, I first ran all of the aligned

partitions through the Gblocks online server 0.91b (Talavera and Castresana, 2007) to remove poorly-aligned highly-divergent areas of alignment. I then analyzed the rapidly evolving gene regions (COI, H3) using DAMBE 5.3.57 (Xia and Xie, 2001; Xia et al., 2003) to test for substitution saturation. When I ran the Gblocks analyses, I chose all options for a less stringent selection.[4] When I ran the DAMBE 5.3.57 analyses I first chose the appropriate genetic code for each of the COI and H3 protein-coding alignments, then I calculated proportion of invariant sites, and then I performed the tests for substitution saturation. For both the CO1 and H3 alignments, I first performed the DAMBE analysis for each of the three codon positions individually, and if the 3rd position was saturated, I then further analyzed the combined 1st and 2nd positions.

The tests for highly-divergent alignment areas (using the Gblocks program) revealed that the 12S and 16S gene alignments had areas of high variability. I therefore created "16S Gblocks" and "12S Gblocks" alignments – alignments with the highly-variable regions removed (HVRR) – that I analyzed further along with the original 12S and 16S (non-Gblocks) alignments (alignments with the highly variable regions still in place). The tests for substitution saturation (using the DAMBE 5.3.57 program) revealed that even though the third codon position of the COI alignment was significantly saturated,

[4] There are three options for a less stringent selection by the Gblocks online server 0.91b (Talavera and Castresana, 2007): 1. Allow smaller final blocks 2. Allow gap positions within the final blocks 3. Allow less strict flanking positions.

the entire COI alignment (with all codon positions present) was not significantly saturated. Nonetheless, I created a "COI 1and2" partition – with only the first and second codon positions included – to be analyzed further, along with the original COI alignment, to see if it made an impact on tree topography and test support. The histone H3 alignment (for each of the individual codon positions and with all codon positions present) was not significantly saturated and thus I did not create another partition for it.

After aligning the data and checking for sequence saturation, and before phylogenetic reconstruction, I used jModelTest 2.1.4 (Darriba et al., 2012) to determine the best-fit models for the maximum likelihood (ML) and Bayesian inference (BI) analyses from among 56 competing models, using Akaike Information Criterion (AIC) calculations. The AIC determined the models and the best-fit parameter values for those models, but because almost all of the alignments or partitions followed the GTR+I+G (GTR: general time reversible model, I: invariable sites, G: gamma distribution) model, I often used the Mesquite 2.75 (Maddison and Maddison, 2011) "MrBayes blocks" to perform the Bayesian analyses. The exceptional gene regions that did not conform to the GTR+I+G model were 1. The second codon position of histone H3, which followed the JC (Jukes Cantor) method, and 2. The third position of histone H3, which followed the GTR+G method. Lastly, protein coding genes (COI and H3)

were partitioned by codon position for the ML and BI analyses using jModelTest 2.14.

2.4 Phylogenetic analyses of individual genes

I conducted Maximum likelihood (ML), Bayesian inference (BI), and Maximum parsimony (MP) analyses on the aligned individual gene partitions (Table 3). Analyzing individual genes before analyzing the concatenated datasets was important for two reasons: 1. I was able to verify if any of the terminals were dramatically out of, what was though to be, their approximate position within the tree, and 2. I was able to assess if the trees displayed higher resolution at their deeper nodes compared to COI trees.

I performed the ML analyses with raxmlGUI 0.93 (Stamatakis, 2006; Silvestro and Michalak, 2012) default settings – "ML Rapid bootstrap," 100 replicates and the "GTRGAMMA" model. A gene-specific codon partition file was also added during the protein coding gene (either COI or H3) analyses.

I performed BI-based phylogenetic analyses, using four Markov chains, running 10 million generations, and sampling every 1000 generations, in MrBayes 3.2.2 (Ronquist and Huelsenbeck, 2003). I used MrBayes 3.2.2 default priors, unlinked parameter estimates, and model parameters from jModeltest 2.1.4 (Darriba et al., 2012). In general, for non-protein coding genes, I exported a

Table 3. Single-gene partitions. "Highly variable regions removed" (HVRR) refers to whether or not the Gblocks online server 0.91b (Talavera and Castresana, 2007) was used to remove poorly-aligned highly-divergent areas from the gene alignment. "3rd COI Positions Excluded" refers to those datasets where the 3rd COI positions were removed from the alignment because DAMBE 5.3.57 (Xia and Xie, 2001; Xia et al., 2003) found their substitution rates to be significantly saturated.

Dataset	Highly Variable Regions Removed?	3rd COI Position Excluded? (if applicable)
16S	No	N/A
16S HVRR	Yes	N/A
12S	No	N/A
12S HVRR	Yes	N/A
18S	No	N/A
28S	No	N/A
H3	No	N/A
COI	No	No
COI (1&2)	No	Yes

MrBayes block from Mesquite 2.75 (Maddison and Maddison, 2011) and then ran it in MrBayes 3.2.2. At the end of each independent iteration, or analysis, I created a majority-rule consensus tree from the trees remaining after an appropriate set (10%) was discarded as burn-in. I checked the efficiency of the burn-in set for each iteration. I performed two or three independent iterations for each of the individual gene partitions, and after all iterations were created I analyzed them for convergence and mixing with Tracer 1.6.0 (Rambaut et al., 2013). Since all iterations from each partition converged and were well mixed, I took one consensus tree from one of the iterations and saved it as the best estimate tree for that dataset. I used the same general methods for the protein coding genes that I used for the non-protein coding genes, except for the protein coding genes I created MrBayes command blocks – which included the appropriate codon partitions.

Lastly, I performed maximum parsimony (MP) analyses using PAUP* 4.0b10 (Swofford, 2003) with all characters weighted equally. To determine the best trees, I conducted heuristic searches using random stepwise addition of the terminals (1000 replicates) with the tree bisection re-connection (TBR) permutation algorithm and with maximum zero-length branches collapsed. I then summarized these trees as a strict consensus tree and subjected them to jackknifing (100 replicates, 100 random additions per iteration, 37% deletion) and

bootstrapping (100 replicates, 100 random additions per iteration) analyses to measure clade support.

After all three tests (ML, BI, and MP) were completed I inspected each best tree (for each of the nine partitions) and noted any terminals that appeared dramatically out of place.

2.5 Phylogenetic analyses of concatenated genes

Once I completed the phylogenetic analyses of the nine single-gene partitions, I performed the same three phylogenetic analyses (ML, BI, and MP) on four concatenated gene datasets (Table 4): "concatenated" (18S, 28S, H3, 16S highly-variable regions included (HVRI), 12S HVRI, COI all codon positions included (ACPI)), "concatenated highly-variable regions removed (HVRR)" (18S, 28S, H3, 16S HVRR, 12S HVRR, COI ACPI), "concatenated COI (1&2)" (18S, 28S, H3, 16S HVRI, 12S HVRI, COI only 1st and 2nd codon positions included), and "concatenated HVRR COI (1&2)" (18S, 28S, H3, 16S HVRR, 12S HVRR, COI only1st and 2nd codon positions included). I later administered an approximately unbiased (AU) test of phylogenetic tree selection on one of these analyzed datasets (Concatenated HVRR) to compare its likelihood to the likelihood of trees produced by recent analyses (more information on the AU test is provided below). I created each of these four datasets using the program

Table 4. Concatenated datasets. "Highly variable regions removed" (HVRR) refers to whether I removed poorly-aligned areas from the gene alignment. "3rd COI Positions Excluded" refers to those datasets where the 3rd COI positions were removed from the alignment because DAMBE 5.3.57 (Xia and Xie, 2001; Xia et al., 2003) found their substitution rates to be significantly saturated.

Dataset	Highly Variable Regions Removed?	3rd COI Position Excluded?
Concatenated	No	No
Concatenated HVRR	Yes	No
Concatenated CO1 (1&2)	No	Yes
Concatenated HVRR CO1 (1&2)	Yes	Yes

Sequence Matrix 1.7.8 (Vaidya et al., 2011), which concatenated the individual partition files as soon as they were loaded. I was then ready to perform the three phylogenetic analyses (ML, MP, and BI) on the four concatenated datasets.

I applied ML, BI, and MP tests on each concatenated (combined) dataset individually. I performed the concatenated dataset ML analyses the same way I performed the single-gene partitions analyses with two differences. First, I imported gene partitions as well as codon partitions into raxmlGUI 0.93 (Stamatakis, 2006; Silvestro and Michalak, 2012) for each dataset. Second, I used a different standard set of settings for all the ML analyses: "ML thorough bootstrap," 100 replicates, "GTRGAMMA" model (as recommended by the program's authors), and both Patiria miniata (Genbank), and Strongylocentrotus purpuratus (Genbank) as outgroup members.

The methods I used when I performed the concatenated dataset BI analyses were slightly different from the ones I used when I performed the BI analyses for the single-gene partition analyses. I used the same settings (four Markov chains, running 10 million generations, sampling every 1000 generations, unlinked parameter estimations, and default priors) for each of the iterations; however, due to time constraints, I used the University of California San Diego CIPRES Science Gateway 3.3 (Miller et al., 2010) to run each of the MrBayes 3.2.2 (Ronquist and Huelsen, 2003) iterations. To run the datasets on the CIPRES Science Gateway I had to create specific command blocks for MrBayes. In these

blocks I included the concatenated dataset alignment and settings, as well as the gene partitions (and their corresponding jModeltest 2.1.4 (Darriba et al., 2012) chosen substitution models) and the codon partitions for the concatenated dataset that I was analyzing. I performed approximately three iterations for each of the four concatenated datasets. Like the single-gene BI analyses, I also used Tracer 1.6.0 (Rambaut et al., 2013) to confirm the convergence and mixing of all of the runs (~6), after which, I took one consensus tree from one of the iterations and used it as the best estimate of the phylogeny.

I performed all of the concatenated dataset MP analyses in PAUP* 4.0b10 (Swofford, 2003) in the same manner (and with the same settings) as the single-gene partition MP analyses.

The approximate unbiased (AU) test of phylogenetic tree selection was the last analysis I completed. I decided to use this test after I evaluated the results from my concatenated datasets and found that my results 1. Differed from many of Pawson and Fell's (1965) clades, and 2. Evinced variation in the position of Molpadida. I wanted to compare the likelihoods of the best tree (Concatenated HVRR) of the current study with both a constrained Pawson and Fell (1965) tree and a tree in which the position of Molpadida was constrained to be sister to a Dendrochirotida+Dactylochirotida group. Thus, I created constrained trees in Mesquite 2.75 (Maddison and Maddison, 2011). I used the same taxa from the current study and followed either Pawson and Fell's (1965) arrangement, or the

arrangement of my result tree with the Molpadida difference. I then loaded both the complete dataset (Concatenated HVRR) and the respective constraint tree (Pawson and Fell (1965) or Molpadida+(Dendrochirotida+Dactylochirotida)) into raxmlGUI 0.93 (Stamatakis, 2006; Silvestro and Michalak, 2012). I ran the raxmlGUI constraint tests under the same conditions (e.g., GTRGAMMA model) as all my concatenated tests. Afterwards, I exported the raxmlGUI "best tree" trees and loaded them into PAUP* 4.0b10 (Swofford, 2003), where I ran the Shimodaira Approximate Unbiased (AU) Test under estimated, 100,000, RELL, and GAMMA settings.

2.6 Vouchers and missing data

A summary of the collected and missing data, along with the locations of the vouchers, are listed in Table 5. Although one or two sequences are missing for some of the terminals (only one, *Paelopatides* sp. AMK19, is missing three), the total amount of missing data is only 11.8%. This amount of missing data is common; in fact, multiple studies have demonstrated that partially incomplete data is unimportant under certain conditions. A study by Wiens (2006) demonstrated that "the placement of highly incomplete taxa in a phylogeny can be

Table 5. Samples and GenBank accession numbers. Asterisks (*) denote vouchers that have not been cataloged yet.

Taxon as Listed On Trees	Location	Date	Depth	Latitude	Longitude	Source	18s	16s	CO1	H3	12s	28s
Psychropotes longicauda E4074	Callifornia, Pulse 43, Sta. M	2/28/04	4065	34.70185° N	123.18642° W	SIO-BIC E4074	-	-		-	-	
Elpidiidae sp. E5110	South Sandwich Island, Antarctica	10/8/11	403	59.38746° S	27.313625° W	SIO-BIC E5110	-	-	-	-	-	
Psolus sp. E5136	Discovery Bank, Antarctica	10/13/11	439	60.111035° S	34.8266° W	SIO-BIC E5136	-	-	-	-	-	
Afrocucumis africana GU038	Asan, Guam	8/13/12	0.5	13.476528° N	144.708333° E	FMNH-IZC*	-	-	-	-		-
Molpadia musculus E5295	Shetland Island, Antarctica	10/27/11	167	62.33746° S	60.7444° W	SIO-BIC E5295	-	-	-	-	-	-
Chiridota hawaiiensis GU056	Tumon, Guam	9/9/12		13.509861° N	144.800667° E	FMNH-IZC*	-	-	-	-	-	-
Holothuria hilla GU047	Tumon, Guam	8/13/12		13.509861° N	144.800667° E	FMNH-IZC*	-	-	-	-	-	-
Bathyplotes cinctus E5111	Herdman Bank, Antarctica	10/10/11	520	59.89862° S	32.4511° W	SIO-BIC E5111	-	-	-	-	-	-
Thelenota anax CHK131	Agat, Guam	9/21/12		13.3585° N	144.6415° E	FMNH-IZC*	-	-	-	-	-	-
Euapta tahitiensis CHK067	Chuuk	9/19/12		7.461° N	151.903667° E	FMNH-IZC*	-		-	-	-	-
Actinopyga mauritiana CHK129	Tumon, Guam	9/20/12		13.509861° N	144.800667° E	FMNH-IZC*	-	-	-	-		
Sclerodactylidae E5613	Disko Island, Greenland	8/1/10	70	69.25° N	53.583° W	SIO-BIC E5613	-	-		-	-	-
Molpadia arenicola SIO1	San Clemente Island, California	11/3/12		32.892444° N	118.530528° W	SIO-BIC*		-	-	-	-	-
Apostichopus californicus SIO2	La Jolla, California	10/23/12		32.871972° N	117.263694° W	SIO-BIC*	-	-	-	-	-	
Ypsilothuria bitentaculata E4760	San Diego, California	7/1/10	500	32.596° N	117.483° W	SIO-BIC E4760	-	-	-	-	-	
Paroriza prouhi AMK8	NE Atlantic					SOC 13314-2	-	-	-	-	-	
Synallactes cf chuni E3566	Mazatlan, Mexico	5/5/04		22.5167° N	106.6992° W	SIO-BIC E3566	-		-	-	-	-
Synallactidae E4365	California, Pulse 49, Sta. M	8/8/06	4100	34.65° N	123.08333° W	SIO-BIC E4365	-	-	-	-	-	-
Stichopus vastus CHK135	Chuuk	9/21/12		7.461° N	151.903667° E	FMNH-IZC*	-	-	-	-		-
Deima validum AMK9	NE Atlantic					SOC 13369-2	-	-	-	-	-	
Paelopatides sp AMK19	Oregon					CAS 115043				-	-	-
Peniagone diaphana AMK3	NE Atlantic					SOC 13369-2	-	-	-	-	-	
Pannychia moseleyi E4625	Monterey Canyon, California	10/26/10	1018	36.7721° N	122.0831° W	SIO-BIC E4625	-	-	-	-	-	
Crucella scotiae E5311	South Orkney, Antarctica	10/20/11	81	60.613° S	45.141685° W	SIO-BIC E5311	-	-	-	-	-	-
Molpadia musculus E5300	South Georgia, Antarctica	9/26/11	316	53.82389° S	37.37297° W	SIO-BIC E5300	-	-	-	-	-	-
Synallactes sp E5607	Spanish Harbor, Florida	3/4/10	0?	24.65416° N	81.324166° W	SIO-BIC E5607	-	-	-	-	-	-
cf Elasipodida E5609	Guaymas Basin, Mexico	4/9/12	2733	26.35495° N	110.746° W	SIO-BIC E5609	-	-	-	-	-	-
Pannychia_cf_moseleyi E5614	Monterey Bay, California	6/2/11	1018	36.772° N	122.083° W	SIO-BIC E5614	-	-	-	-	-	-
Chiridota_sp E5611	San Diego, California	7/2/10	100	32.596° N	117.483° W	SIO-BIC E5611	-	-	-	-	-	-
Sigmodota_sp E5135	South Sandwich Island, Antarctica	10/6/11	147	57.03685° S	26.747445° W	SIO-BIC E5135	-			-	-	-

Taxon as Listed On Trees	Location	Date	Depth	Latitude	Longitude	Source	18s	16s	CO1	H3	12s	28s
Oneirophanta setigera UF9706	Moorea, French Polynesia	10/22/09	880			FMNH-IZC UF9706	-	-	-	-		-
Mesothuria_sp UF9746	Moorea, French Polynesia	10/22/09	678			FMNH-IZC UF9746	-	-	-	-	-	-
Crucella scotiae E5296	Shag Rock, Antarctica	9/23/11	156	53.42147° S	42.01879° W	SIO-BIC E5296	-	-	-	-		-
Chiridota_sp E5602	Disko Island, Greenland	8/2/10	5	69.48431° N	53.939° W	SIO-BIC E5602	-		-	-	-	
Chiridota sp E5604	Bransfield Strait, Antarctica	10/24/11	150	63.3252° S	59.86298° W	SIO-BIC E5604	-			-	-	
Crucella scotiae VMA05	South Shetland Islands, Antarctica	1/4/12		62.4472° S	55.2648° W	MV-F193785	-	-	-	-	-	-
Paracucumis turricata VMA06	South Orkney Islands, Antarctica	9/3/09		63.2385° S	59.4203° W	MV-F169314	-	-	-	-	-	-
Placothuria squamata NW1	Pegasus Bay, New Zealand	10/13/73	0	43.1582985° S	172.8217010° E	SIO-BIC*			-	-	-	
Enypniastes eximia NW3	Bay of Plenty, New Zealand	4/26/12	1078	37.3345000° S	176.9597000° E	SIO-BIC*	-	-	-	-	-	-
Heterothyone alba NW5	New Zealand	4/18/07	451	44.0681600° S	178.5492000° E	SIO-BIC*	-	-	-	-	-	-
cf_*Cucumariidae S20192*	Antarctica, Sta.SMIc	4/10/13				SIO-BIC*	-	-	-	-	-	-
cf_*Pseudostichopus S20595*	Antarctica, Sta. BBE2, event 38	4/25/13				SIO-BIC*	-	-	-	-		-
cf_*Heterothyonidae S20758*	Antarctica, Sta. BBE3, event 42	4/26/13				SIO-BIC*	-	-	-	-	-	-
cf_*Dendrochirotida S20863*	Antarctica, Sta. COF, event 56	4/30/13				SIO-BIC*	-	-	-	-	-	-
cf_*Psolidae S20868*	Antarctica, Sta. BBE3, event 43	4/26/13				SIO-BIC*	-	-	-	-	-	-
cf_*Pseudostichopus S21014*	Antarctica, Sta. POF, event 55	4/29/13				SIO-BIC*	-	-	-	-	-	-
cf_*Synallactidae S21020*	Antarctica, Sta. POF, events 55	4/29/13				SIO-BIC*	-	-	-	-	-	-
Molpadia arenicola AMK16	California					CAS 115044	-	-	-	-	-	-
Molpadiodemas villosus AMK	NE Atlantic					SOC 13627-10	-	-	-	-		
Bohadschia koellikeri AMK	Guam					US NMNH E51759	-	-	-	-		

resolved with perfect accuracy (based on simulations) and with strong statistical support (based on empirical analyses)." The critical factors, in resolving phylogenetic relationships have to do with the quality (Philippe et al., 2014) and the overall quantity of the data that is present in the study (Wiens, 2006), not the specific missing components. Multiple successful case studies have demonstrated that combined-gene analyses with only a moderate amount of missing data can produce phylogenetically accurate results (Baldauf et al., 2000; Bouchenak-Khelladi et al., 2008; Rouse et al., 2013; Philippe et al., 2014).

CHAPTER 3: RESULTS

3.1 Highly-variable regions, saturation, model selection, and MCMC output

Tests for regions of high variability discovered poorly aligned regions in only the 16S and 12S alignments. Consequently, two separate 16S HVRR and 12S HVRR partitions (with the highly-variable regions removed) were added to the set of single-gene partitions (Table 3).

DAMBE 5.3.57 (Xia and Xie, 2001; Xia et al., 2003) saturation plots (scattergrams) of nucleotide transitions and transversions against the GTR (generalized time-reversible) and TN93 (Tamura and Nei, 1993) corrected genetic distances were created for the COI and H3 (protein coding) partitions. The plots for (1) the 3rd COI codon position, (2) the 1st/2nd COI codon positions (combined), and (3) all of the COI codon positions (1st/2nd/3rd) (combined) are depicted in Figure 7. The tests revealed that the third codon positions of the COI sequences were significantly saturated; however, the tests did not show that the 1st/2nd combined or the all of the COI codon positions (1st/2nd/3rd) combined were significantly saturated. In other words, although there were more transversions ("v" and green in Figure 7) than transitions ("s" and blue in Figure 7), no obvious plateau of transitions was observed, which is what would be seen if significant

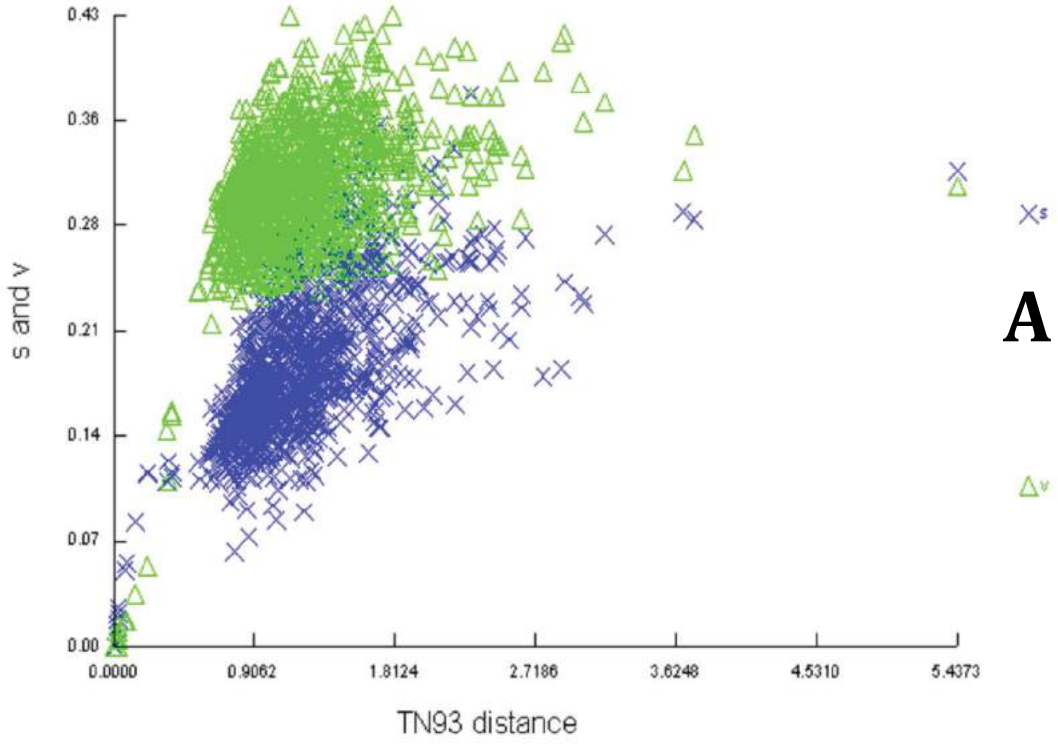
0.43
0.36
0.28
0.21
0.14
0.07
0.00
s and v
0.0000
0.9062
1.8124
2.7186
3.6248
4.5310
5.4373
TN93 distance
s
v

A

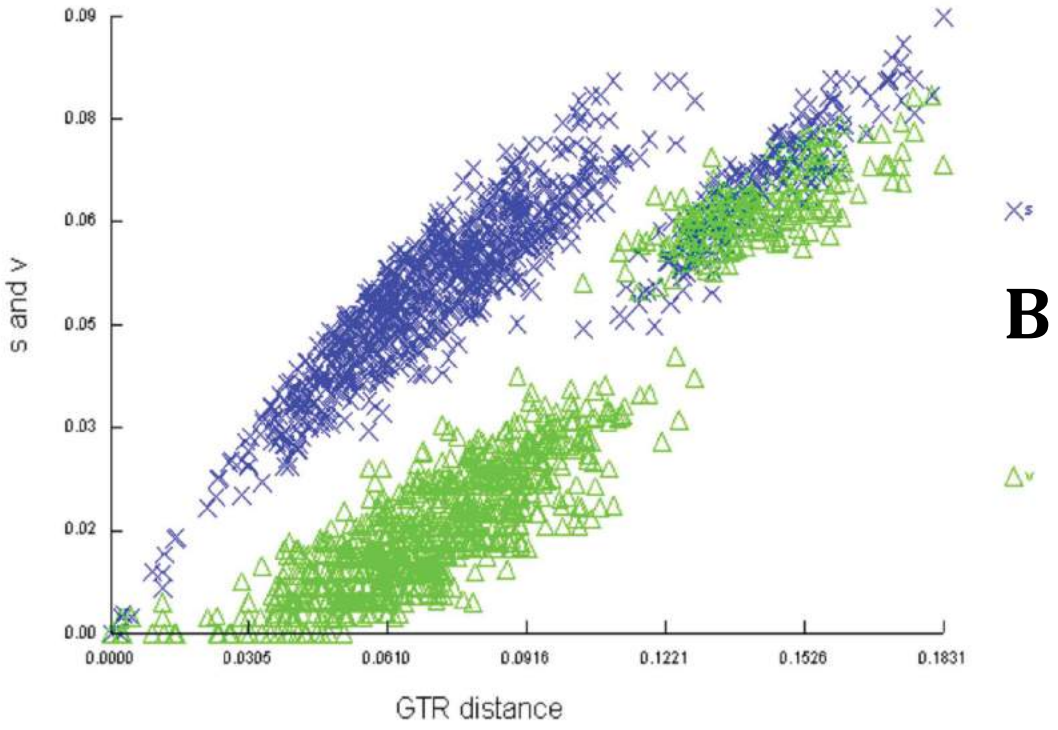
0.09
0.08
0.06
0.05
0.03
0.02
0.00
s and v
0.0000
0.0305
0.0610
0.0916
0.1221
0.1526
0.1831
GTR distance
s
v

B

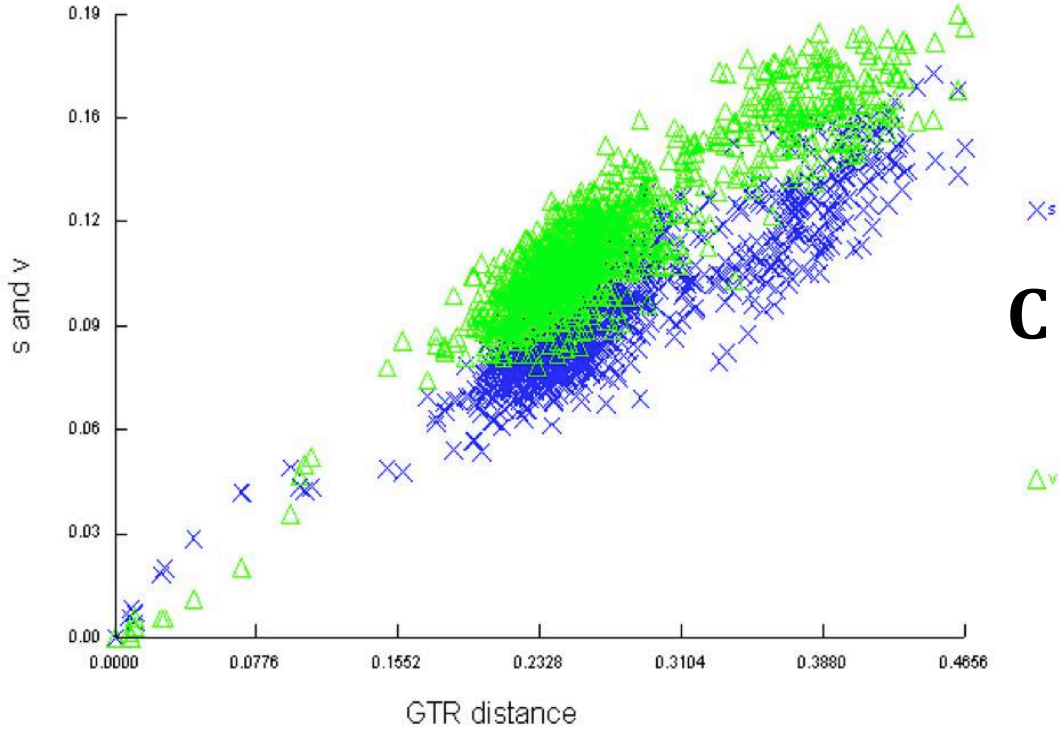

Figure 7. DAMBE 5.3.57 saturation plots. DAMBE 5.3.57 (Xia and Xie, 2001; Xia et al., 2003) was used in this study to create saturation plots (scattergrams) of transversion ("v" and green) and transition ("s" and blue) rates against GTR and TN93 distances at **A.** COI 3rd codon position, **B.** 1st/2nd COI codon positions (combined), and **C.** all COI positions (1st/2nd/3rd) (combined). The COI 3rd codon position was also plotted over GTR distance (not shown here) and produced the same transition/transversion relationship as that in graph **A**.

saturation had occurred. Therefore, it was not necessary to exclude the third codon positions, but as a precautionary measure, a COI (1&2) partition (Table 3) was created and analyzed. None of the H3 codon positions were saturated and, therefore, no new partitions were created for the H3 gene.

Tests for the best-fit models of nucleotide substitution for each partition found that all of the gene datasets, and almost all of the COI and H3 codon partitions followed the GTR+I+G (GTR: general time reversible model, I: invariable sites, G: gamma distribution) model. The H3 second codon position (model: JC (Jukes-Cantor) and the H3 third codon position (model: GTR+G) were the two exceptions.

Tracer 1.6.0 (Rambaut et al., 2013) was used to analyze the trace files generated by the BI MCMC runs. Combined trace plots (plots of the log-likelihood (LnL) through time) created by Tracer 1.6.0 (Rambaut et al., 2013) showed efficient mixing and repeated convergence (upon a -LnL value) for each of the 13 partitions (Table 3 and 4). As a result, the use of one consensus tree from one iteration was justified. An example of a Tracer 1.6.0 four iteration combined trace plot is portrayed in Figure 8.

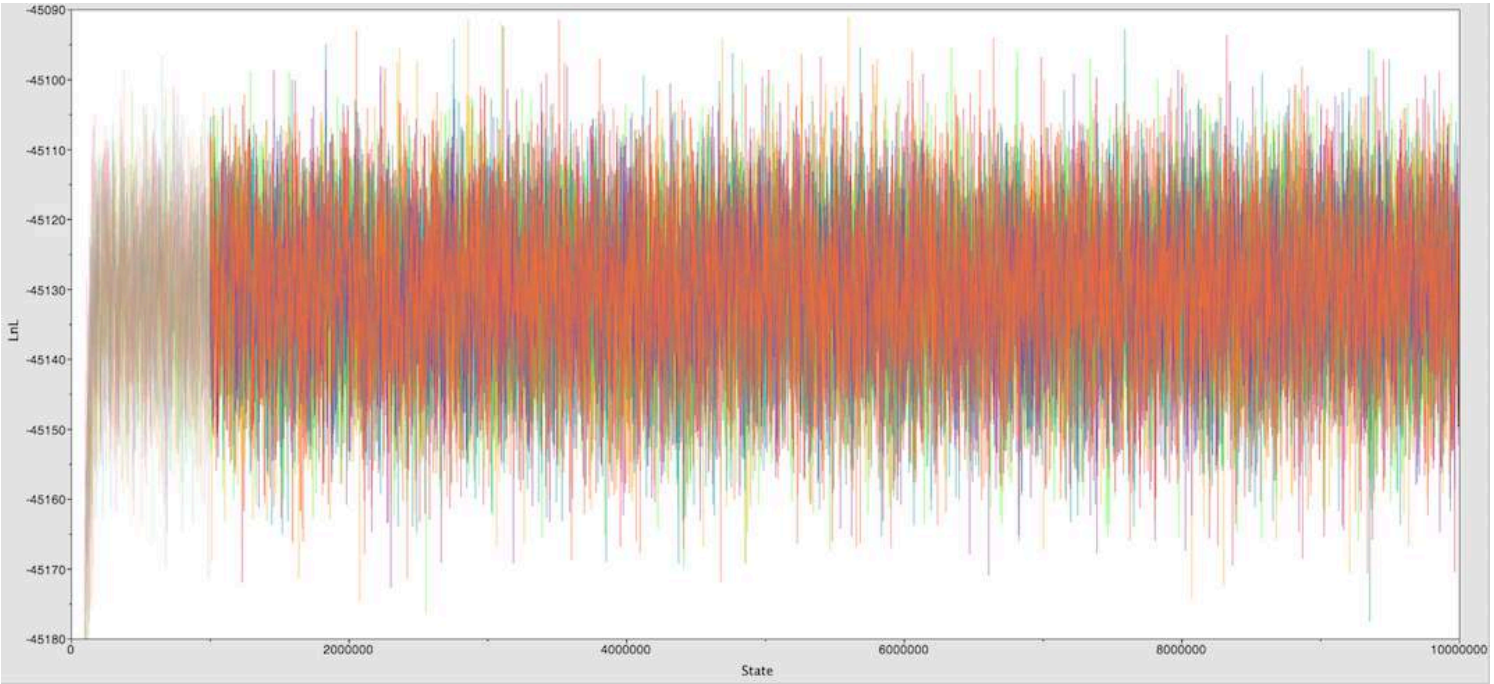

Figure 8. Example of a Tracer 1.6.0 four-iteration combined trace plot. Tracer 1.6.0 (Rambaut et al., 2013) was used in this study to analyze the trace files generated by the BI MCMC runs. The plot of the log-likelihood (LnL) through time (represented as the State) shows an adequate burn in period, efficient mixing, and congruent convergent upon an LnL value.

3.2 Phylogenetic analyses

Table 6 provides the summary statistics from the MP, ML, and BI analyses, including the number of taxa, characters, parsimony-informative characters, and most parsimonious trees (MP analyses), tree lengths and likelihoods for the 13 analyses. Single gene trees are displayed in Appendix, 1 Figures 14– 22.

Of the four six-gene (18S, 28S, 16S, 12S, COI, and H3) concatenated datasets, one (Concatenated HVRR dataset) was chosen as the 'complete,' or best estimate, dataset (the trees for all four concatenated datasets for each of the three analyses are listed in Appendix 2, Figures 23-26). Figure 9 presents the topologies generated from the complete dataset, analyzed using MP (Figure 9A), ML (Figure 9B), and BI (Figure 9C). It was possible to select a complete dataset because there were no major analytical differences in the topologies and support values of the four concatenated datasets.[5] This indicated that the four concatenated datasets were largely the same regardless of their various forms (highly variable regions and significantly saturated regions) of missing data. As a result, the Concatenated HVRR dataset – the dataset with the highly-variable regions removed – was

[5] There were no major analytical differences in the topologies and support values of the four concatenated datasets besides the fluctuation of the position of Molpadida, which was found across all datasets, and one major clade difference that appeared to be linked to the MP analyses.

Table 6. Overview of single-gene partitions and concatenated dataset analyses. *C*: number of characters analyzed, *PIC*: parsimony-informative characters, *MPTs*: number of most parsimonious trees, *MPT L*: most parsimonious tree lengths in MP analyses. Models represent those selected for the maximum likelihood (ML) and Bayesian inference (BI) analyses: *GTR*: general time reversible model, *TVM:* transversion model *I*: invariable sites, *G*: gamma distribution, *L*: likelihood of the tree obtained from the maximum likelihood analyses. The same models for the single-gene partitions were used in the concatenated datasets. The trees from each analysis can be found in Appendices 1-2. Datasets are the 13 alignments used in this study. HVRR: highly variable regions removed, (1&2): first and second codons included.

Dataset	C	PIC	MPTs	MPT L	Model	L
16S	671	317	2	2459	GTR+I+G	-10176
16S HVRR	516	258	1	1860	GTR+I+G	-8049
12S	474	270	2	1871	GTR+I+G	-7745
12S HVRR	377	231	10	1539	GTR+G	-6543
18S	1973	428	67997	1390	GTR+I+G	-10005
28S	995	223	63	862	GTR+I+G	-5315
H3	335	110	10	812	TVM+I+G	-3772
COI	700	315	2	3103	GTR+I+G	-11574
COI (1&2)	467	100	22	535	GTR+I+G	-2899
Concatenated	5148	1718	1	10838		-50421
Concatenated HVRR	4896	1611	1	9891		-47048
Concatenated CO1 (1&2)	4915	1503	5	8162		-41591
Concatenated HVRR CO1 (1&2)	4663	1396	1	7209		-38210

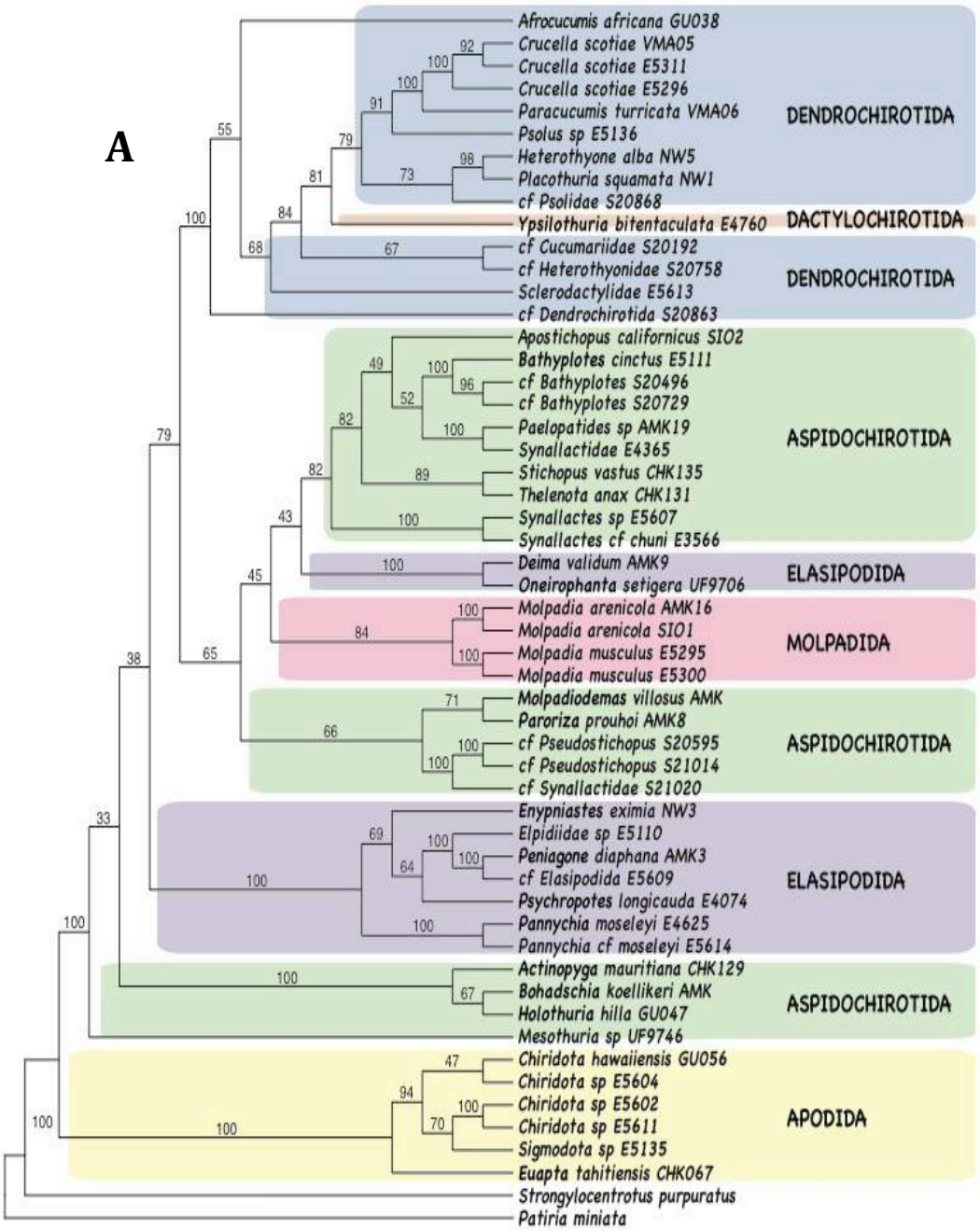
A
Afrocucumis africana GU038
Crucella scotiae VMA05
Crucella scotiae E5311
Crucella scotiae E5296
Paracucumis turricata VMA06
Psolus sp E5136
Heterothyone alba NW5
Placothuria squamata NW1
cf Psolidae S20868
DENDROCHIROTIDA
Ypsilothuria bitentaculata E4760
DACTYLOCHIROTIDA
cf Cucumariidae S20192
cf Heterothyonidae S20758
Sclerodactylidae E5613
cf Dendrochirotida S20863
DENDROCHIROTIDA
Apostichopus californicus SIO2
Bathyplotes cinctus E5111
cf Bathyplotes S20496
cf Bathyplotes S20729
Paelopatides sp AMK19
Synallactidae E4365
Stichopus vastus CHK135
Thelenota anax CHK131
Synallactes sp E5607
Synallactes cf chuni E3566
ASPIDOCHIROTIDA
Deima validum AMK9
Oneirophanta setigera UF9706
ELASIPODIDA
Molpadia arenicola AMK16
Molpadia arenicola SIO1
Molpadia musculus E5295
Molpadia musculus E5300
MOLPADIDA
Molpadiodemas villosus AMK
Paroriza prouhoi AMK8
cf Pseudostichopus S20595
cf Pseudostichopus S21014
cf Synallactidae S21020
ASPIDOCHIROTIDA
Enypniastes eximia NW3
Elpidiidae sp E5110
Peniagone diaphana AMK3
cf Elasipodida E5609
Psychropotes longicauda E4074
Pannychia moseleyi E4625
Pannychia cf moseleyi E5614
ELASIPODIDA
Actinopyga mauritiana CHK129
Bohadschia koellikeri AMK
Holothuria hilla GU047
Mesothuria sp UF9746
ASPIDOCHIROTIDA
Chiridota hawaiiensis GU056
Chiridota sp E5604
Chiridota sp E5602
Chiridota sp E5611
Sigmodota sp E5135
Euapta tahitiensis CHK067
APODIDA
Strongylocentrotus purpuratus
Patiria miniata

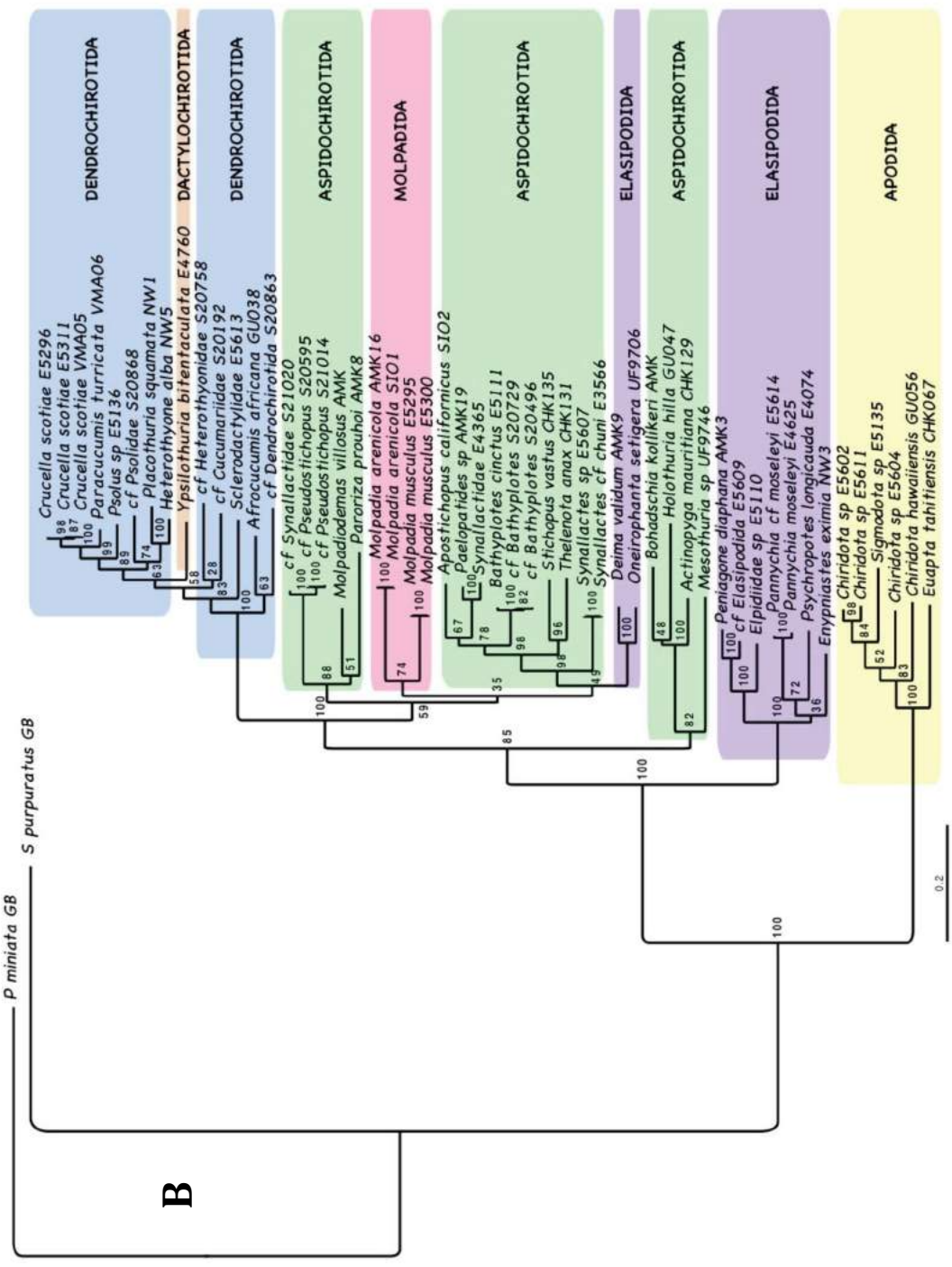
B
P miniata GB
S purpuratus GB
Crucella scotiae E5296
Crucella scotiae E5311
Crucella scotiae VMA05
Paracucumis turricata VMA06
Psolus sp E5136
cf Psolidae S20868
Placothuria squamata NW1
Heterothyone alba NW5
Ypsilothuria bitentaculata E4760
cf Heterothyonidae S20758
cf Cucumariidae S20192
Sclerodactylidae E5613
Afrocucumis africana GU038
cf Dendrochirotida S20863
cf Synallactidae S21020
cf Pseudostichopus S20595
cf Pseudostichopus S21014
Molpadiodemas villosus AMK
Paroriza prouhoi AMK8
Molpadia arenicola AMK16
Molpadia arenicola SIO1
Molpadia musculus E5295
Molpadia musculus E5300
Apostichopus californicus SIO2
Paelopatides sp AMK19
Synallactidae E4365
Bathyplotes cinctus E5111
cf Bathyplotes S20729
cf Bathyplotes S20496
Stichopus vastus CHK135
Thelenota anax CHK131
Synallactes sp E5607
Synallactes cf chuni E3566
Deima validum AMK9
Oneirophanta setigera UF9706
Bohadschia kollikeri AMK
Holothuria hilla GU047
Actinopyga mauritiana CHK129
Mesothuria sp UF9746
Peniagone diaphana AMK3
cf Elasipodida E5609
Elpidiidae sp E5110
Pannychia cf moseleyi E5614
Pannychia moseleyi E4625
Psychropotes longicauda E4074
Enypniastes eximia NW3
Chiridota sp E5602
Chiridota sp E5611
Sigmadota sp E5135
Chiridota sp E5604
Chiridota hawaiiensis GU056
Euapta tahitiensis CHK067
DENDROCHIROTIDA
DACTYLOCHIROTIDA
DENDROCHIROTIDA
ASPIDOCHIROTIDA
MOLPADIDA
ASPIDOCHIROTIDA
ELASIPODIDA
ASPIDOCHIROTIDA
ELASIPODIDA
APODIDA
0.2

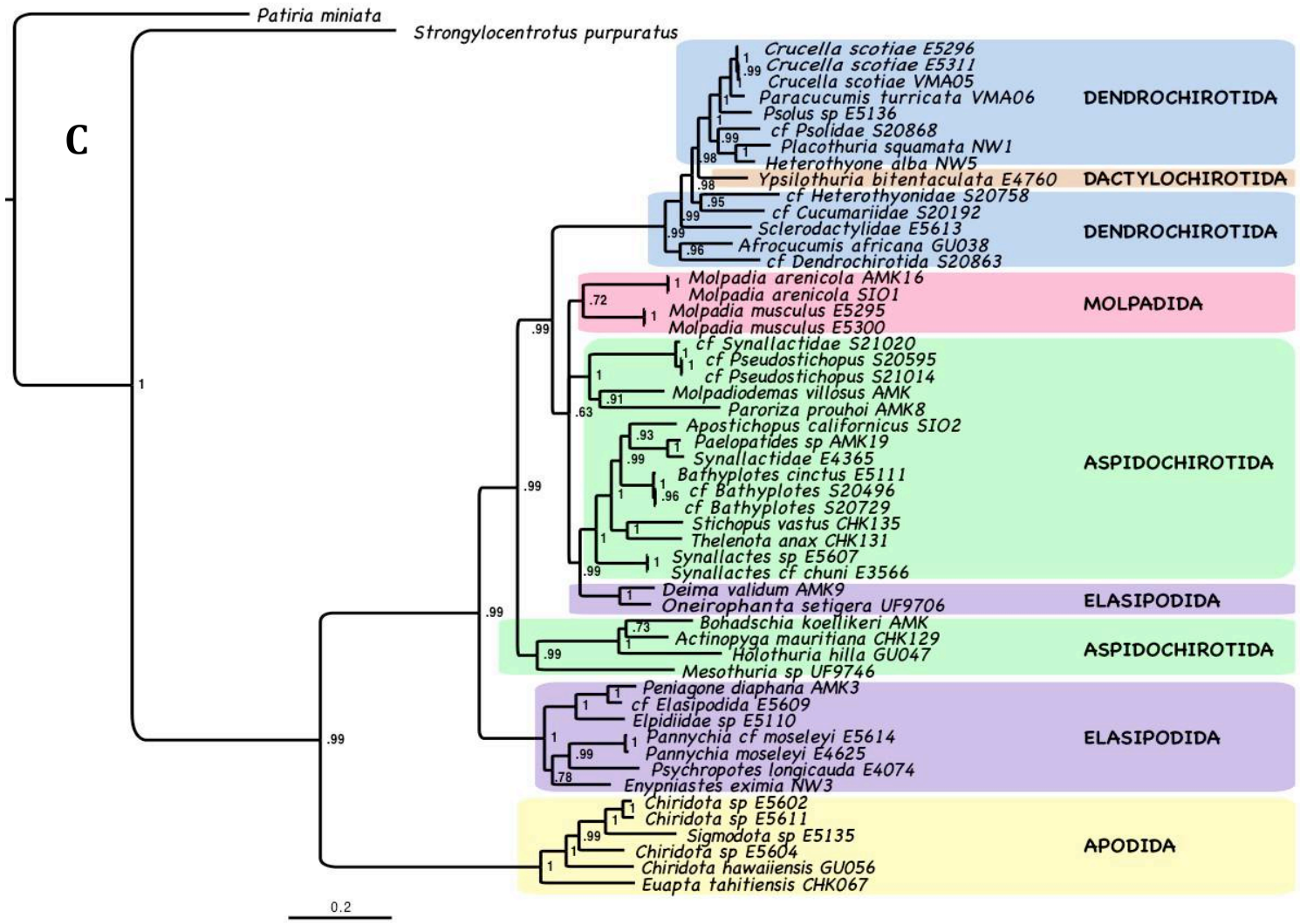
C
Patiria miniata
Strongylocentrotus purpuratus
Crucella scotiae E5296
Crucella scotiae E5311
Crucella scotiae VMA05
Paracucumis turricata VMA06
Psolus sp E5136
cf Psolidae S20868
Placothuria squamata NW1
Heterothyone alba NW5
DENDROCHIROTIDA
Ypsilothuria bitentaculata E4760
DACTYLOCHIROTIDA
cf Heterothyonidae S20758
cf Cucumariidae S20192
Sclerodactylidae E5613
Afrocucumis africana GU038
cf Dendrochirotida S20863
DENDROCHIROTIDA
Molpadia arenicola AMK16
Molpadia arenicola SIO1
Molpadia musculus E5295
Molpadia musculus E5300
MOLPADIDA
cf Synallactidae S21020
cf Pseudostichopus S20595
cf Pseudostichopus S21014
Molpadiodemas villosus AMK
Paroriza prouhoi AMK8
Apostichopus californicus SIO2
Paelopatides sp AMK19
Synallactidae E4365
Bathyplotes cinctus E5111
cf Bathyplotes S20496
cf Bathyplotes S20729
Stichopus vastus CHK135
Thelenota anax CHK131
Synallactes sp E5607
Synallactes cf chuni E3566
ASPIDOCHIROTIDA
Deima validum AMK9
Oneirophanta setigera UF9706
ELASIPODIDA
Bohadschia koellikeri AMK
Actinopyga mauritiana CHK129
Holothuria hilla GU047
Mesothuria sp UF9746
ASPIDOCHIROTIDA
Peniagone diaphana AMK3
cf Elasipodida E5609
Elpidiidae sp E5110
Pannychia cf moseleyi E5614
Pannychia moseleyi E4625
Psychropotes longicauda E4074
Enypniastes eximia NW3
ELASIPODIDA
Chiridota sp E5602
Chiridota sp E5611
Sigmodota sp E5135
Chiridota sp E5604
Chiridota hawaiiensis GU056
Euapta tahitiensis CHK067
APODIDA
0.2

Figure 9. Maximum parsimony (MP), maximum likelihood (ML), and Bayesian inference (BI) trees inferred from the six-gene concatenated complete dataset (highly-variable regions removed). **A.** Complete dataset MP bootstrap tree. **B.** Complete dataset ML tree. **C.** Complete dataset BI tree. Numbers immediately after taxon names are field numbers used to distinguish same species leaves. Numbers above or adjacent to nodes represent bootstrap scores (MP and ML analyses, **A** and **B**) or posterior probability values (BI analysis, **C**). Colored boxes designate orders: Blue = Dendrochirotida; Orange = Dactylochirotida; Green = Aspidochirotida; Red = Molpadida; Purple = Elasipodida; Yellow = Apodida. Taxon designations are from Pawson and Fell (1965).

chosen as the complete dataset because it best represented the topologies seen across all datasets.

Figure 10 summarizes the relationships of Pawson and Fell's (1965) families and orders as depicted by the BI and ML analyses of the current study. The MP analyses were excluded from the summary tree because of the difference in branch structure at several sites on the MP tree, all of which had poor support values.[6] The differences in the MP tree topology were likely due to the analyses lack of incorporation of a specific model of nucleotide substitution and resulting problems, such as long-branch attraction (Felsenstein, 1978). Regardless, the MP tree topology was nearly congruent to the ML and BI tree topologies, indicating minimal issues with site saturation.

The monophyly of extant Holothuroidea was always strongly supported, irrespective of the estimation method (ML, MP, and BI). Likewise, seven clades were strongly supported (ML and BI) within the class (Figure 10, Clades I-VII). The first clade, Apodida, was always highly supported as the monophyletic sister group to all other holothuroids (Figure 10, Clade I). Within Apodida, Chiridotidae was also strongly supported as monophyletic.

The deep-sea Elasipodida was polyphyletic in all analyses; elasipodan members were found in two evolutionarily distant clades (Figure 10, Clades II and VI). One of the elasipodan clades included only members from the family

[6] I define poor phylogenetic support as < 75% bootstrap values in the MP and ML trees and < 0.95 posterior probabilities in the BI trees.

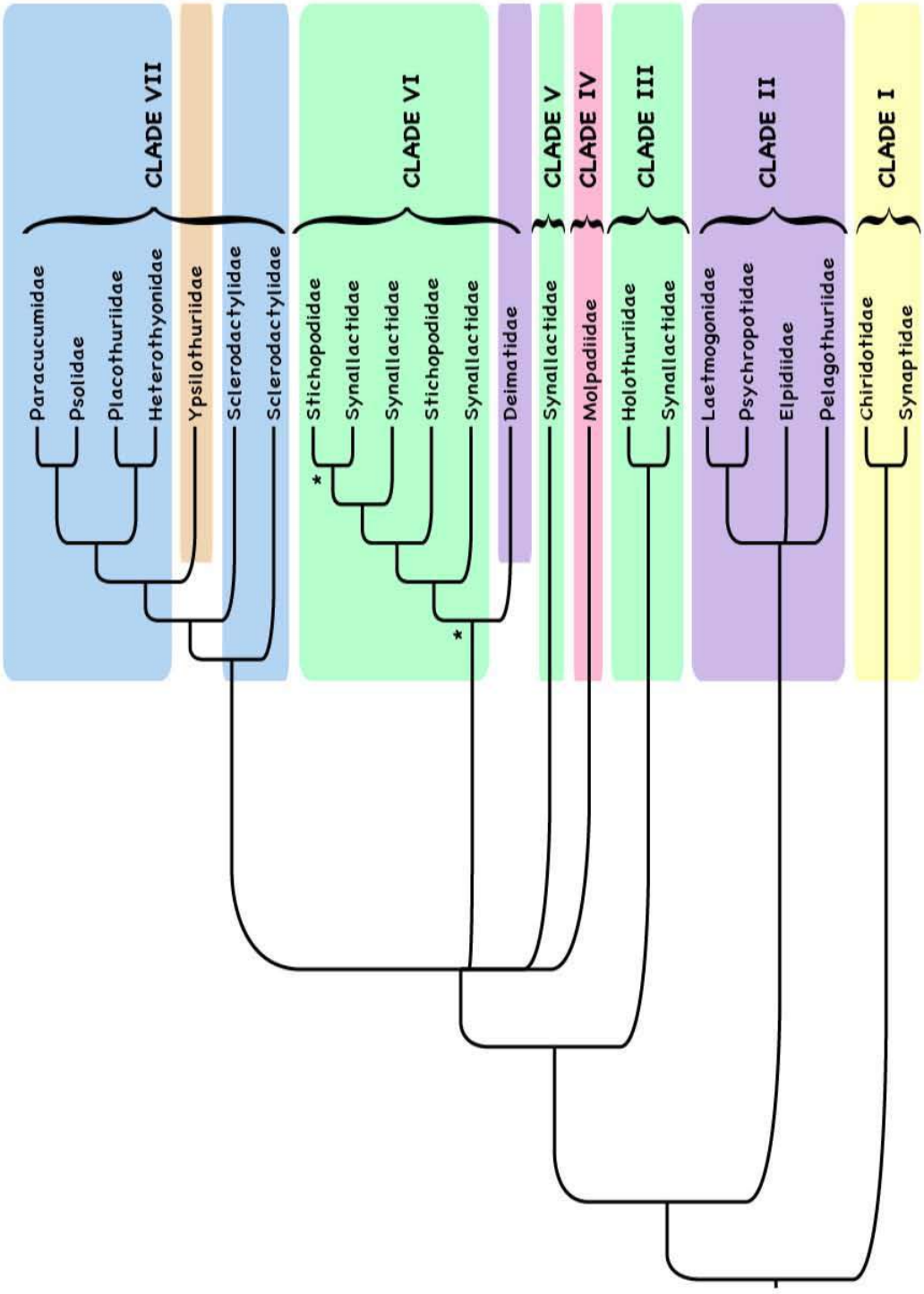
CLADE VII
Paracucumidae
Psolidae
Placothuriidae
Heterothyonidae
Ypsilothuriidae
Sclerodactylidae
Sclerodactylidae
CLADE VI
Stichopodidae
Synallactidae
Synallactidae
Stichopodidae
Synallactidae
Deimatidae
CLADE V
Synallactidae
CLADE IV
Molpadiidae
CLADE III
Holothuriidae
Synallactidae
CLADE II
Laetmogonidae
Psychropotidae
Elpidiidae
Pelagothuriidae
CLADE I
Chiridotidae
Synaptidae
*
*

Figure 10. Best estimate of holothuroid relationships based on Bayesian inference (BI) and maximum likelihood (ML) analyses. Branches with less than 0.95 Bayesian probability support are collapsed. Asterisks indicate branches with less than 75% maximum likelihood bootstrap support, all other nodes have maximum likelihood support values greater than 75% and Bayesian probability support values greater than 0.95. Colored boxes designate orders: Blue = Dendrochirotida; Orange = Dactylochirotida; Green = Aspidochirotida; Red = Molpadida; Purple = Elasipodida; Yellow = Apodida. Taxon designations are from Pawson and Fell (1965).

Deimatidae and is discussed in the paragraphs below. The second elasipodan clade (with members from Laetmogonidae, Psychropotidae, Elpidiidae, and Pelagothuriidae) was sister to the holothuroids, excluding Apodida (Figure 10, Clade II). Within this group Laetmogonidae was a well-supported sister group to Psychropotidae in the ML and BI analyses. Elpidiidae was sister to the clade comprising Laetmogonidae and Psychropotidae in the ML and BI analyses. The position of Pelagothuriidae was poorly supported. Pelagothuriidae was sister to the group (Laetmogonidae+Psychropotidae) in the Concatenated trees (Appendix 2, Figure 23 A-D), the Concatenated HVRR trees (Appendix 2, Figure 25A-B), and the Concatenated HVRR COI (1&2) trees (Appendix 2, Figure 26A-D), but not the rest of the trees.

Surprisingly, a clade containing the aspidochirotan families Holothuriidae and Synallactidae (*Mesothuria* sp. Ludwig, 1894) was strongly supported in all of the ML and BI trees (Figure 10, Clade III). This third clade was sister to the rest of the holothuroids excluding Clades I and II. Two of the MP datasets, MP Concatenated and Concatenated HVRR, showed the synallactid *Mesothuria* sp. as a monotypic group between the elasipodan Clade II and the rest of the holothuroids (Appendix 2, Figures 22C-D, 24C-D). Arrangement at the genus level varied within this clade (Figure 9). In the BI analyses *Bohadschia koellikeri* Semper, 1868 always formed a clade with *Actinopyga mauritiana* Quoy and

Gaimard, 1834, but was variable in the ML and MP analyses. In all trees the support at the node of the two most derived taxa in the clade was low.

The nodes for the last four clades (Figure 10, Clades IV-VII) were poorly supported in all analyses and were thus represented as a polytomy in Figure 10.

The first clade in this four-clade polytomy included members from the rat-tailed Molpadiidae (Figure 10, Clade IV). The position of this enigmatic group was the least stable in almost every analysis and it was the primary impetus for the four-clade polytomy in Figure 10 (see below for further explanation).

The next clade in the polytomy included only genera from the Aspidochirotan family Synallactidae (Figure 10, Clade V). This clade of benthic to partially burrowing species was recovered with medium to high support by all tests and in all datasets. The arrangement of the genera within Clade V was also universal across datasets: *Molpadiodemas villosus* Théel, 1886 and *Paroriza prouhoi* Hérouard, 1902 were always sister to *cf Pseudostichopus* and *cf Synallactidae*.

The second largest clade in the polytomy included members from Aspidochirotida and, surprisingly, Elasipodida (Figure 10, Clade VI). As noted by the asterisk in Figure 10, the node for Clade VI was weakly supported by the ML analyses (49% - 75% ML bootstrap support), but strongly supported by the BI analyses. The MP support values were also low for the group (49% - 75% MP jackknife values). Still, the group was recovered in every analysis. Elasipodida

members of the group were from Deimatidae, and Aspidochirotida members of the group were from Synallactidae and Stichopodidae. As mentioned briefly above, the elasipodan Deimatidae, represented by *Deima validum* (now represented as *Deima validum validum* Théel, 1879) and *Oneirophanta setigera*, was the only elasipodan family represented in Clade VI; thus, the order Elasipodida was rendered polyphyletic. Synallactidae and Stichopodidae formed a clade sister to the deimatids. In this clade, the same family relationships were recovered for all datasets by both the BI and ML analyses with strong support except for the most derived stichopodid member (*Apostichopus californicus* Stimpson, 1857), which had low ML support values (<75% ML bootstrap support, denoted by asterisk in Figure 10). The MP analyses were not congruent with the BI and ML analyses in Clade VI (Figure 9). The MP concatenated dataset depicted the same relationship of the BI and ML tests with one exception; *Apostichopus californicus* formed a clade with *Stichopus vastus* Sluiter, 1887 and *Thelenota anax* Clark, 1921. All other MP datasets depicted the same relationships of the BI and ML tests with another exception: *Apostichopus californicus* formed a clade with *Bathyplotes cinctus* Koehler and Vaney, 1910, and the two other *cf Bathyplotes* species.

The last clade in the polytomy included members from Dendrochirotida and Dactylochirotida (Figure 10, Clade VII). This clade was recovered with very high support in all datasets by all analyses. Dactylochirotida, represented by one

member *Ypsilothuria bitentaculata* Ludwig, 1893, was nested between several Sclerodactylidae species and the clade ((Paracucumidae+Psolidae) (Placothuriidae+Heterothyonidae)) in all trees, thus rendering Dendrochirotida paraphyletic. The same genera-level organization was seen in all datasets by all analyses (Figure 9). Only two MP datasets differed. The one relationship difference that differentiated the two MP datasets (Concatenated and Concatenated COI (1&2)) from the BI and ML datasets was the position of *Afrocucumis Africana* Semper, 1867 as sister to the rest of the clade.

The position of these last four clades (Clades IV through VII) within the polytomy (Figure 10) remains largely unclear. One trend, however, stood out. All ML and MP tests appeared to have the same four-clade organization: a monophyletic Clade IV (Molpadida) was sister to Clade VI (Elasipodida+Aspidochirotida) with Clade V (Synallactidae) sister to the group (Clade IV+Clade VI) (Figure 9 A-B). The support for this arrangement, however, was low. Unlike the ML and MP analyses, the BI analyses of three of the four datasets revealed a paraphyletic Clade IV. In these trees, two molpadidan groups, instead of one (Clade IV), were sister to Clade VII (Dendrochirotida+Dactylochirotida) (Appendix 2, Figures 22B, 23B, and 25B). The support for this clade arrangement, however, was also low. The fourth BI analysis of the complete dataset (Concatenated HVRR) was different from the other three BI tests. The fourth BI test, like the MP and ML analyses, displayed

Clade IV (Molpadida) with Clade VI (Elasipodida+Aspidochirotida) and Clade V (Synallactidae), except the arrangement was presented as a polytomy (Figure 9C). This polytomy was determined to be a sister group to Clade VII (Dendrochirotida+Dactylochirotida) with high support.

Results from an approximately unbiased (AU) test showed that a ML tree (analyzed the same way as all other ML test in this study) constraining Clade IV (Molpadida) as a sister group to Clade VII (Dendrochirotida+Dactylochirotida) was significantly ($P < 0.05$) less likely (ln L -49880.9) than the unconstrained ML tree (ln L - 48912.2). This result was also supported by the likelihood values given by the raxmlGUI 0.93 (Stamatakis, 2006; Silvestro and Michalak, 2012) ML tests of both the Clade IV-constrained dataset (ln L - 50156.1) and the complete unconstrained dataset (ln L - 47048.8).

CHAPTER 4: DISCUSSION

This is the first phylogenetic study to estimate the higher-level relationships of Holothuroidea using a multi-gene molecular approach and to include taxa from difficult-to-access deep-sea and polar environments.

4.1 Current taxonomic uncertainty

Pawson and Fell (1965) remains the most widely accepted higher classification of Holothuroidea. These authors proposed three subclasses (Dendrochirotacea, Aspidochirotacea, and Apodacea) which they divided into six orders (Molpadida, Apodida, Aspidochirotida, Elasipodida, Dendrochirotida, and Dactylochirotida) (Figure 6I). Kerr and Kim (2001) using a morphology-based phylogeny of all 26 holothuroid families, found that two of Pawson and Fell's (1965) subclasses (Apodacea and Aspidochirotacea) and one of their orders (Dendrochirotida) was paraphyletic (Figure 6L). In 2005, Lacey et al. analyzed partial 18S rDNA sequences from eight families in four orders (Aspidochirotida, Elasipodida, Apodida, Dendrochirotida) and found Aspidochirotida paraphyletic (Figure 6M). Most recently, Smirnov (2012) considered these studies in a complete revision of the class (Figure 6P) that included many novel higher-level arrangements.

Below, I first compare the phylogenetic findings of this study with Pawson and Fell's (1965) taxonomic system. Then, I compare this study's findings to those of previous cladistic works and propose a novel cladistic nomenclature for them.

4.2 Systematics

4.2.1 Comparison to Pawson and Fell's (1965) system

Similar to recent phylogenetic analyses (Kerr and Kim, 2001; Lacey et al., 2005), this study found low support for the monophyly of two of the three subclasses proposed by Pawson and Fell (1965). First, Aspidochirotacea (Aspidochirotida+Elasipodida) is rendered paraphyletic by the presence of three clades comprised of members from four orders (Molpadida, Elasipodida, Dendrochirotida, and Dactylochirotida). Pawson and Fell (1965) defined Aspidochirotacea based on shield-shaped tentacles and conspicuous bilateral symmetry. Instead, this study indicates that these synapomorphies either arose at the base of a more inclusive clade or have evolved multiple times (Figure 10). Pawson and Fell's subclass Apodacea (Apodida+Molpadida) is also paraphyletic. Pawson and Fell (1965) defined this subclass for holothuroids lacking tubefeet. Pawson and Fell (1965) acknowledged, and most now agree, that the absence of tubefeet is a convergent trait in Apodida and Molpadida (Kerr, 2000; Kerr and

Kim, 2001; Lacey et al., 2005; Smirnov, 2012; this study). Finally, this study finds that Dendrochirotacea (Dendrochirotida+Dactylochirotida) comprises Dactylochirotida nested within Dendrochirotida, which renders the latter paraphyletic. Pawson and Fell (1965) diagnosed Dendrochirotacea via the presence of oral introverts and retractile muscles, which are well-supported synapomorphies in this study and in Kerr and Kim (2001).

As well, three of the orders proposed by Pawson and Fell (1965) – Aspidochirotida, Dendrochirotida, and Elasipodida – are recovered as non-monophyletic in the current study. The first of the three non-monophyletic orders, Aspidochirotida, is rendered paraphyletic across all analyses by the inclusion of members from Molpadida (Molpadiidae), Elasipodida (Deimatidae), and all of Dendrochirotida+Dactylochirotida. The paraphyly of Aspidochirotida has been proposed previously (Perrier, 1902; MacBride, 1906; Lacey et al., 2005); however, the arrangement revealed here appears new. Dendrochirotida is also non-monophyletic because the sole representative in this study (Ypsilothuriidae), of Pawson and Fell's (1965) Dactylochirotida, is nested within. Kerr and Kim (2001) agree and additionally found Dactylochirotida monophyletic. Smirnov (2012) also agrees, but felt Dactylochirotida was polyphyletic.

Elasipodida is polyphyletic, with one family, Deimatidae, consistently recovered within Aspidochirotida. The remaining elasipodan families formed a monophyletic group sister to the rest of the holothuroids except Apodida. Becher

(1909) hypothesized Deimatidae as a clade within Aspidochirotida very early on, but his idea was overlooked until Smirnov (2012) agreed that the "morphology of the calcareous ring and sclerites in the family Deimatidae [were] more similar to that in aspidochirotids [aspidochirotans] than in elasipodids [elasipodans]." In contrast to the rest of Pawson and Fell's (1965) orders, Apodida appears to be the only well supported monophyletic group. However, I cannot say whether the clade is monophyletic without including members of Myriotrochidae. Kerr and Kim's (2001) morphological analysis found Apodida monophyletic when including Myriotrochidae; however, Smirnov (2012) hypothesized that Myriotrochidae was sister to all the other apodans in his taxonomy. Lastly, Molpadida and Dactylochirotida might also be monophyletic, but greater sampling is needed.

4.2.2 Novel and recently hypothesized clades: Suggestions for nomenclature

Figure 10 summarizes this study's results according to the widely used Pawson and Fell (1965) taxonomic nomenclature. Figure 11 depicts the

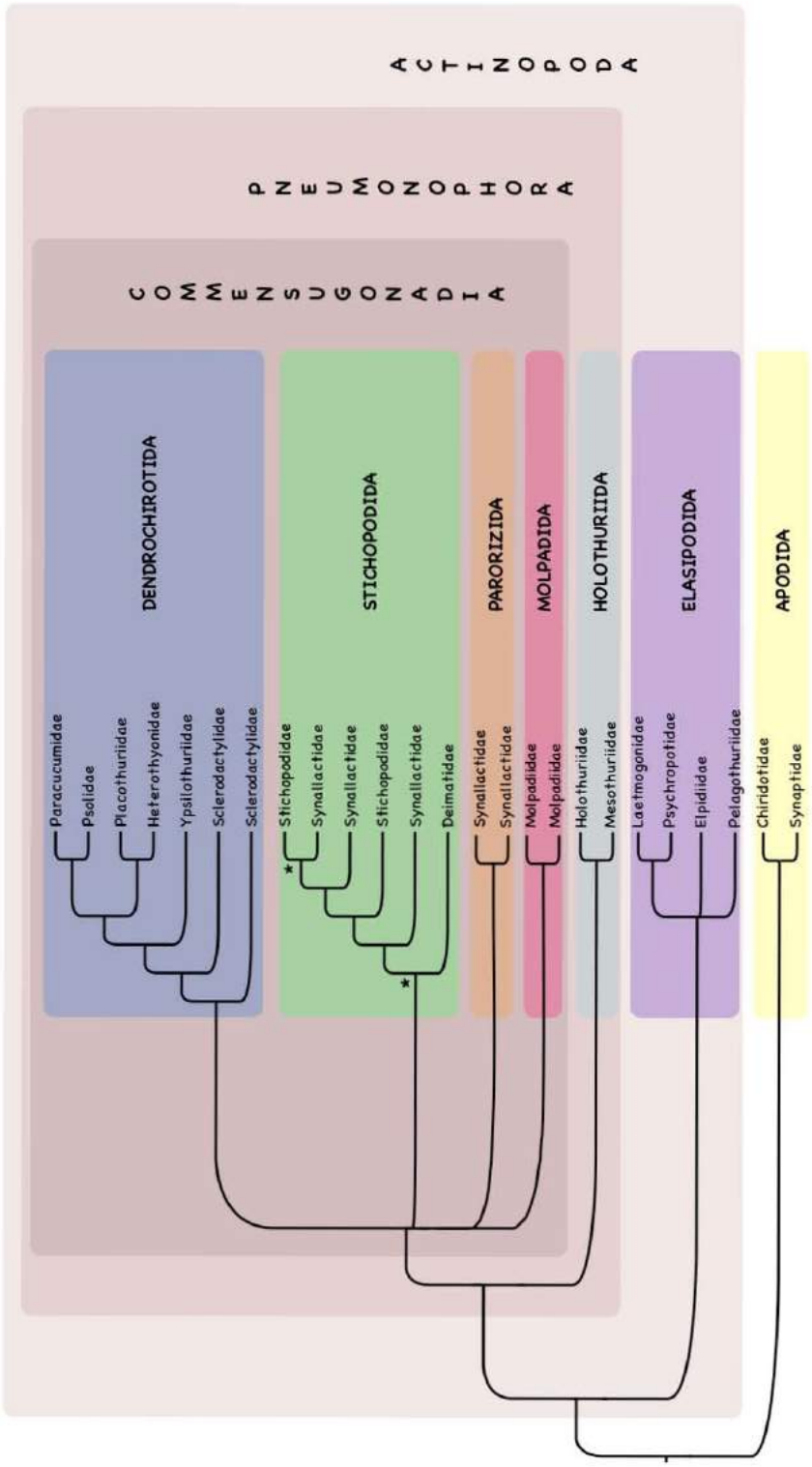
ACTINOPODA
PNEUMONOPHORA
COMMENSUGONADIA
DENDROCHIROTIDA
Paracucumidae
Psolidae
Placothuriidae
Heterothyonidae
Ypsilothuriidae
Sclerodactylidae
Sclerodactylidae
STICHOPODIDA
Stichopodidae
Synallactidae
Synallactidae
Stichopodidae
Synallactidae
Deimatidae
PARORIZIDA
Synallactidae
Synallactidae
MOLPADIDA
Molpadiidae
Molpadiidae
HOLOTHURIIDA
Holothuriidae
Mesothuriidae
ELASIPODIDA
Laetmogonidae
Psychropotidae
Elpidiidae
Pelagothuriidae
APODIDA
Chiridotidae
Synaptidae

Figure 11. Summary of holothuroid relationships based on BI and ML analyses with the clade and group names proposed in this study. The tree is taken from the summary tree in Figure 10, of which the large clade names have been modified and the colors have been re-defined. To compare the new clade and group names listed here to the old taxonomic names (those of Pawson and Fell (1965)), simply compare the branches of the two trees. Parorizida and Molpadida differ from Figure 10 in that they are divided into two groups. This was done to better display groups that might warrant renaming in the future. Asterisks (*) indicate branches with less than 75% maximum likelihood bootstrap support, all other nodes have maximum likelihood support values greater than 75% and Bayesian probability support values greater than 0.95.

results using the proposed cladistic nomenclature. Some of these clade names, such as Holothuriida are new, while others, such as Pneumonophora Selenka, 1867, have been resurrected.

The current study recovered three large clades (Pneumonophora, Aspidochirotida, and Commensugonadia) that appear to be united by several morphological apomorphies. Recent phylogenetic studies (Littlewood et al., 1997; Kerr and Kim, 2001; Lacey et al., 2005) mirror even the earliest taxonomic accounts (Müller, 1850; Selenka, 1867; Semper, 1868) in supporting a division of Holothuroidea into groups with and without respiratory trees. This study also recovered a lunged clade that is equivalent to Smirnov's (2012) subclass Holothuriacea, but here designated Pneumonophora (after Selenka, 1867).[7] This clade (of subclades Dendrochirotida, Stichopodida, Parorizida, Molpadida, and Holothuriida) lies above a grade without respiratory trees (Apodida and Elasipodida). The clades Pneumonophora and Elasipodida together form the clade Actinopoda (after Ludwig's system, 1889-1892).[8] This clade appears subtended by shield-shaped tentacles and extensions (tubefeet and tentacles) from the

[7] Jaeger (1833) was the first to consider the presence or absence of respiratory trees in his classification; however, Jaeger divided the class into three groups based on respiratory tree presence as well as body morphology and the position of tubefeet. Müeller (1850) was the first to weight the presence or absence of respiratory trees greater than any other morphological character, but his classifications did not follow the laws of common descent and could not be defended phylogenetically (Samyn, 2003).

[8] Ludwig (1889-1892), in his system of the class, divided Holothuroidea into two orders Actinopoda and Paractinopoda, which he based on the morphology of the ambulacral system. Actinopoda included representatives from the families Aspidochirotae (Aspidochirotida), Elasipoda (Elasipodida), Dendrochirotae (Dendrochirotida), and Molpadiidae (Molpadida). Paractinopoda included representatives from one family Synaptidae (Apodida). Interestingly, Ludwig's (1891) phylogeny (one of the first for the class) is not congruent with his system. For example, in his phylogeny Paractinopoda is included in with molpadiids (Molpadida) and dendrochirotids (Dendrochirotida) in Dendrochirotenstamm.

ambulacral system, although these characters have subsequently undergone many parallel reversals. Lastly, recent work by Solís-Marín (2003) and Smirnov (2012) suggested a group of holothuroids with gonads on one side of the dorsal mesentery. This study shows a clear split between a clade with gonads to the left of the dorsal mesentery (Holothuriida) and a large clade with gonads on both sides of the dorsal mesentery, Commensugonadia (Molpadida, Parorizida, Stichopodida, and Dendrochirotida).

In contrast to the clear apomorphies that unite the larger holothuroid clades, the morphological traits defining their subclades are less obvious. As proposed by multiple authors (Semper, 1868; MacBride, 1906; Becher, 1909; Cuénot, 1948; Haude, 1992; Littlewood et al., 1997; Kerr, 2000; Kerr and Kim, 2001; Lacey et al., 2005; Reich, 2010; Smirnov, 2012), Apodida appears monophyletic and sister to the rest of Holothuroidea (Figure 11, in yellow). It was thought early on that within Apodida, Synaptidae was most closely related to Chiridotidae (Östergren, 1907; Frizzel and Exline, 1966), and currently there is morphological (Smirnov, 1998; Kerr and Kim, 2001) and fossil (Gilliland, 1993) evidence to support this idea. In the current study, Chiridotidae appears monophyletic within Apodida. However, because there was only one representative from Synaptidae and none from Myriotrochidae, their arrangement within Apodida and the monophyly of Chiridotidae remain uncertain.

Sister to Apodida is Pneumonophora, within which most elasipodans form a basal subclade (Figure 11, in purple). In this study this group is comprised of all elasipodan families excluding Deimatidae. Taxonomic relationships among the elasipodan families have varied dramatically over the years (Théel, 1882; Ludwig, 1891; Haeckel, 1896; Perrier, 1902; MacBride, 1906; Östergren, 1907; Becher, 1909; and Cuénot, 1948).[9] Most recently Smirnov (2012) removed the family Deimatidae from Elasipodida and placed it in Synallactidae on the basis of calcareous ring shape, ossicle morphology, and phylogenetic analyses (Solís-Marín, 2003).

In agreement with Smirnov (2012), this analysis recovered two evolutionarily disparate clades of elasipodans: the clade Elasipodida containing exemplars from Psychropotidae, Laetmogonidae, Elpidiidae and Pelagothuriidae, plus the distant clade Deimatidae (Figure 11). Within the clade Elasipodida, Psychropotidae and Laetmogonidae formed a clade in most analyses that was sister to either Elpidiidae or Pelagothuriidae, rendering Hansen's (1975) subclass, Psychropotina, paraphyletic. The evolutionary position of Pelagothuriidae has

[9] Théel (1882) originally separated his order Elasipoda into a polytomy of three families: Elpidiidae, Deimatidae, and Psychropotidae. Ludwig (1891) and later Haeckel (1896) followed this division; however, Haeckel placed his family Dehnatida (Deimatidae) as sister to Psychropotida (Psychropotidae) and placed Pelagothuria (Pelagothuriidae in part) distantly within Synaptonia (Apodida). Thus began a trend of scattered elasipodan members across taxonomic trees (Figure 6C-G); Haeckel (1896), Perrier (1902), MacBride (1906), Östergren (1907), and Becher (1909) all had different ideas of where elasipodan families and genera were positioned with respect to the rest of the holothuroids. The trend came to halt when Cuénot (1948), declared that Elasipodes (Elasipodida) were primitive compared to the water-lung holothurians (those with respiratory trees) and, thus, evolved separately from the rest (Figure 6H). In 1975, Hansen, after evaluating many preserved (and some live) specimens, divided the order into two suborders Deimatina (Deimatidae+Laetmogonidae) and Psychropotina (Psychropotidae+Elpidiidae).

long been debated (Haeckel, 1896; Perrier, 1902; Östergren, 1907; Cuénot, 1948; Hansen, 1975; Kerr and Kim, 2001). Unfortunately, this study did not resolve the position of Pelagothuriidae within Elasipodida. However, it did reveal that Pelagothuriidae lies within a grade of other psychropotines below Laetmogonidae. It would be beneficial if the only other pelagothuriid, the morphologically distinct *Pelagothuria natatrix* Ludwig, 1893 (Figure 12) (the only wholly pelagic echinoderm), was included in future phylogenetic analyses.

In contrast to the other elasipodans, Deimatidae is nested within a clade of aspidochirotans, which renders Hansen's (1975) other subclass, Deimatina, polyphyletic. Furthermore, the results from this study are the first to support Smirnov's (2012) taxonomic separation of Deimatidae from Elasipodida (*contra* Kerr and Kim, 2001). They also support Smirnov's (2012) placement of Deimatidae within a largely aspidochirotan clade subtended by the presence of respiratory trees. Further, the current study places Deimatidae within Stichopodida (comprises members from the aspidochirotan families Stichopodidae and Synallactidae). Since I used the type species for Deimatidae, I retain the name Deimatidae for the clade. I also propose that the clade name Elasipodida remain with the larger clade of primarily psychropotine elasipodans because the clade likely holds all non-deimatid elasipodans.

Figure 12. *Pelagothuria natatrix* (photo taken from a video by Dr. Dave L. Pawson).

A recent study by Kerr and Kim (2001) recovered a clade of holothuroids united by the presence of respiratory trees. The current study also provides strong support for a respiratory-tree clade (Pneumonophora), as well as strong to medium support for five clades within it: Holothuriida, Parorizida, Stichopodida, Dendrochirotida, and Molpadida (Figure 11).

Holothuriida is strongly supported as sister to the other clades in Pneumonophora (Figure 11, in light blue). Holothuriida holds members from Synallactidae (as *Mesothuria*) and Holothuriidae (as *Bohadschia*, *Holothuria*, and *Actinopyga*) with *Mesothuria* sister to the clade of holothuriids. Becher (1909) hypothesized a similar branch order in his evolutionary tree (Figure 6G). Using a phylogenetic approach, Solís-Marín (2003) also noted the distance of *Mesothuria* (as well as *Zygothuria* Perrier, 1898) from the rest of the synallactids. He found that Synallactidae was broken into '"Mesothuriidae,"' a clade with gonads in a single tuft, and a clade of all other synallactids possessing paired gonads. Based on this, Smirnov (2012) created the taxonomic family Mesothuriidae, which he placed in his taxonomic order Aspidochirotida (Figure 6P). This study recovered a clade in which Holothuriidae is sister to *Mesothuria* sp., here designated Holothuriida.

Sister to Holothuriida is the large clade Commensugonadia consisting of a polytomy of four clades Parorizida, Stichopodida, Dendrochirotida, and Molpadida (Figure 11). Solís-Marín (2003) found Synallactidae to consist of two

deeply divergent basal subclades. The current study also found two primarily synallactid clades within Commensugonadia roughly corresponding to Solís-Marín's division. The first, here designated Parorizida (Figure 11, in orange), corresponds to a group potentially typified by a unique secondary chemistry (Silchenko et. al., 2004; Kalinin et al., 2005) and shared morphological characters. O'Loughlin and Ahearn (2005) defined a "pygal-furrowed" synallactid group containing *Molpadiodemas* and *Pseudostichopus* as one lacking body wall ossicles and possessing a pygal (posterior) furrow. The current study extends this description to also include *Paroriza* in the clade Parorizida.

The remaining synallactid exemplars were recovered in a second clade, here designated Stichopodida (Figure 11, in green). This clade consists of six well-supported subclades that additionally include taxa from Stichopodidae, Synallactidae, and Deimatidae. It is currently unclear what morphological synapomorphies might unite this clade, although most species reside in the deep-sea and are epibenthic. The stichopodid exemplars derived positions within this clade renders the family Synallactidae paraphyletic as speculated previously (Kerr and Kim, 2001; Solís-Marín, 2003; Smirnov, 2012). The two synallactid clades (Parorizida and Stichopodida) recovered here support Smirnov's (2012) speculation that Synallactidae be divided into two subfamilies, respectively, "Pseudostichopodinae" and "Synallactinae." If this is the case, another potential

taxonomic implication of this study is that at least some stichopodids would be reassigned to the latter subfamily.

Dendrochirotida is likely the largest subclade within the paired-gonad clade, Commensugonadia (Figure 11, in dark blue). The current study found that a member of the order Dactylochirotida, *Ypsilothuria bitentaculata* (Ypsilothuriidae), was nested within this clade, therefore rendering the order Dendrochirotida paraphyletic. Pawson and Fell (1965) distinguished the order Dactylochirotida via unique tentacle and ossicle morphology, clearly derived characters in the clade Dendrochirotida. Nevertheless, all members of this clade possess a character unique to Holothuroidea, the pharyngeal introvert. For this reason, Smirnov (2012) considered all dactylochirotes, albeit with considerable family-level rearrangement, within his conception of the order Dendrochirotida. Unfortunately, I cannot say at this time whether or not the elusive Dactylochirotida comprises a monophyletic group within Dendrochirotida. If so, the name for such a clade might be Dactylochirotina.

The current study includes only a few dendrochirote representatives from six taxonomic families. Thus, it is difficult for me to say with certainty how all of the families are related to each other. In 2001 Kerr and Kim recovered a multi-family 'testaceous' clade (those with large imbricating plates) that inserted above a grade of 'soft-bodied' families. The current study also recovers this division, but

with low support in almost all analyses (Figure 9A-B). Future studies sampling "soft-bodied" taxa (e.g., from Cucumariidae) should resolve this debate.

The last clade within the Commensugonadia is Molpadida (Figure 11, in red). In the past, taxonomists have grouped molpadidans and apodans together because they both lacked tubefeet (Brandt, 1835; Burmeister, 1837, Bronn, 1860; Théel, 1886; Perrier, 1902; Pawson and Fell, 1965). Using a morphological phylogenetic analysis, Kerr and Kim (2001) found Molpadida sister to Dendrochirotida, a relationship first proposed by other taxonomists (Ludwig, 1891; Ludwig, 1889-1892; Haeckel, 1896; MacBride, 1906; Clark, 1910). The current study finds the clade Molpadida well outside Apodida and within a polytomy of Dendrochirotida, Parorizida, and Stichopodida (Figure 11). It appears that the loss of tubefeet in Holothuroidea is an evolutionarily labile trait, one that was probably repeatedly lost when benthic holothurians switched to an infaunal lifestyle. Currently, few synapomorphies have been hypothesized that link Molpadida's position as either sister to Dendrochirotida, or nested within the Stichopodida+Parorizida clade. Smirnov (2012) discusses a character that unites his orders Dendrochirotida and Molpadida, the development of the tentacles and their contact with the radial ambulacral canals. It might also be possible that the fused calcareous ring plates of Molpadida unite the two groups (M. Reich, pers. comm). Contrary to these two hypotheses is the idea that a clade of Dendrochirotida and Molpadida is not preferred over a resolution of a

Molpadida+Stichopodida+Parorizida group via an approximately unbiased test for branching order (constrained (Dendrochirotida+Molpadida) = ln L -49880.9, unconstrained = ln L - 48912.2). Since only one family from Molpadida (Molpadiidae) is represented in this study, I propose that the name remain.

4.3 Conclusions

The results of the current study complement those of recent molecular (Lacey et al., 2005) and morphological (Kerr and Kim, 2001) cladistic analyses, as well as taxonomic work incorporating these findings (Smirnov, 2012). However, this study also reveals that a further large-scale systematic revision of Holothuroidea is necessary. Contrary to all recent analyses, the majority of extant holothuroids appear to fall into three large nested clades (Aspidochirotida, Pneumonophora, and Commensugonadia), which are further divided into seven smaller clades (Apodida, Elasipodida, Holothuriida, Molpadida, Parorizida, Stichopodida, and Dendrochirotida). Although there is strong support for most of the seven smaller clades, low support for a few (Molpadida, Stichopodida, and Parorizida) illustrates the amount of research still necessary. Fortunately, advances in next-generation sequencing methods now allow for the fast and relatively easy processing of more than 100 genes at one time (Ozsolak and Patrice, 2010; Liang et al., 2013). Future molecular phylogenetic studies that

utilize this technology and incorporate more taxa might resolve many of the remaining higher-order Holothuroidea polytomies within the Holothuroidea. Molecular-clock analyses are needed to estimate dates of divergences, and would lead to inferences about the pace of past radiation events. Morphological traits should also be mapped to provide insight about the evolution of life history and ecology within the class. Interestingly, like many echinoderm classes, holothuroids appear to have re-acquired traits, such as large multi-layered plate ossicles, simple tentacles, and the absence of tubefeet, numerous times over their evolutionary history. Although it is apparent how some of these traits evolved over the holothuroid tree, the evolution of many others remains unclear. Future studies that include multiple character types, such as fossil evidence, should resolve these uncertainties.

LITERATURE CITED

Ababneh, F., Jermiin, L., Ma, C., Robinson, J., 2006. Matched-pairs tests of homogeneity with applications to homologous nucleotide sequences. Bioinformatics. 22, 1225-1231.

Ahmed, M.I., Lawrence, A.J., 2007. The status of commercial sea cucumbers from Egypt's northern Red Sea Coast. SPC Beche-de-mer Inf. Bull. 26, 14-18.

Alaska Department of Fish and Game, 2013. Red Sea Cucumber (*Parastichopus californicus).* <http://www.adfg.alaska.gov/index.cfm?adfg=%20redsea cucumber.uses>.

Alcock, N., 2013. Shedding new light on the humble sea cucumber. <http://www.niwa.co.nz/aquatic-biodiversity-and-biosecurity/ update/issue-03-2003/shedding-new-light-on-the-humble-sea-cucumber>.

Arndt, A., Marquez, C., Lambert, P., and Smith, M., 1996. Molecular Phylogeny of Eastern Pacific Sea Cucumbers (Echinodermata: Holothuroidea) Based on Mitochondrial DNA Sequence. Mol. Phylo. Evol. 6, 425-437.

Bakus, G. J., 1973. The biology and ecology of tropical holothurians, In: Jones, O.A., Endean, R. (Eds), Biology and Geology of Coral Reefs. Volume 2 Biology 1. Academic Press London pp., 325-367.

Baldauf, S.L., Roger, A.J., Wenk-Siefert, I., Doolittle, W.F., 2000. A kingdom-level phylogeny of eukaryotes based on combined protein data. Sci. 290, 972-977.

Becher, S., 1909. Die Stammesgeschichte der Seewalzen, Ergebnisse und Fortschritte der Zoologie. 1, 403–490.

Bernhard, D., Stechmann, A., Foissner, W., Ammermann, D., 2001. Phylogenetic relationships within the class Spirotrichea. Mol. Phylo. Evol. 21(1), 86-92.

Bouchenak-Khelladi, Y., Salamin, N., Savolainen, V., Forest, F., Van der Bank, M., Chase, M.W., Hodkinson, T.R., 2008. Large multi-gene phylogenetic trees of grasses (Poaceae): Progress towards complete tribal and generic level sampling. Mol. Phylo. Evol. 47, 488-505.

Brandt, J.F., 1835. Prodromus descriptionis animalium ab H. Mertensio in orbis terrarium circumnavigatione observatorum, Petropoli: Sumptibus Academiae.

Bronn, H.G., 1860. Die Klassen und Ordnungen der Strahlenthiere (Actinozoa): wissenschaftlich dargestellt in Wort und Bild. Leipzig und Heidelberg: C.F. Winter'sche Verlagshandlung, Leipzig.

Bruckner, A.W., 2005. The recent status of sea cucumber fisheries in the continental United States of America. SPC Beche-de-mer Inf. Bull. 22, 39-46.

Burmeister, H., 1837. Handbuch der naturgeschichte. Zweite Abt. Zoologie, Theod. Chr. Friedr. Gnelin, Berlin.

Byrne, M., Rowe, F., Uthicke, S., 2010. Molecular taxonomy, phylogeny and evolution in the family Stichopodidae (Aspidochirotida: Holothuroidea) based on COI and 16S mitochondrial DNA. Mol. Phylo. Evol. 56, 1068-1081.

Caldeira, K., Wickett, M.E. 2003. Anthropogenic carbon and ocean pH. Nature. 425, 365.

Christiansen, B., Thiel, H., 1992. Deep-Sea Epibenthic megafauna of the Northeast Atlantic: Abundance and biomass at three mid-oceanic locations estimated from photographic transects. Deep-Sea Food Chains and the Global Carbon Cycle. 360, 125-138.

Clark, H.L., 1910. The development of an apodous holothurian (*Chiridota rotifer*). J. Exp. Zool. 9, 497-516.

Clark, A.M., Rowe, F.W.E., 1971. Monograph of shallow-water Indo-West Pacific echinoderms. Trustees of the British Museum (Natural History), London.

Colgan, D.J., McLauchlan, A., Wilson, GDF, Livingston, S.P., Edgecombe, G.D., Macaranas, J., Cassis, G., Gray, M.R., 1998. Histone H3 and U2 snRNA DNA sequences and arthropod molecular evolution. Aus. J. Zool. 46, 419-437.

Conand, C., 1989. Les holothuries aspidochirotes du lagon de Nouvelle-Caledonie: biologie, écologie et exploitation. Ph.D Thesis, Université de Bretagne Occidentale, Brest.

Conand, C., 1996. Asexual reproduction by fission in *Holothuria atra*: Variability of some parameters in populations from the tropical Indo-Pacific. Oceanologica Acta. 19, 209-216.

Conand, C., Byrne, M., 1993. A review of recent developments in the world sea cucumber fisheries. Marine Fisheries Review 55, 1–13.

Conand, C., Galet-Lalande, N., Randriamiarana, H., Razafintseheno, G., de San, M., 1997. Sea cucumbers in Madagascar: difficulties in the fishery and sustainable management. SPC Beche-de-mer Inf. Bull. 9, 4-5.

Coppard, S.E., Alvvarado, J.J., 2013. Echinoderm diversity in Panama: 144 years of research across the isthmus, In: Alvarado, J.J., Solís-Marín, F.A. (Eds.), Echinoderm Research and Diversity in Latin America. Springer., Heidelberg, pp. 107-144.

Cuénot, L., 1948. Anatomie, Éthologie et systématique des echinodermes, In: Grassé, P., (Ed), Traité de zoologie, vol 11. Masson, Paris. pp. 3-272.

Cuénot, L., 1891. Études morphologiques sur les Echinodermes. Archives de Biol. 11, 313–680, pl. 24–31.

Cutress, B.M., 1996. Changes in dermal ossicles during somatic growth in Caribbean littoral sea cucumbers (Echinoidea [sic]: Holothuroidea: Aspidochirotida). Bull. Mar. Sci. 58, 44-116.

Darriba, D., Taboada, G.L., Doallo, R., Posada, D., 2012. jModelTest 2: more models, new heuristics and parallel computing. Nature Methods. 9, 772.

Darwin, C., 1859. On the origin of species, John Murray, London.

Deichmann, E., 1930. The holothurians of the western part of the Atlantic Ocean. Bull. Mus. Comp. Zool. Harv. 71(3), 43–226.

Felsenstein, J., 1978. Cases in which parsimony and compatibility methods will be positively misleading. Sys. Zoo. 27 (4), 401-410.

Ekman, S., 1926. Systematisch-phylogenetische Studien über Elasipoden und Aspidochiroten. Zool. Jb. (Anat.). 47(4), 429-540.

Frizzell, D., Exline, H., 1966. Holothuroidea – fossil record, In: Moore, R.C. (Ed.), Treatise on Invertebrate Paleontology. Part U, Echinodermata 3(2). Geological Society of America, Lawrence, Kansas, pp. U646-U672.

Fulton, T.L., Strobeck, C., 2006. Molecular phylogeny of the Arctoidea (Carnivora): Effect of missing data on supertree and supermatrix analyses of multiple gene data sets. Mol. Phylo. Evol. 41, 165-181.

Gallo, N., 2015. Challenger Deep 2013. Unpublished. Ph.D dissertation, Scripps Institution of Oceanography.

Gilliland, P.M., 1993. The skeletal morphology, systematics and evolutionary history of holothurians. Palaeontological Assoc. 47, 1-147.

Giribet, G., Carranza, S., Baguna, J., Riutort, M., Ribera, C., 1996. First molecular evidence for the existence of a Tardigrade + Arthropoda clade. Mol. Biol. Evol. 13, 76-84.

Gouy, M., Guindon, S., Gascuel, O., 2010. SeaView version 4: a multiplatform graphical user interface for sequence alignment and phylogenetic tree building. Mol. Biol. Evol. 27, 221-224.

Gray, J.E., 1853. Description of *Rhopalodina*, a new form of Echinodermata. J. Nat. Hist. 11 (64), 301-302.

Grube, A.E., 1840. Actinien, Echinodermen und Wurmer des Adriatischen – und Mitteelmeers. J. H. Bon, Konigsberg.

Guindon, S., Gascuel, O., 2003. A simple, fast and accurate method to estimate large phylogenies by maximum-likelihood. Syst. Biol. 52, 696-704.

Haeckel, E., 1896. Systematische Phylogenie der Wirbellosen Thiere (Invertebrata). Zweiter Theil. Des Entwurfs einer systematischen Stammesgeschichte. Georg Reimer, Berlin.

Hamel, J., Mercier, A., 2000. Cuvierian tubules in tropical holothurians: usefulness and efficiency as a defense mechanism. Mar. Fresh. Behav. Physiol. 33, 115-139.

Hansen, B., 1975. Systematics and biology of the deep-sea holothurians. Part 1. Elasipoda. Galathea Report. 13, 1-262.

Hansen, B. & Madsen, F.J., 1956. On two bathypelagic holothurians from the South China Sea. *Galatheathuria* n.g. *aspera* (Théel) and *Enypniastes globosa* n. sp.. Galathea Report. 2, 55-5.

Hasbún, C.R., Lawrence, A.J., 2002. An annotated description of shallow water holothurians (Echinodermata: Holothuroidea) from Cayos Cochinos, Honduras. Rev. Biol. Trop. 50, 669-678.

Haude, R., 1992. Fossil holothurians: ossicle aggregates as 'good' species, In: Scalera-Liaci, L., Canicatti, C., (Eds.), Echinoderm Research. Balkema, Rotterdam, pp. 29–33.

Hillis, D.M., Dixon, M.T., 1991. Ribosomal DNA: Molecular evolution and phylogenetic inference. Quart. Rev. Biol. 66, 411-453.

Honey-Escandón, M., Laguarda-Figueras, A., Solís-Marín, F., 2012. Molecular phylogeny of the subgenus *Holothuria (Selenkothuria)* Deichmann, 1958 (Holothuroidea: Aspidochirotida). Zool. J. Linn. Soc. 165, 109-120.

Hughes, S.J.M., Ruhl, H.A., Hawkins, L.E., Hauton, C., Boorman, B., Billett, D.S.M., 2011. Deep-sea echinoderm oxygen consumption rates and an interclass comparison of metabolic rates in Asteroidea, Crinoidea, Echinoidea, Holothuroidea and Ophiuroidea. J. Exp. Biol. 214, 2512-2521.

Huxley, T.H., 1878. Anatomy of Invertebrated Animals. Murray, London.

Janies, D.A., Voight, J.R., Daly, M., 2011. Echinoderm phylogeny including *Xyloplax*, a progenetic asteroid. Syst. Biol. 60(4), 420-438.

Jayaswal, V., Jermiin, L.S., Poladian, L, Robinson, J., 2011. Two stationary, non-homogeneous Markov models of nucleotide sequence evolution. Syst. Biol. 60, 74-86.

Jaeger, G.F., 1833. De Holothuriis. Stuttgardiensis, Turici.

Kalinin, V.I., Silchenko, A.S., Avilov, S.A., Stonik, V.A., Smirnov, A.V., 2005. Sea cucumber triterpene glycosides, the recent progress in structural elucidation and chemotaxonomy. Phytochem. Rev. 4(2-3), 221-236.

Kamarudin, K.R., Hashim, R., Usup, G., 2010. Phylogeny of sea cucumber (Echinodermata: Holothuroidea) as inferred from 16S mitochondrial rRNA gene sequence. Sains Malaysiana. 39, 209-218.

Katoh, K., Standley, D., 2013. MAFFT multiple sequence alignment software version 7: improvements in performance and usability. Mol. Biol. Evol. 30(4), 772-780.

Kearse, M., Moir, R., Wilson, A., Stones-Hava, S., Cheung, M., Sturrock, S., Buxton, S., Cooper, A., Markowitz, S., Duran, C., Thierer, T., Ashton, B., Mentjies, P., Drummond, A., 2012. Geneious Basic: an integrated and extendable desktop software platform for the organization and analysis of sequence data. Bioinformatics, 28(12), 1647-1649.

Kerr, A.M., Norris, D.R., Schupp, P.J., Meyer, K.D., Pitlik, T.J., 1992. Range Extensions of Echinoderms (Asteroidea, Echinoidea and Holothuroidea) to Guam, Mariana Islands. Micronesica. 25(2), 201-216.

Kerr, A., Kim, J., 1999. Bi-penta-bi-decaradial symmetry: a review of evolutionary and developmental trends in Holothuroidea (Echinodermata). J. Exp. Zool. 285, 93-103.

Kerr, A., 2000. Evolution and systematics of Holothuroidea (Echinodermata). Ph.D Thesis, Yale University.

Kerr, A., 2001. Phylogeny of the apodan holothurians (Echinodermata) inferred from morphology. Zool. J. Linn. Soc. 133, 53-62.

Kerr, A., 2000. Holothuroidea. Sea cucumbers. Version 01 December 2000. <http://tolweb.org/Holothuroidea/19240/2000.12.01>, In: The Tree of Life Web Project, <http://tolweb.org/>.

Kerr, A. and Kim, J., 2001. Phylogeny of Holothuroidea (Echinodermata) inferred from morphology. Zool. J. Linn. Soc. 133, 63-8.

Kim, S., 2013. Color, confusion, and crossing: resolution of species problems in *Bohadschia* (Echinodermata: Holothuroidea). Zool. J. Linn. Soc. 168, 81-97.

Lacey, K., McCormack, G., Keegan, B., Powell, R., 2005. Phylogenetic relationships within the class Holothuroidea, inferred from 18S rRNA gene data. Mar. Biol. 147, 1149-1154.

Lambert, P., 1997. Sea cucumbers of British Columbia. Southeast Alaska and Puget Sound. UBC Press, Vancouver.

Liang, D., Xing Shen, X., Zhang, P., 2013. One thousand two hundred and ninety nuclear genes from a genome-wide survey support lungfishes as the sister group of tetrapods. Mol. Biol. Evo. 30(8), 1803-1807.

Littlewood, D.T., Smith, A.B., Clough, K.A., Emson, F.L., 1997. The interrelationships of the echinoderm classes: morphological and molecular evidence. Biol. J. Linn. Soc. 61, 409-438.

Ludwig, H., 1889-1892. Echinodermen. Die Seewalzen, In: Bronn, H.G. (Ed.), Bronn's Klassen und Ordnungen des Their Reichs., C. F. Winter'sche Verlagshandlung, Leipzig, pp. 1-17.

Ludwig, H., 1891. *Ankyroderma musculus* (Risso), eine Molpadiide des Mittelmeeres, nebst Bemerkungen zur Phylogenie und Systematik der Holothurien. Zeitschrift für wissenschaftliche Zool. 51, 569–612.

Ludwig, H., 1894. The Holothuroidea. Reports on an exploration off the west coast of Mexico, Central and South America, and off the Galapagos Islands, in charge of Alexander Agassiz, by the U.S. Fish Commission Steamer "Albatross," during 1891. XII. Mem. Mus. Comp. Zool. 17(3), 1-183.

MacBride, E.W., 1906. Echinodermata, In: Harmer, S.F., Shipley, A.E., (Eds.) The Cambridge Natural History, Vol. 1. MacMillan, London, pp. 425-623.

Maddison, W.P., Maddison, D.R., 2011. Mesquite: a modular system for evolutionary analysis. Version 2.75. <http://mesquiteproject.org>.

Massin, C., 1994. Ossicle variation in Antarctic dendrochirote holothurians (Echinodermata). Bulletin van het Koninklijk Belgish Instituut voor Natuurwetenschappen. Biologie. 64, 129-146.

Massin, C., Mercier, A., Hamel, J-F., 2000. Ossicle change in *Holothuria scabra* with a discussion of ossicle evolution within the Holothuriidae (Echinodermata). Acta Zool. 81, 77-91.

Máñez, K.S., Ferse, S.C.A. 2010. The history of Makassan trepang fishing and trade. PloS ONE. 5(6), 1-8.

Martínez, P.C., 2001. The Galápagos sea cucumber fishery: risk or an opportunity for conservation? SPC Beche-de-Mer Inf. Bull. 14, 22-23.

Miller, J.E., Pawson, D.L., 1990. Swimming sea cucumbers (Echinodermata: Holothuroidea): a survey, with analysis of swimming behavior in four bathyal species. Smith. Contrib. Mar. Sci. 35, 1–18.

Miller, M.A., Pfeiffer, W., Schwartz, T., 2010. Creating the CIPRES Science Gateway for inference of large phylogenetic trees, In: Proceedings of the Gateway Computing Environments Workshop (GCE), 14 Nov. 2010., New Orleans, Louisiana, pp. 1-8.

Mortensen, T.H., 1925. On a Small Collection of Echinoderms from the Antarctic Sea. Ark. Zool. 17A(31), 1–12.

Müller, J., 1850. Anatomische studien über die echinodermen. Archiv für Anatomie und Physiologie. 1850, 117-155.

Nadler, S.A., 1995. Advantages and disadvantages of molecular phylogenetics: A case study of ascaridoid nematodes. J. Nematology. 27, 423-432.

Ohta, S., 1985. Photographic observations of the swimming behavior of the deep-sea pelagothuriid holothurian *Enypniastes* (Elasipoda, Holothuroidea). J. Oceanographical Soc. Jap. 41, 121-133.

O'Loughlin, M.P., Alcock, N., 2000. The New Zealand Cucumariidae (Echinodermata, Holothuroidea). Mem. Mus. Vict. 58(1), 1-24.

O'Loughlin, M.P., Paulay, G., Davey, N., Michonneau, F., 2010a. The Antarctic region as a marine biodiversity hotspot for echinoderms: Diversity and diversification of sea cucumbers. Deep-Sea Res. II.

O'Loughlin, M.P., Vanden Spiegel, D., 2010b. A revision of Antarctic and some Indo-Pacific apodid sea cucumbers (Echinodermata: Holothuroidea: Apodida). Mem. Mus. Vict. 67, 61-95.

Östergren, H. 1907. Zur Phylogenie und Systematik der Seewalzen. Särtryck ur Zoologiska Studier Tillägnade Professor T. Tullberg, Almquist & Wiksells Buchdruckerei-Aktiengesellschaft, Upsala pp. 191-215.

Ozsolak, F., Milos, P.M., 2010. RNA sequencing: advances, challenges, and opportunities. Nature Reviews Genetics. 12, 87-98.

Palumbi, S.R., 1996. Nucleic acids II: The polymerase chain reaction, In: Hillis, D.M., Moritz, C., Mable, B.K. (Eds.), Molecular Systematics. Sinauer Associates, Sunderland, Massachusetts, pp. 205-247.

Parmentier, E., Vandewalle, P., 2005. Further insight on carapid – holothuroid relationships. Mar. Biol. 146, 455-465.

Pawson, D.L., Fell, H.B., 1965. A revised classification of the dendrochirote holothurians. Breviora. 214, 1-7.

Pawson, D.L., 1977. Marine flora and fauna of the Northeastern United States. Echinodermata: Holothuroidea. NOAA Tech. Report NMFS Circular 405. U.S. Department of Commerce, NOAA Nat. Mar. Fisheries Serv. Washington, D.C.

Pawson, D.L., 1982. Holothuroidea, In: Parker, S.P. (Ed.), Synopsis and classification of living organisms. McGraw-Hill, New York, pp. 813-818.

Pérezrul, M.D.H., Chávez, E.A., 2005. Optimum fishing strategies for *Isostichopus fuscus* (Echinodermata: Holothuroidea) in the Gulf of California, México. Rev. Biol. Trop. 53, 357-366.

Perrier, R., 1902. Holothuries, in Expédition scientifique du "Travailleur" et du "Talisman" pendant les années 1880, 1881, 1882, 1883. VI Cirrhipèdes, Némertiens, Opistobranches, Holothuries. Masson, Paris.

Pawson, D.L., 1982. Deep-sea echinoderms in the Tongue of the Ocean, Bahama Islands: a survey using the research submersible 'Alvin'. Mem. Aus. Mus. 16, 129-145.

Philippe, H., Snell, E.A., Bapteste, E., Lopez, P., Holland, P.W.H., Casane, D., 2014. Phylogenomics of eukaryotes: Impact of missing data on large alignments. Mol. Biol. Evol. 21(9), 1740-1752.

Purcell, S.W, Samyn, Y., Conand, C., 2012. Commercially important sea cucumbers of the world. FAO Species Catalogue for Fishery Purposes. No. 6. FAO, Rome.

Raff, R.A., Field, K.G., Ghiselin, M.T., Lane, D.J., Olsen, G.J., Pace, N.R., Parks, A.L., Parr, B.A., Raff, E.C., 1988. Molecular analysis of distant phylogenetic relationships in echinoderms, In: Paul, C.R.C., Smith, A.B. (Eds.), Echinoderm phylogeny and evolutionary biology. Current Geological Concepts 1. Oxford Science Publications and Liverpool Geological Society, Oxford, pp. 29-41.

Rambaut, A., Suchard, M.A., Xie, D., Drummond, A.J., 2013. Tracer v1.5. <http://beast.bio.ed.ac.uk/Tracer>.

Reich, M., 2010a. The early evolution and diversification of holothurians (Echinozoa), In: Harris, L.G., Böttger, S.A., Walker, C.W., Lesser, M.P., (Eds.), Echinoderms: Durham. Taylor & Francis Group, London, pp. 55-59.

Reich, M., 2010b. The oldest synallactid sea cucumber (Echinodermata: Holothuroidea: Aspidochirotida). Paläontologische Zeitschrift. 84, 541–546.

Rhoads, D.C., Young, D.K., 1971. Animal-sediment relations in Cape Cod Bay, Massachusetts II. Reworking by *Molpadia oolitica* (Holothuroidea). Mar. Biol. 11, 255-261.

Rouse, G.W., Jermiin, L.S., Wilson, N.G., Eeckhaut, I., Lanterbecq, D., Oji, T., Young, C.M., Browning, T., Cisternas, P., Helgen, L., Stuckey, M., Messing, C., 2013. Fixed, free, and fixed: The fickle phylogeny of extant Crinoidea (Echinodermata) and their Permian-Triassic origin. Mol. Phylogenet. Evol. 66(1), 161-181.

Ronquist, F., Huelsenbeck, J.P., 2003. MRBAYES 3: Bayesian phylogenetic inference under mixed models. Bioinfor. 19, 1572-1574.

Ruhl, H.A., 2007. Abundance and size distribution dynamics of abyssal epibenthic megafauna in the Northeast Pacific. Ecology. 88(5), 1250-1262.

Samyn, Y., 2003. Towards an understanding of the shallow-water holothuroid fauna (Echinodermata: Holothuroidea) of the western Indian Ocean: Ch.1. Vrije Universiteit Brussel, Brussels.

Samyn, Y., 2005. Phylogeny of *Labidodemas* and Holothuriiae (Holothuroidea: Aspidochirotida) as inferred from morphology. Zool. J. Linn. Soc. 144, 103-120.

Schoch, C.L., Crous, P.W., Groenewald, J.Z., Boehm, E.W.A., Burgess, T.I., de Gruyter, J., de Hoog, G.S., Dixon, L.J., Grube, M., Gueidan, C., Harada, Y., Hatakeyama, S., Hirayama, K., Hosoya, T., Huhndorf, S.M., Hyde, K.D., Jones, E.B.G., Kohlmeyer, J., Kruys, A., Li, Y.M., Lucking, R., Lumbsch, H.T., Marvanova, L., Mbatchou, J.S., McVay, A.H., Miller, A.N., Mugambi, G.K., Muggia, L., Nelsen, M.P., Nelson, P., Owensby, C.A., Phillips, A.J L., Phongpaichit, S., Pointing, S.B., Pujade-Renaud, V., Raja, H.A., Plata, E Rivas., Robbertse, B., Ruibal, C., Sakayaroj, J., Sano, T., Selbmann, L., Shearer, C.A., Shirouzu, T., Slippers, B., Suetrong, S., Tanaka, K., Volkmann-Kohlmeyer, B., Wingfield, M.J., Wood, A R., Woudenberg, J.H.C., Yonezawa, H., Zhang, Y., Spatafora, J.W., 2009. A class-wide phylogenetic assessment of *Dothideomycetes*. Studies in Mycol. 64, 1-15.

Seilacher, A., 1961. Holothurien im Hunsrückschiefer (Unter Devon), Notizblatt des hessischen Landesamtes fur Bodenforsch zu Wiesbaden. 89, 66–72.

Semon, R., 1888. Die Entwickelung der *Synapta digitata* und die Stammesgeschichte der Echinodermen. Jenaische Zeitchrift fur Naturwissenschaft. 22, 1-135.

Schneider, K., Silverman, J., Woolsey, E., Eriksson, H., Byrne, M., and Caldeira, K., 2011. Potential influence of sea cucumbers on coral reef CaCO3 budget: A case study at One Tree Reef. J. Geophysical. Res. 116, 1-6.

Selenka, E., 1867. Beitrage zur anatomie und systematik der holothurien. Zeitschrift fur wissenschaftliche zoologie. 17, 291-374.

Semper, D.C., 1868. Reisen im Archipel der Philippinen. II. Theil. Wissenschaftliche Resultate. Erster Band. Holothurien. Wihelm Engelmann, Leipzig.

Silchenko, A.S., Avilov, S.A., Kalinin, V.I., Kalinovsky, A.I., Stonik, V.A., Smirnov, A.V., 2004. Pseudostichoposide B – New triterpene glycoside with unprecedent type of sulfatation from the deep-water North-Pacific sea cucumber *Pseudostichopus trachus.* Nat. Prod. Res. 18(6), 565-570.

Silvestro, D., Michalak, I., 2012. RaxmlGUI: a graphical front-end for RAxML. Organism Diversity and Evolution. 12, 335-337.

Smiley, S., 1994. Holothuroidea, In: Harrison, F.W., Chia, F.S., (Eds.), Microscopic anatomy of invertebrates, vol.14: Echinodermata. Wiley-Liss, New York, pp. 401-471.

Smirnov, A.V., 1984. Notes on the system Holothuroidea. Zoologicheskii zhurnal. 63, 547-553.

Smirnov, A.V., 1998. On the classification of the apodid holothurians, In: Mooi, R., Telford, M. (Eds.), Echinoderms: Proceedings of the 9th International

Conference, San Francisco, California, USA, 1996. Rotterdam, Brookfield, pp. 393-395.

Smirnov, A.V., 2012. System of the Class Holothuroidea. Paleontological. J. 46, 793-832.

Smith. A,B.. 1997. Echinoderm larvae and phylogeny. Annual Review of Ecology and Systematics. 28, 219–241.

Solís-Marín, F.A., 2003. Systematics and Phylogeny of the Holothurian Family Synallactidae. Thesis, University of Southampton.

Solís-Marín, F.A., Hooker, Y., Laguarda, A., 2012. First record of swimming sea cucumber *Enypniastes eximia* Thèel, 1882 (Echinodermata: Holothuroidea) in Peruvian waters. Rev. Peru. Biol. 19(1), 95-96.

Solís-Marín, F.A., Billet, D.S.M., Preston, J., Rogers, A.D., 2004. Mitochondrial DNA sequence evidence supporting the recognition of a new North Atlantic *Pseudostichopus* species (Echinodermata: Holothuroidea). J. Mar. Biol. Ass. U.K. 84, 1077-1084.

Solomon, S., Qin, D., Maning, M., Marquis, M., Averyt, K., Tignor, M.M.B., Miller, H.L., 2007. Climate change 2007 – The physical science basis. Cambridge University Press, Cambridge.

Stamatakis, A., 2006. RAxML-VI-HPC: Maximum Likelihood-based Phylogenetic Analyses with Thousands of Taxa and Mixed Models. Bioinformatics. 22(21), 2688–2690.

Stamatakis, A., Hoover, P., Rougemont, J., 2008. A rapid bootstrap algorithm for the RAxML web servers. Syst. Biol. 57(5), 758-771.

Swofford, D. L., 2003. PAUP*. Phylogenetic Analysis Using Parsimony (*and Other Methods). Version 4. Sinauer Associates, Sunderland, Massachusetts.

Talavera, G., Castresana, J., 2007. Improvement of phylogenies after removing divergent and ambiguously aligned blocks from protein sequence alignments. Systematic Biol. 56, 564-577.

Tamura, K., Nei, M., 1993. Estimation of the number of nucleotide substitutions in the control region of mitochondrial DNA in humans and chimpanzees. Mol. Biol. Evol. 10, 512-526.

Thandar, A.S., 2001. The holothuroid family Rhopalodinidae – its composition, distribution, phylogeny and taxonomic status. African Zool. 36, 229-243.

Thandar, A.S., Arumugam, P., 2011. A new family within the holothuroid order Dactylochirotida with description of a new species from South Africa and comments on the dendrochirotid genus *Neoamphicyclus* Hickman, 1962 and the molpadid genus *Cherbonniera* Sibuet, 1974 (Echinodermata). Zootaxa. 2971, 40-48.

Théel, H., 1879. Preliminary report on the Holothuridea of the Exploring Voyage of H.M.S. Challenger under Professor Sir C. Wyville Thomson. I, Bihang Till K. Svenska Vetensk Akad. Handlingar. 5(19), 1-20.

Théel, H., 1882. Report on the Holothuroidea dredged by H.M.S. Challenger during the Years 1873 – 1876. Part I. Report on the Scientific Results of the voyage of H.M.S. Challenger during the years 1873-1876. Zool. 14(39), 1-290.

Théel, H., 1886. Report on the Holothuroidea dredged by H.M.S. Challenger during the Years 1873 – 1876. Part II. Report on the Scientific Results of the voyage of H.M.S. Challenger during the years 1873-1876. Zool. 14(39), 1-290.

Thuy, B., Gale, A.S., Kroh, A., Kucera, M., Numberger-Thuy, D.L., Reich, M., Stöhr, S., 2012. Ancient origin of the modern deep-sea fauna. PLoS ONE. 7(10): e46913.

Toral-Granda, V., 2008. Population status, fisheries and trade of sea cucumbers in Latin America and the Caribbean. In: Toral-Granda, V., Lovatelli, A., Vasconcellos, M. (Eds.), Sea Cucumbers: A Global Review of Fisheries and Trade. Fisheries and Aquaculture Technical Paper 516. Food and Agriculture Organization of the United Nations, Rome, pp. 231–253.

Uthicke, S., 1994. Distribution patterns and growth of two reef flat holothurians, *Holothuria atra* and *Stichopus chloronotus,* In: David, B., Guille, A., Feral, J.P., Roux, M. (Eds.), Echinoderms Through Time: Proceedings of the Eighth International Echinoderm Conference. Balkema, Rotterdam, pp. 569–576.

Uthicke, S., 2001a. Nutrient regeneration by abundant coral reef holothurians. J. Exp. Mar. Biol. Ecol. 265, 153-170.

Uthicke, S., 2001b. Interactions between sediment-feeders and microalgae on coral reefs: grazing losses versus production enhancement. Mar. Ecol. Prog. Ser. 210, 125-138.

Uthicke, S., O'Hara, T.D., Byrne, M., 2004. Species composition and molecular phylogeny of the Indo-Pacific teatfish (Echinodermata: Holothuroidea) beche-de-mer fishery. Mar. Freshwater Res. 55, 837-848.

Uthicke, S., Byrne, M., Conand, C., 2010. Genetic barcoding of commercial Bêche-de-mer species (Echinodermata: Holothuroidea). Mol. Eco. Res. 10, 634-646.

Uthicke, S., O'Hara, T.D., Byrne, M., 2004. Species composition and molecular phylogeny of the Indo-Pacific teatfish (Echinodermata: Holothuroidea) bêche-de-mer fishery. Mar. Freshwater Res. 55, 837-848.

Vaidya, G., Lohman, D. J., Meier, R., 2011. SequenceMatrix: concatenation software for the fast assembly of multi-gene datasets with character set and codon information. Cladistics. 27, 171-180.

Wada, H., Satoh, N., 1994. Phylogenetic relationships among extant classes of echinoderms, as inferred from sequences of 18S rDNA, coincide with relationships deduced from the fossil record. J. Mol. Evo. 38, 41-49.

Wiens, J.J., 2006. Missing data and the design of phylogenetic analyses. J. Bio. Inf. 39, 34-42.

Wolkenhauer, S., Uthicke, S., Burridge, C., Skewes, T., Pitcher, R., 2009. The ecological role of *Holothuria scabra* (Echinodermata: Holothuroidea) within subtropical seagrass beds. J. Mar. Biol. Ass. U.K. 90(2), 215-223.

Xia, X., Lemey, P., 2009. Assessing substitution saturation with DAMBE, In: Lemey, P., Salem, M., Vandamme, A.M. (Eds.), The Phylogenetic Handbook: A Practical Approach to DNA and Protein Phylogeny, second ed. Cambridge University Press, Cambridge, pp. 615–630.

Xia, X., Xie, Z., 2001. DAMBE: data analysis in molecular biology and evolution. J. Hered. 92, 371–373.

Xia, X., Xie, Z., Salemi, M., Chen, L., Wang, Y., 2003. An index of substitution saturation and its application. Mol. Phyl. Evol. 26, 1–7.

APPENDICES

Appendix 1. Maximum parsimony (MP), maximum likelihood (ML), and Bayesian inference (BI) trees for the nine individual gene alignments. *HVRR*: "highly variable regions removed" dataset. *COI (1&2)*: COI dataset with the 3rd codon position removed. *Note: the following taxon names were changed (names following "->" are the most recent identification). E5311 -> *Crucella scotiae,* E5296 – *Crucella scotiae,* AMK19 – *Paelopatides* sp, E4365 – Synallactidae, E5607 – *Synallactes* sp, E3566 – *Synallactes* cf *chuni,* AMK16 – *Molpadia arenicola*, SIO1 – *Molpadia arenicola*, E5295 – *Molpadia musculus*, E5300 – *Molpadia musculus*, E5609 – cf Elasipodida, and E5604 – *Chiridota* sp.

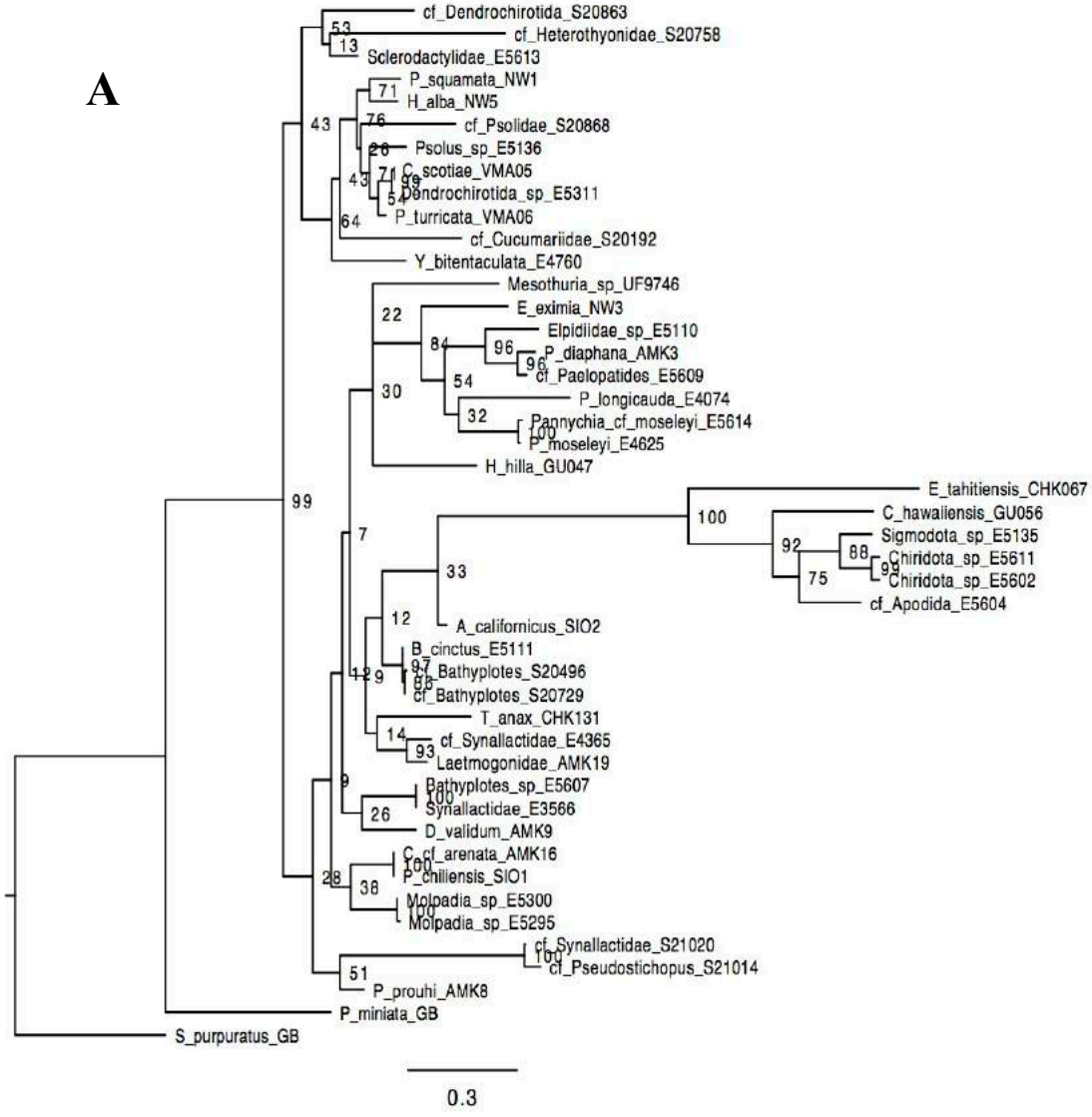

Appendix 1 continued.

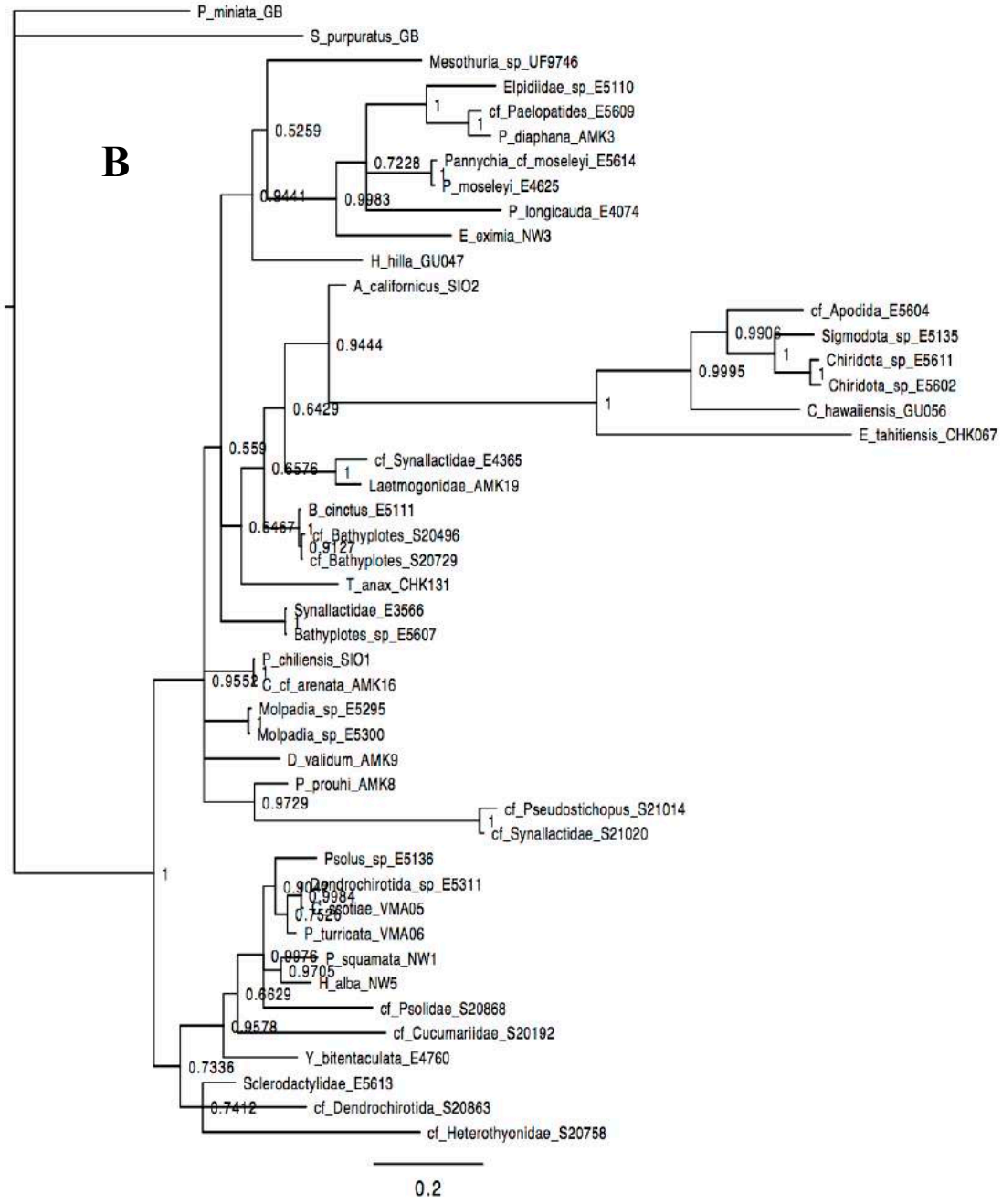

Appendix 1 continued.

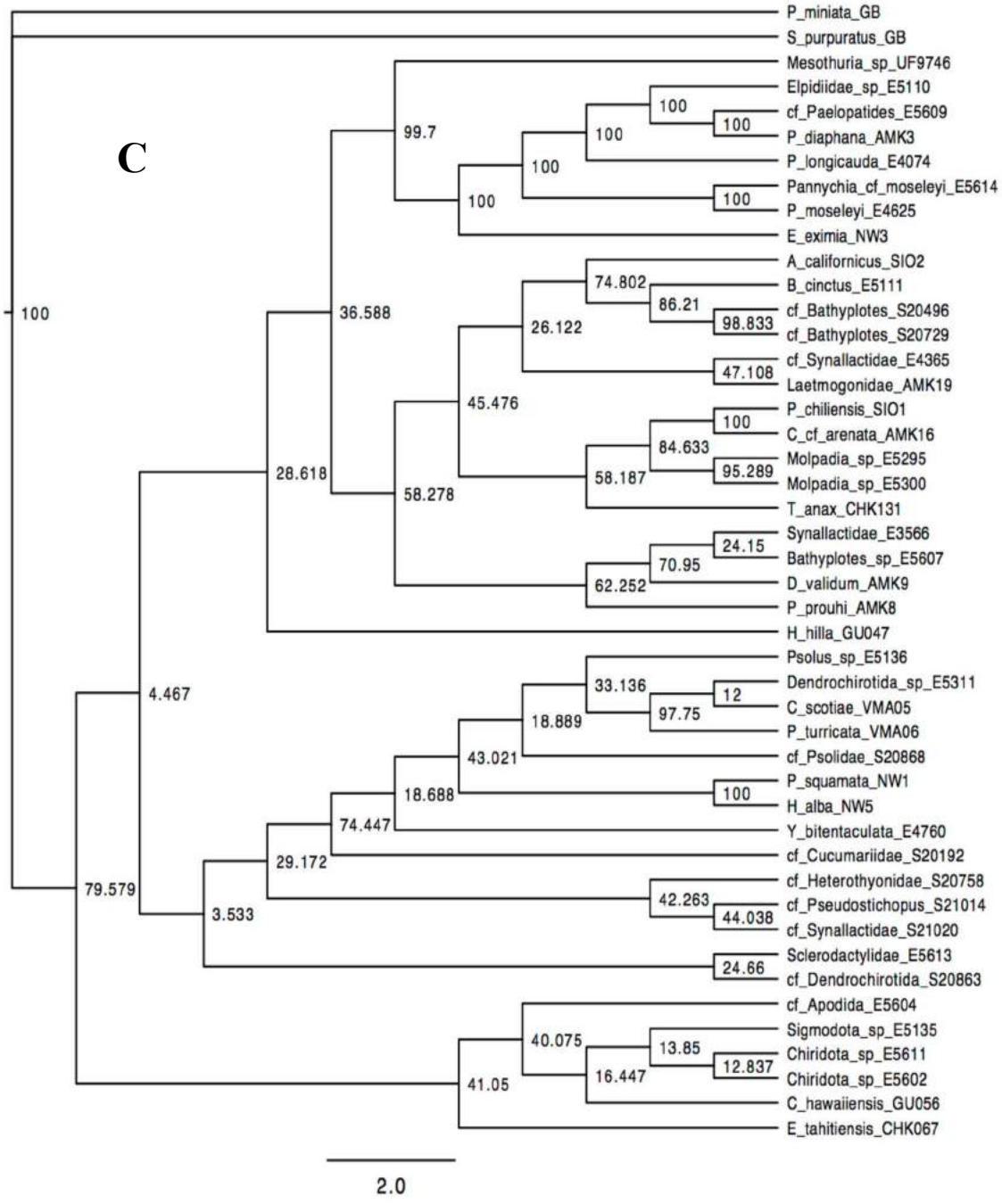

Appendix 1 continued.

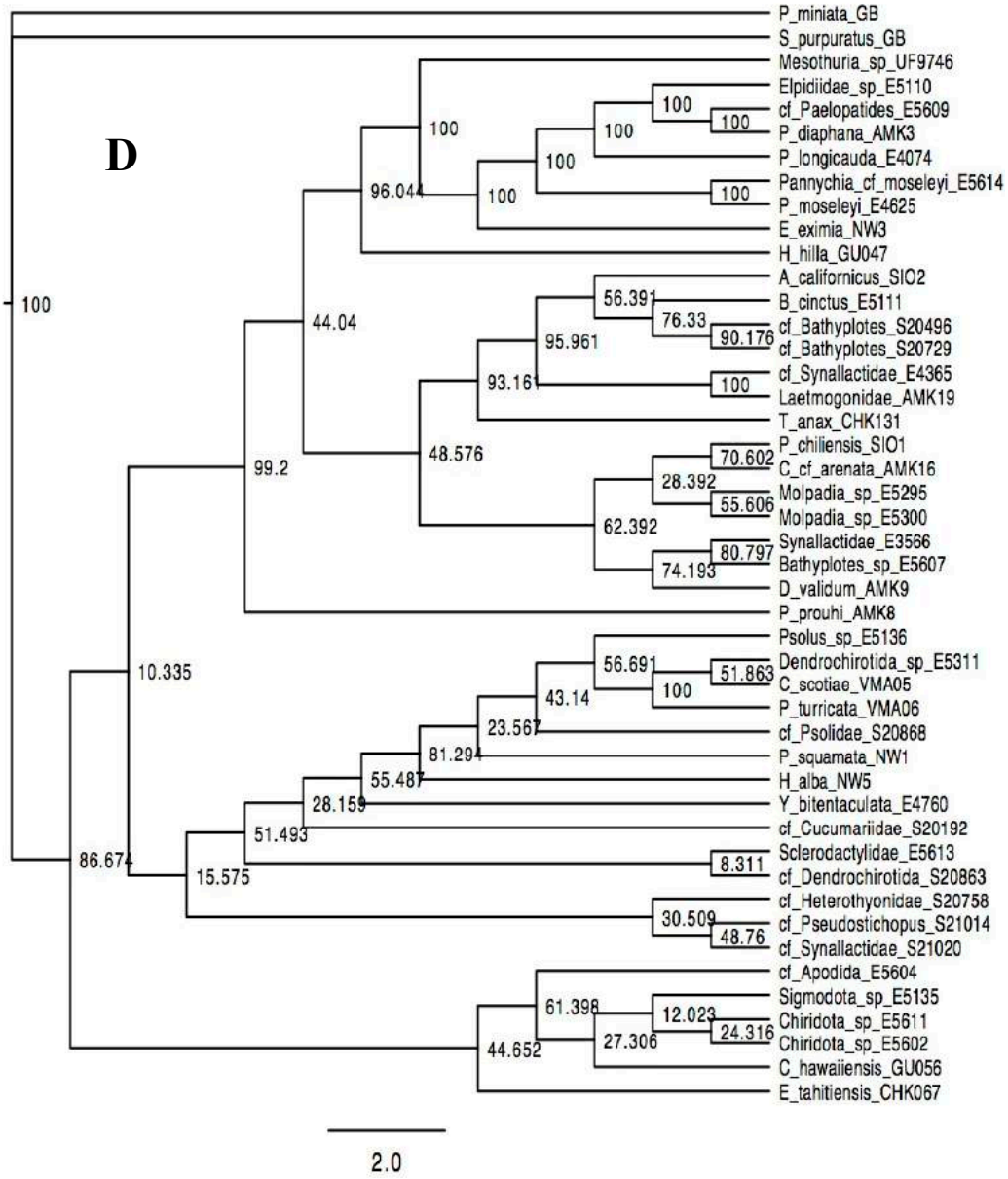

Figure 13. 12S ***A.*** ML, ***B.*** BI, ***C.*** MP (bootstrap) and, ***D.*** MP (jackknife) trees. The numbers at or adjacent to the nodes represent the bootstrap support values (***A.*** and ***C.***), Bayesian posterior probabilities values (***B.***), and jackknife support values (***D.***)

Appendix 1 continued.

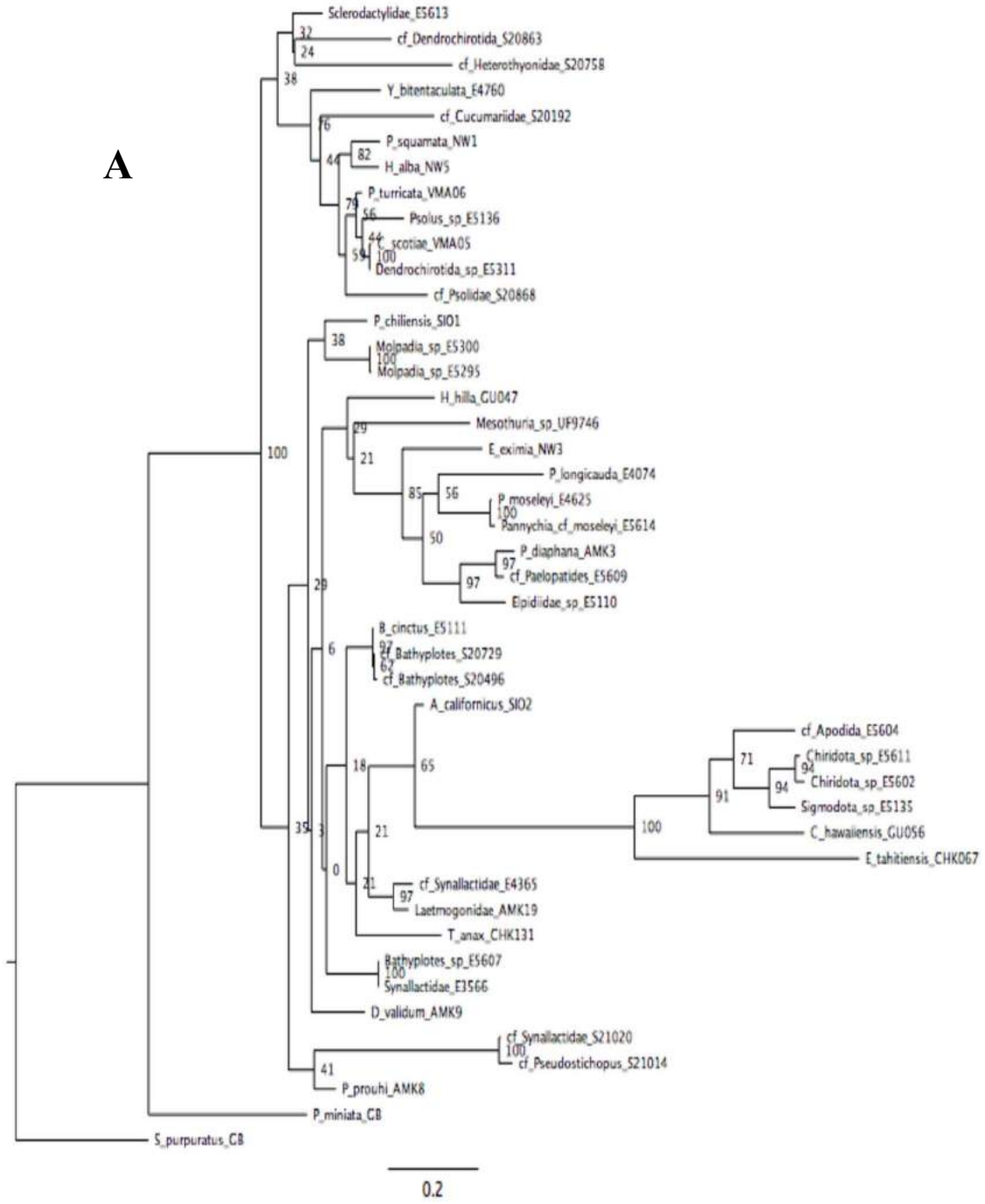

Appendix 1 continued.

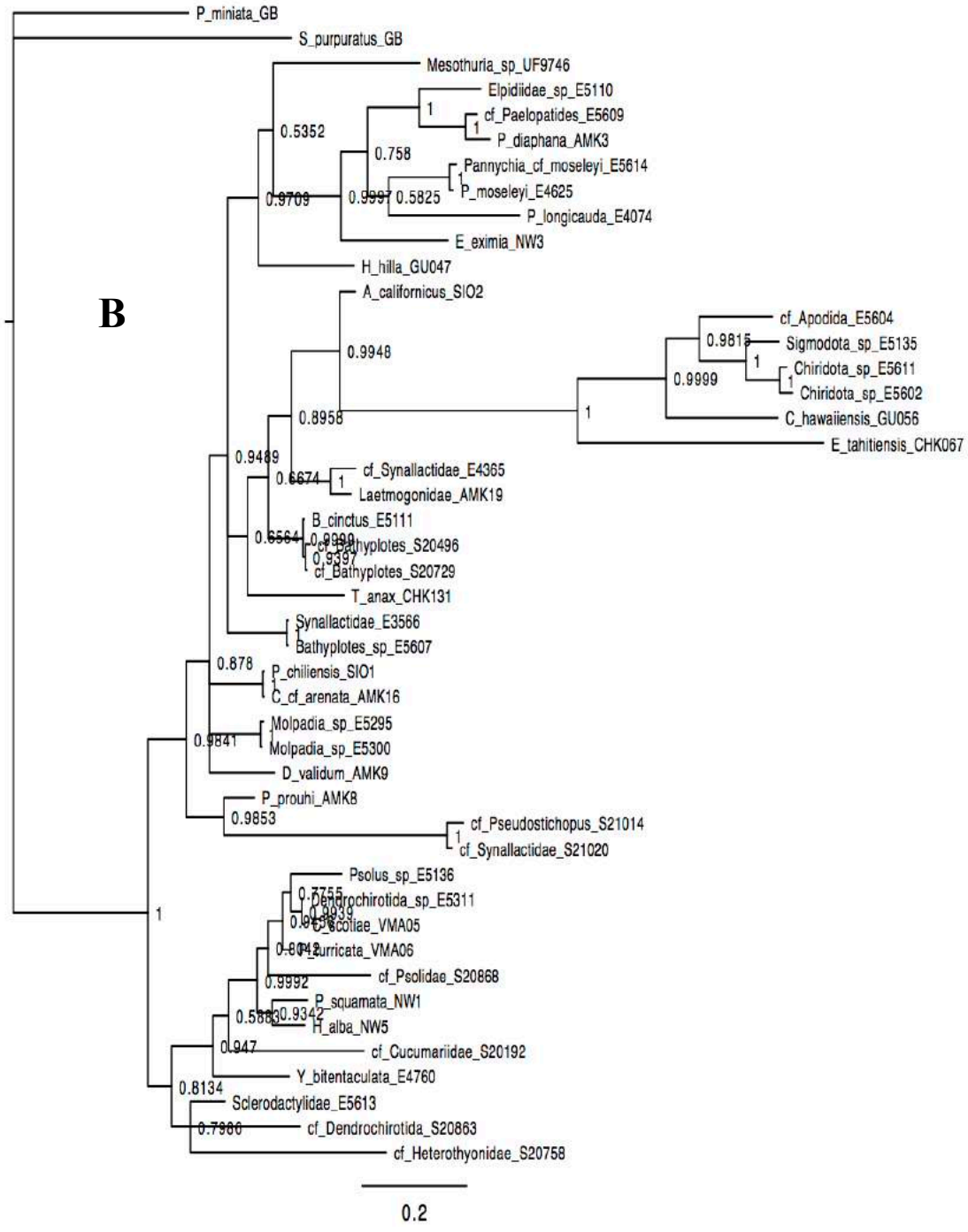

Appendix 1 continued.

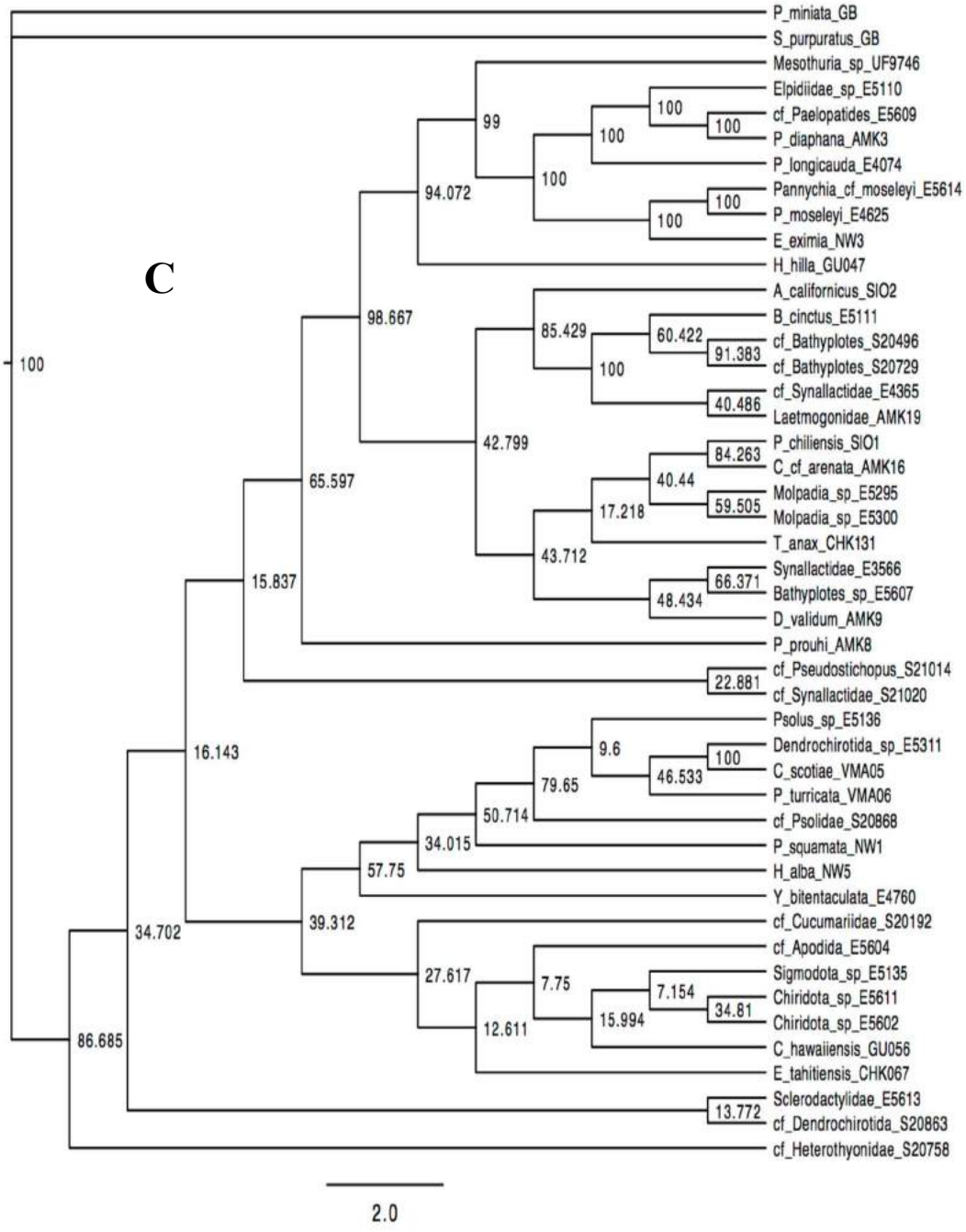

Appendix 1 continued.

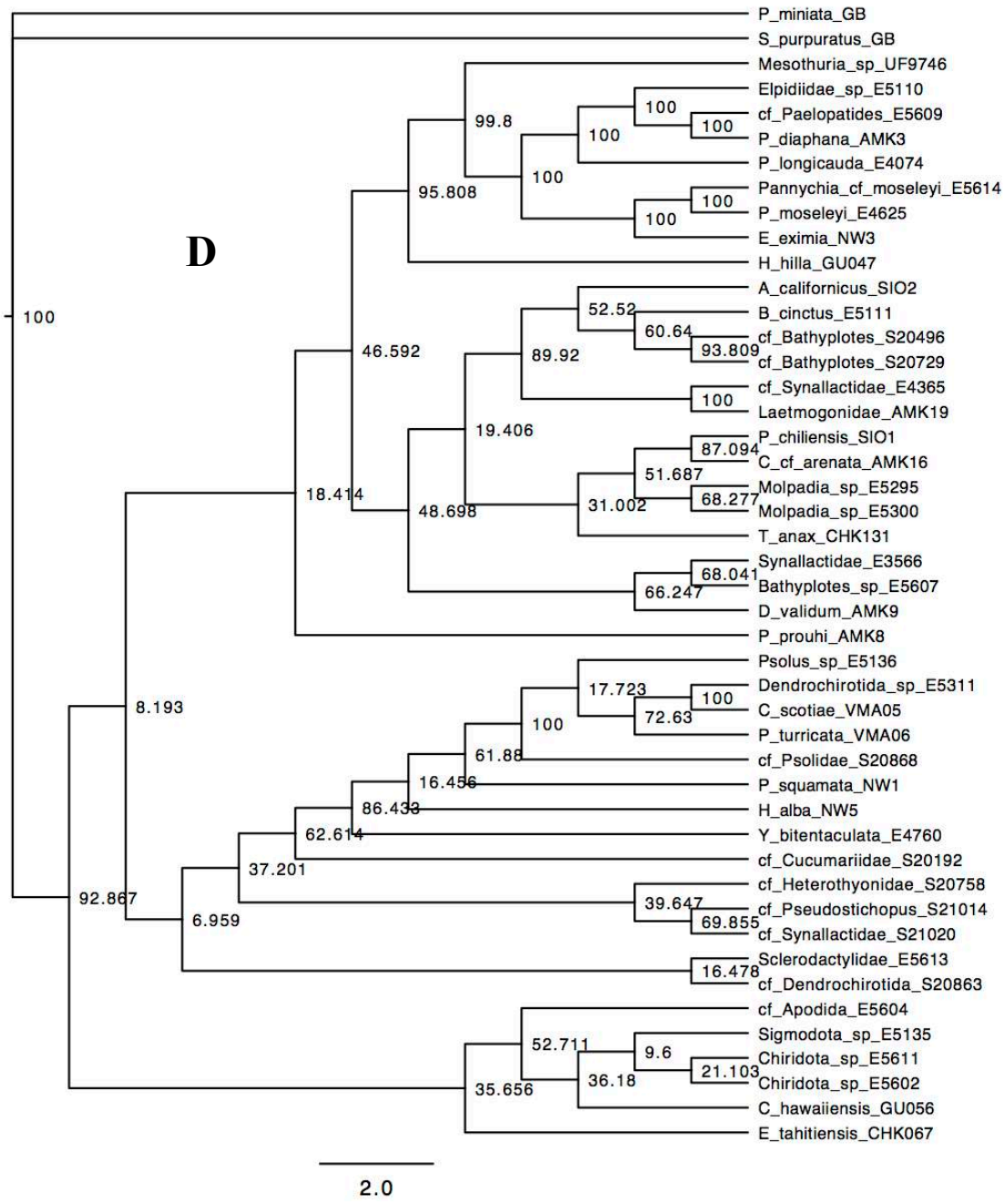

Figure 14. 12S HVRR ***A.*** ML, ***B.*** BI, ***C.*** MP (bootstrap) and, ***D.*** MP (jackknife) trees. The numbers at or adjacent to the nodes represent the bootstrap support values (***A.*** and ***C.***), Bayesian posterior probabilities values (***B.***), and jackknife support values (***D.***)

Appendix 1 continued.

Appendix 1 continued.

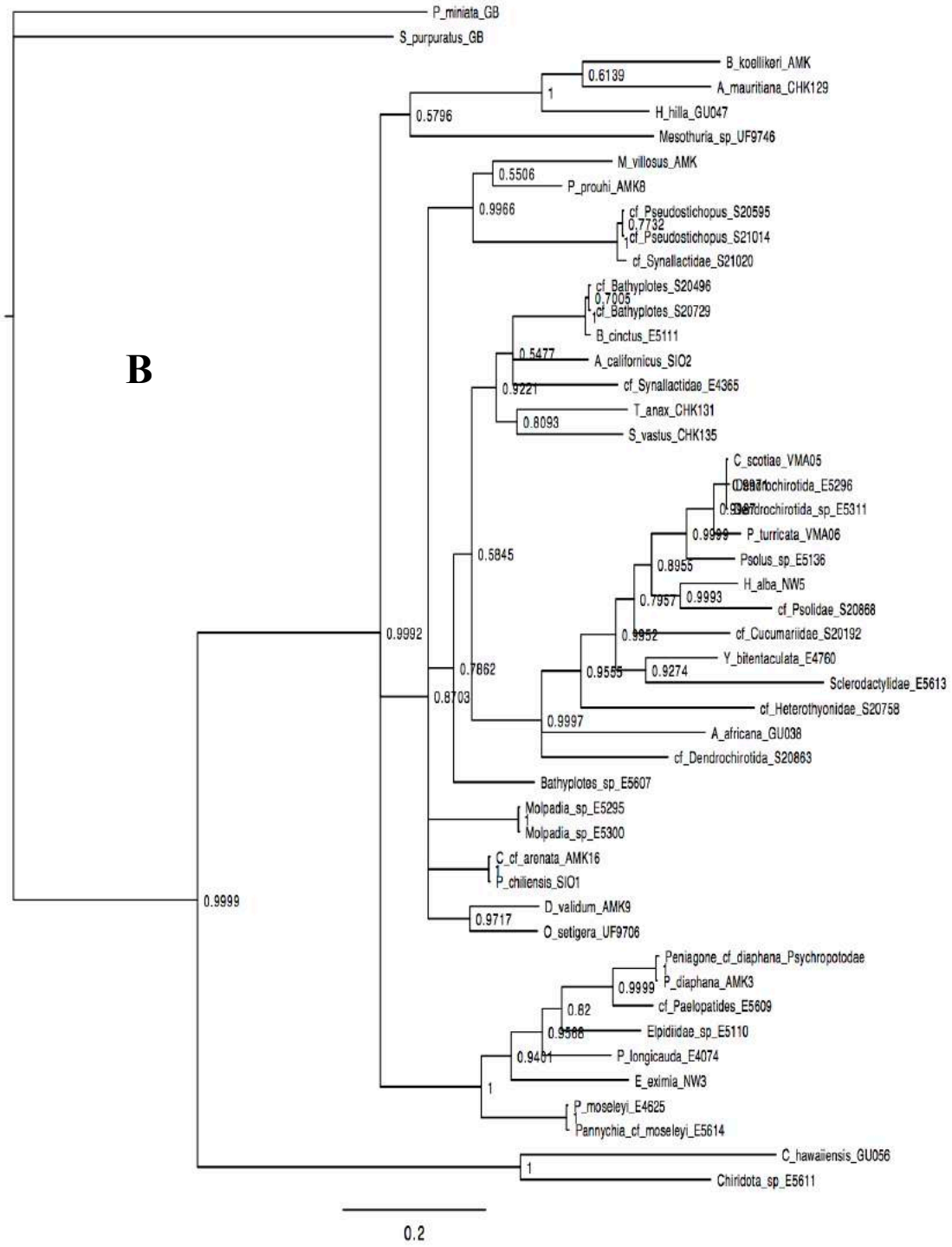

Appendix 1 continued.

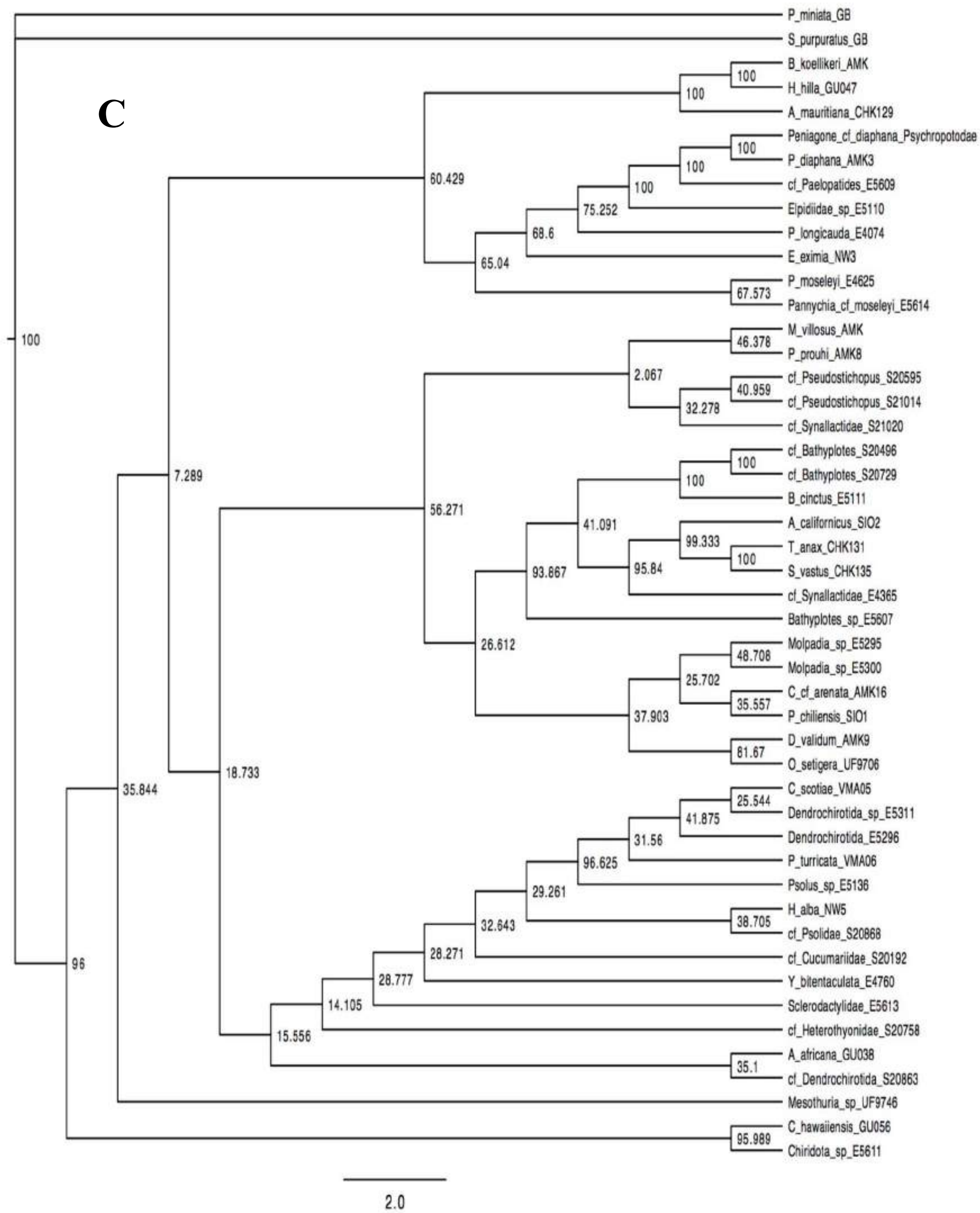

Appendix 1 continued.

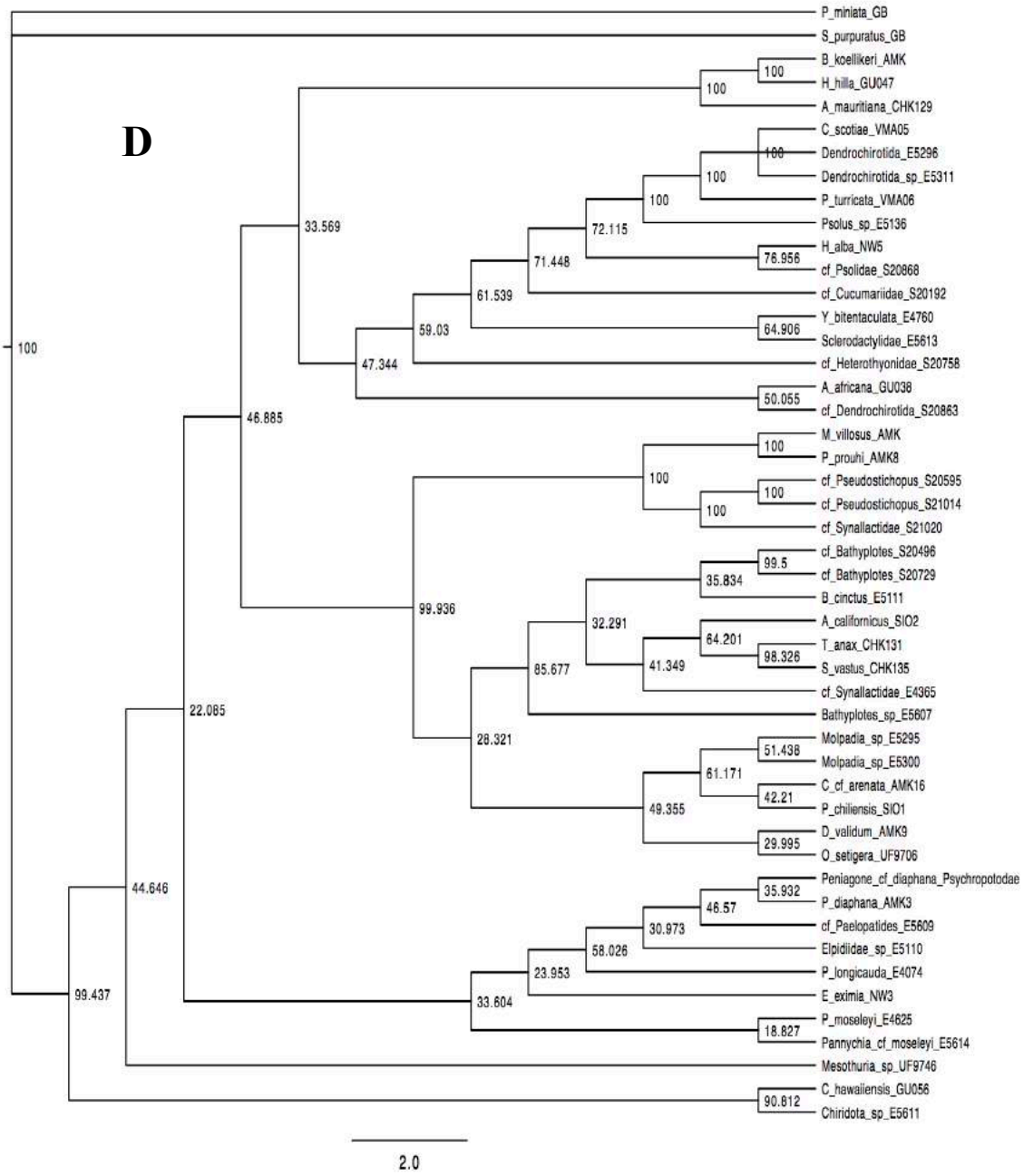

Figure 15. 16S HVRR ***A.*** ML, ***B.*** BI, ***C.*** MP (bootstrap) and, ***D.*** MP (jackknife) trees. The numbers at or adjacent to the nodes represent the bootstrap support values (***A.*** and ***C.***), Bayesian posterior probabilities values (***B.***), and jackknife support values (***D.***)

Appendix 1 continued.

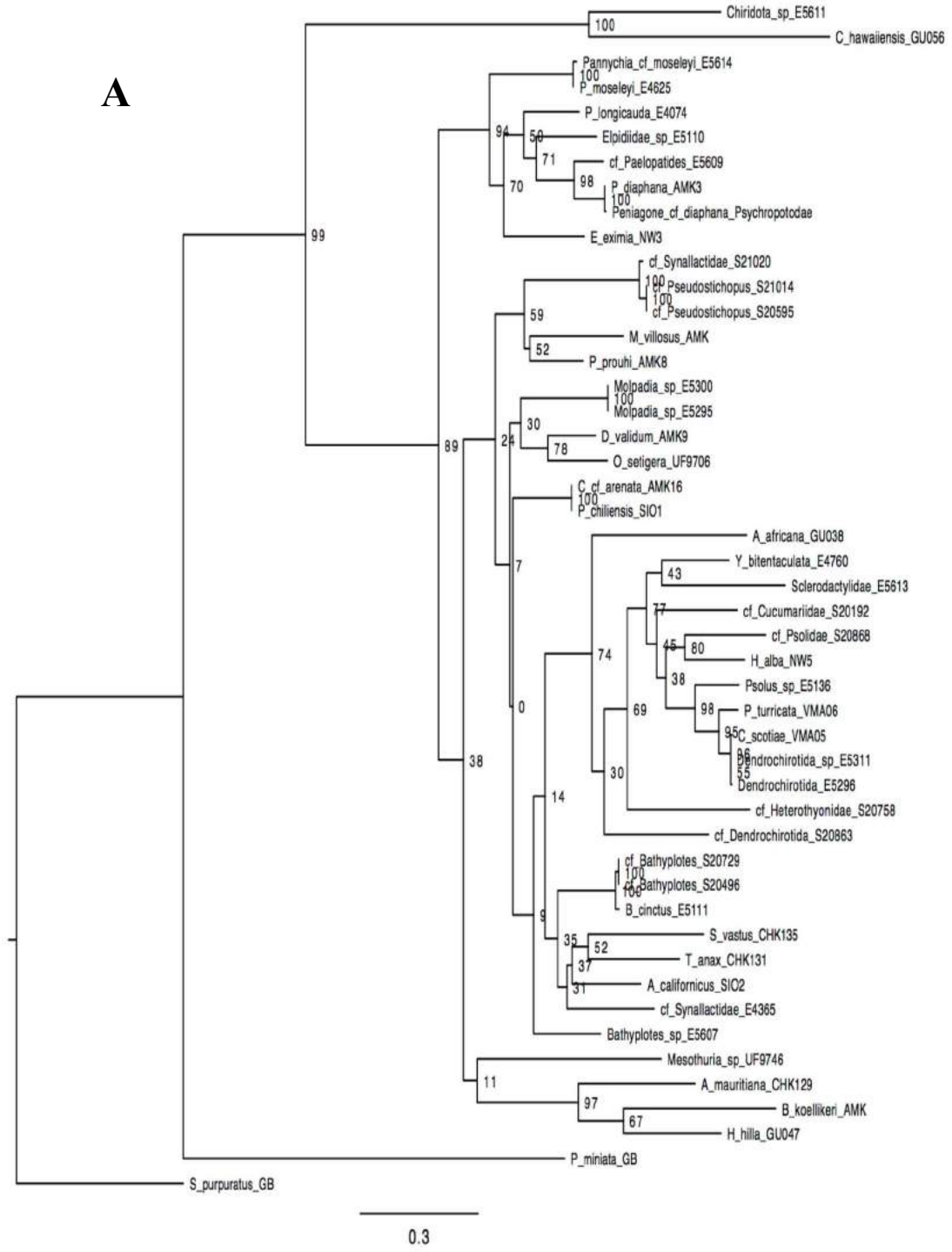

Appendix 1 continued.

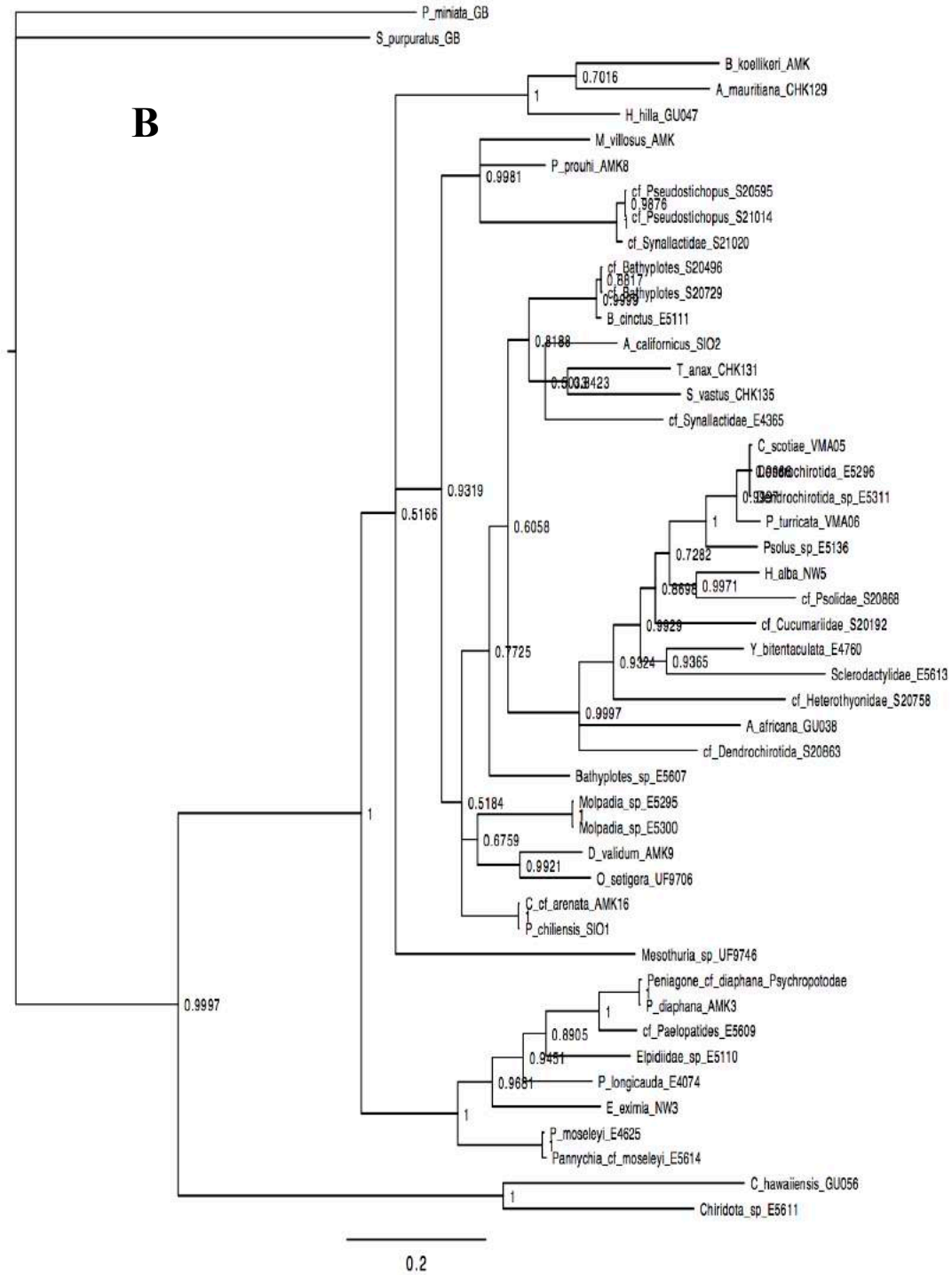

Appendix 1 continued.

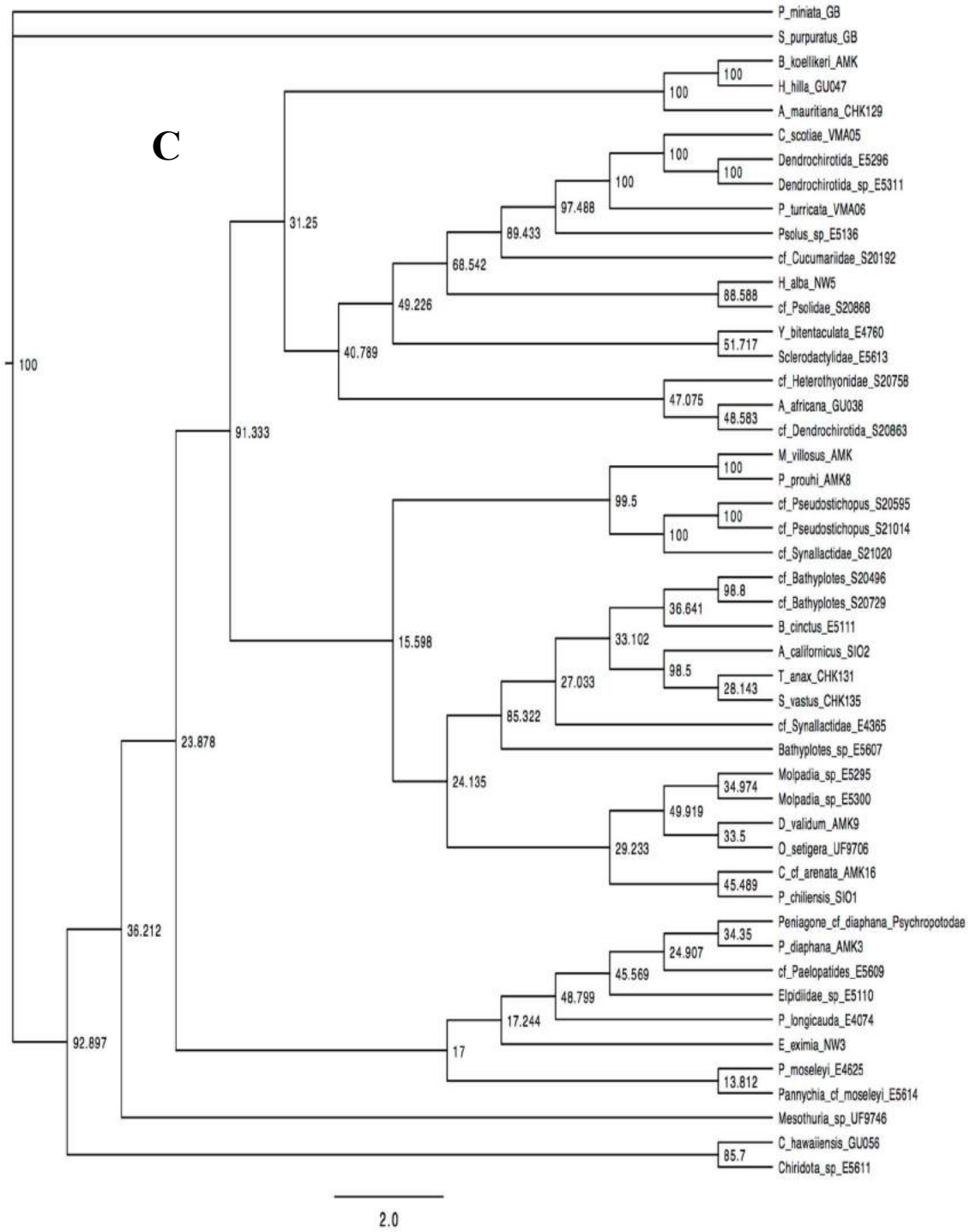

Appendix 1 continued.

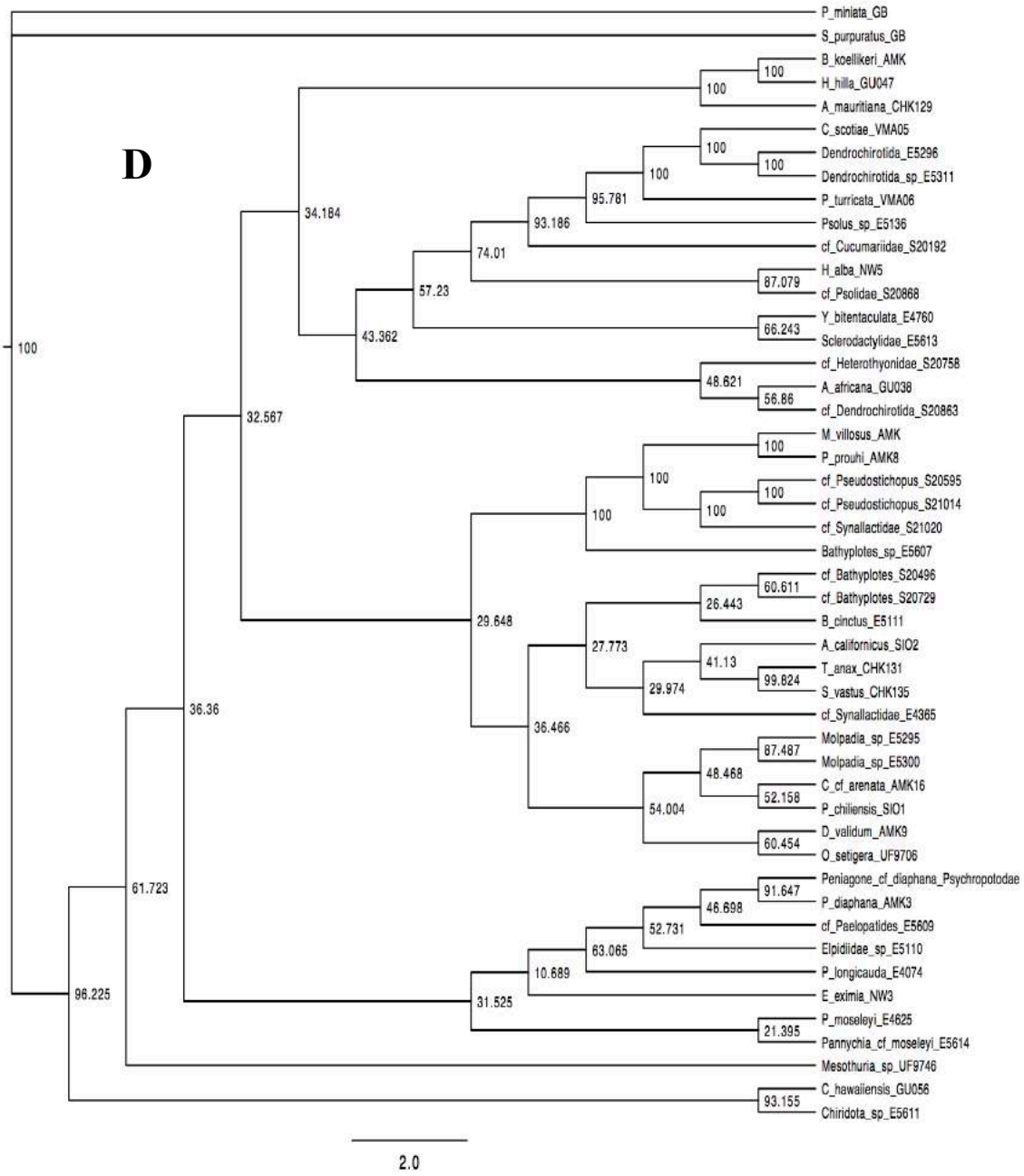

Figure 16. 16S ***A.*** ML, ***B.*** BI, ***C.*** MP (bootstrap) and, ***D.*** MP (jackknife) trees. The numbers at or adjacent to the nodes represent the bootstrap support values (***A.*** and ***C.***), Bayesian posterior probabilities values (***B.***), and jackknife support values (***D.***)

Appendix 1 continued.

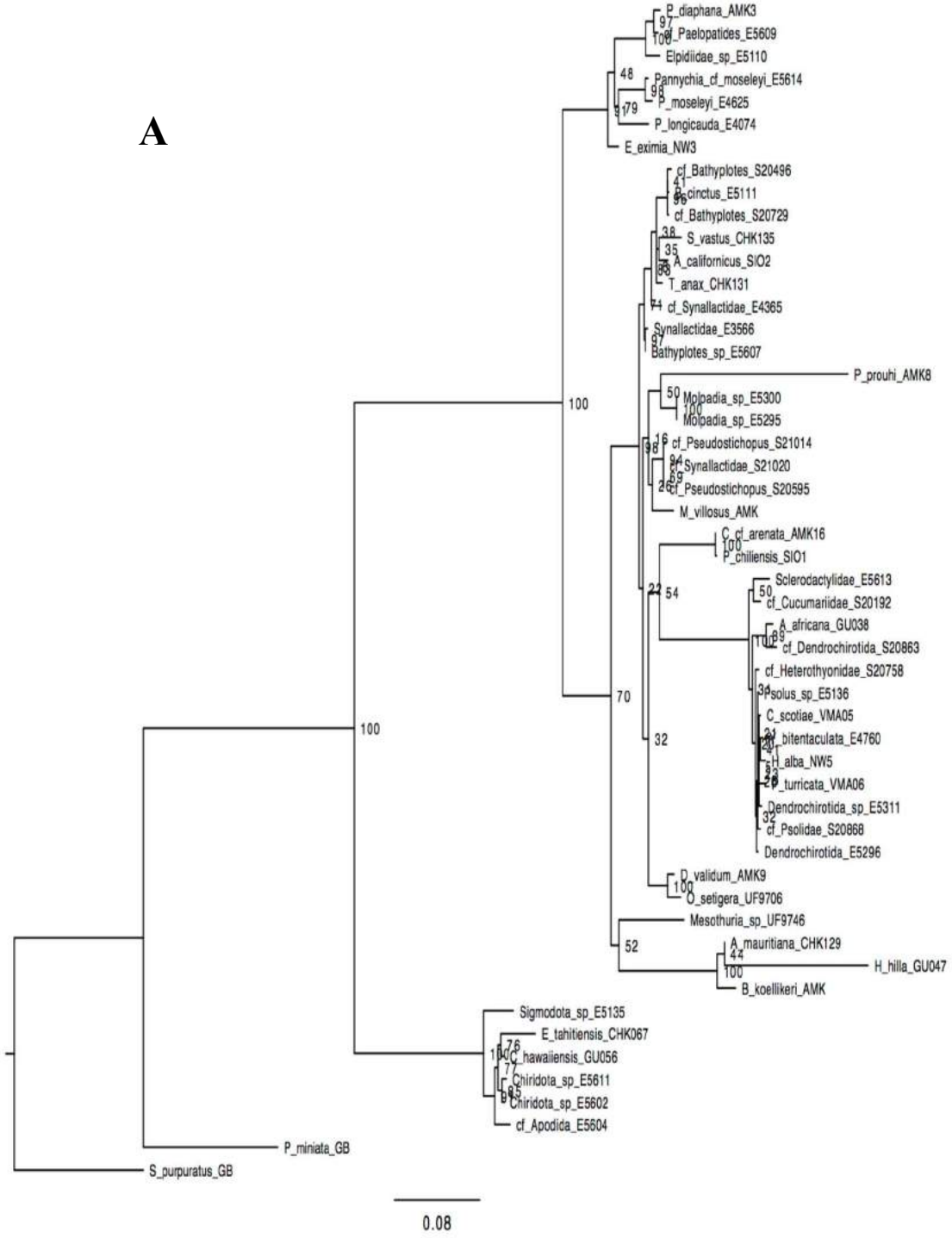

Appendix 1 continued.

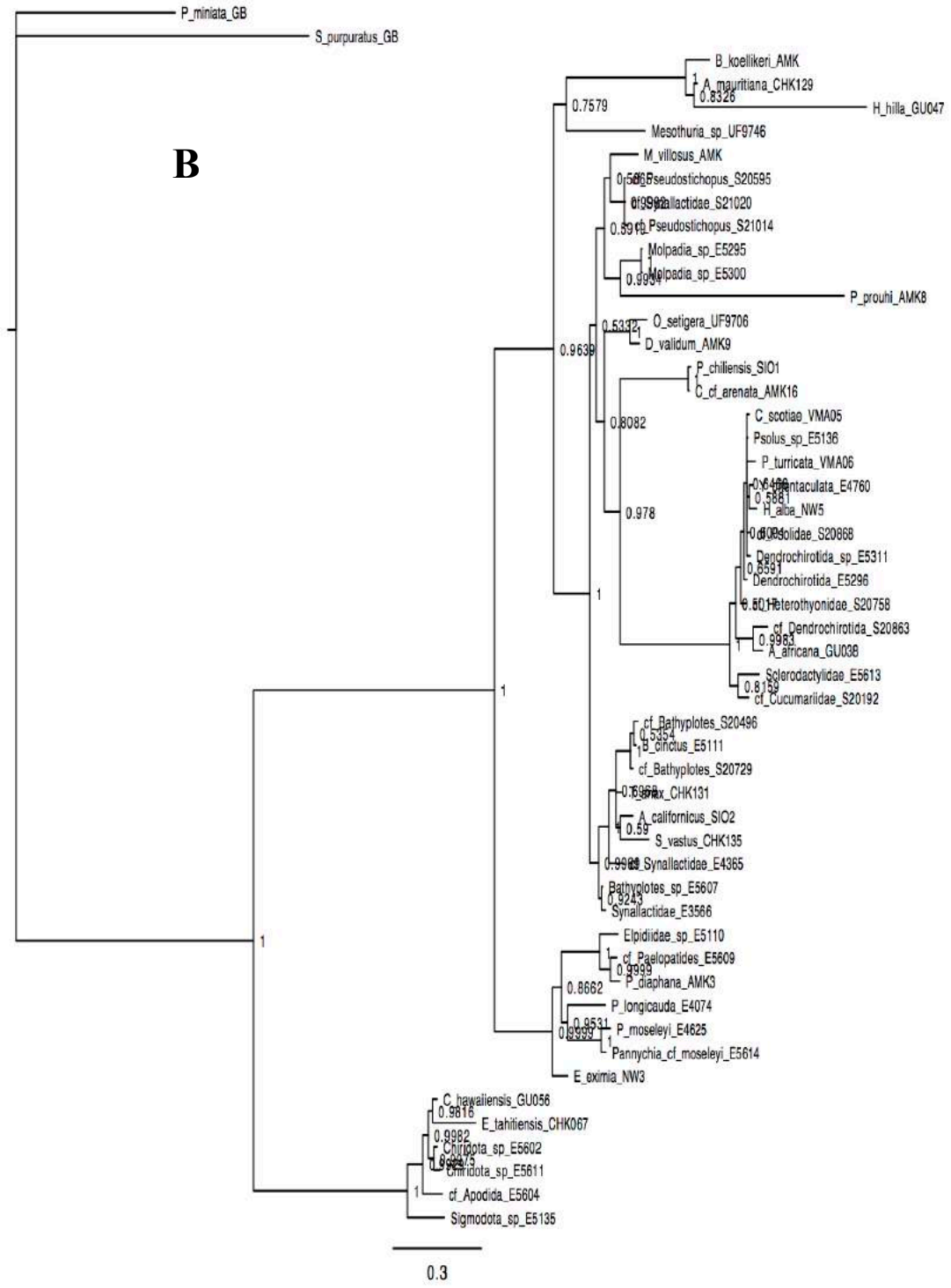

Appendix 1 continued.

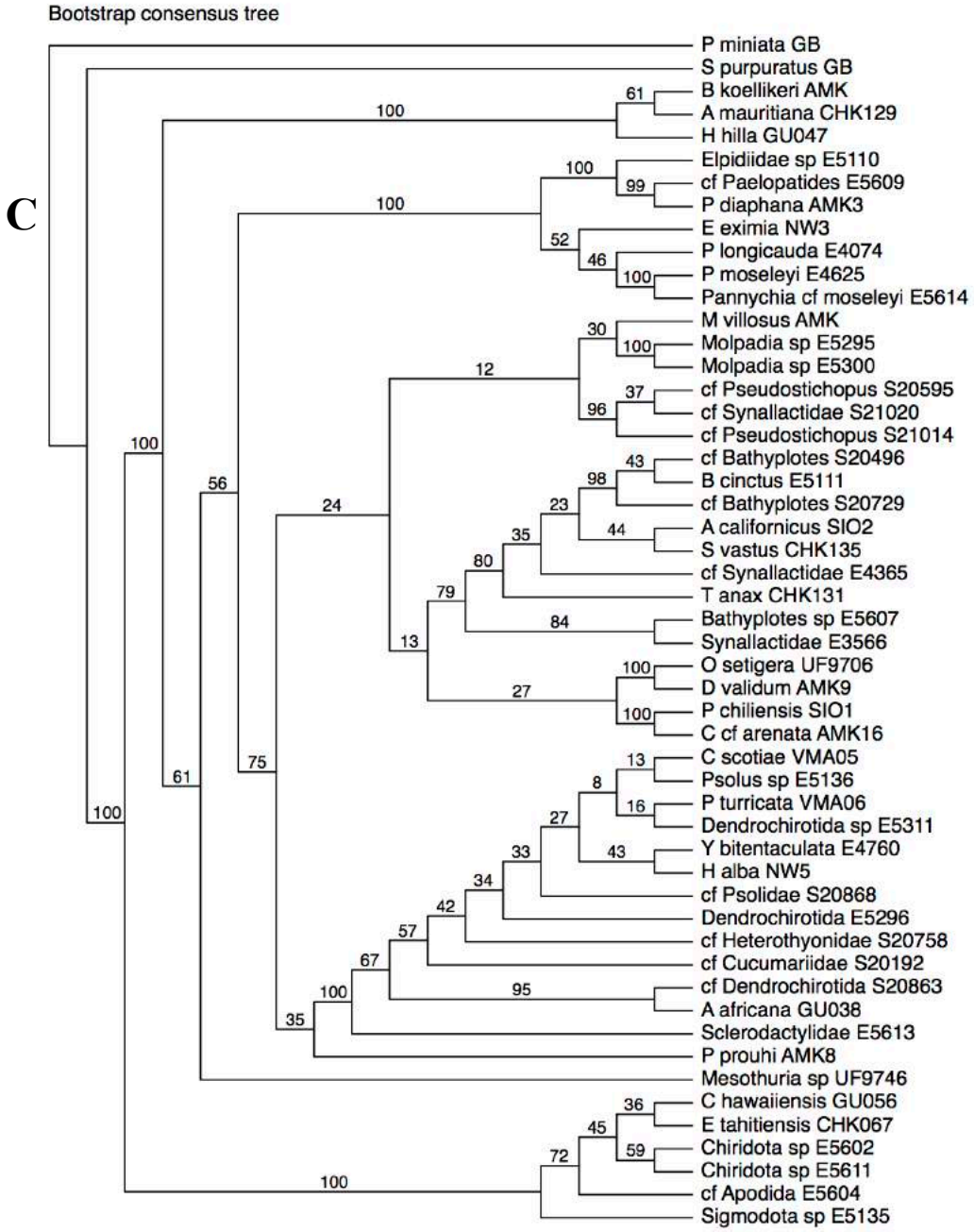

Appendix 1 continued.

D

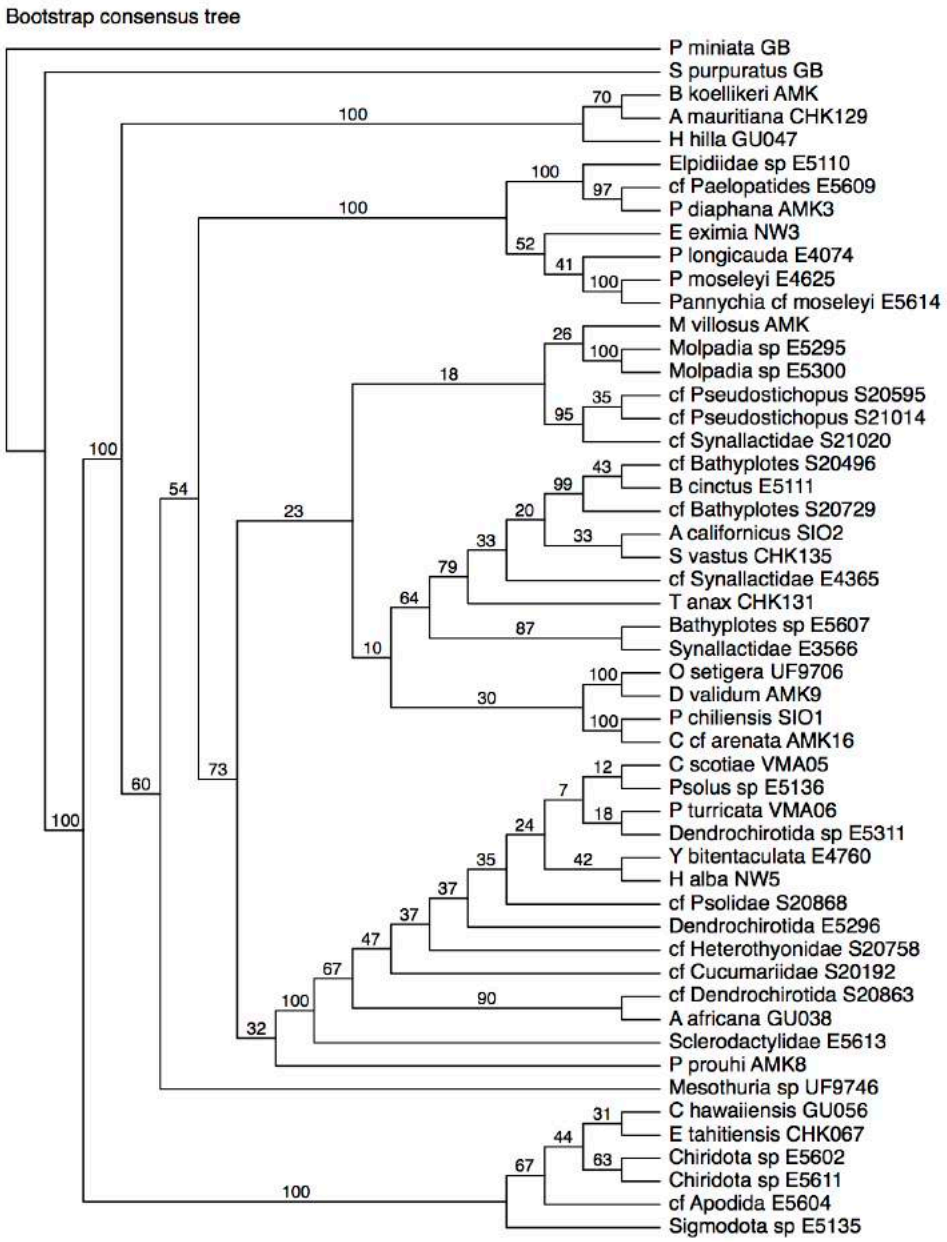

Figure 17. 18S ***A.*** ML, ***B.*** BI, ***C.*** MP (bootstrap) and, ***D.*** MP (jackknife) trees. The numbers at or adjacent to the nodes represent the bootstrap support values (***A.*** and ***C.***), Bayesian posterior probabilities values (***B.***), and jackknife support values (***D.***)

Appendix 1 continued.

Appendix 1 continued.

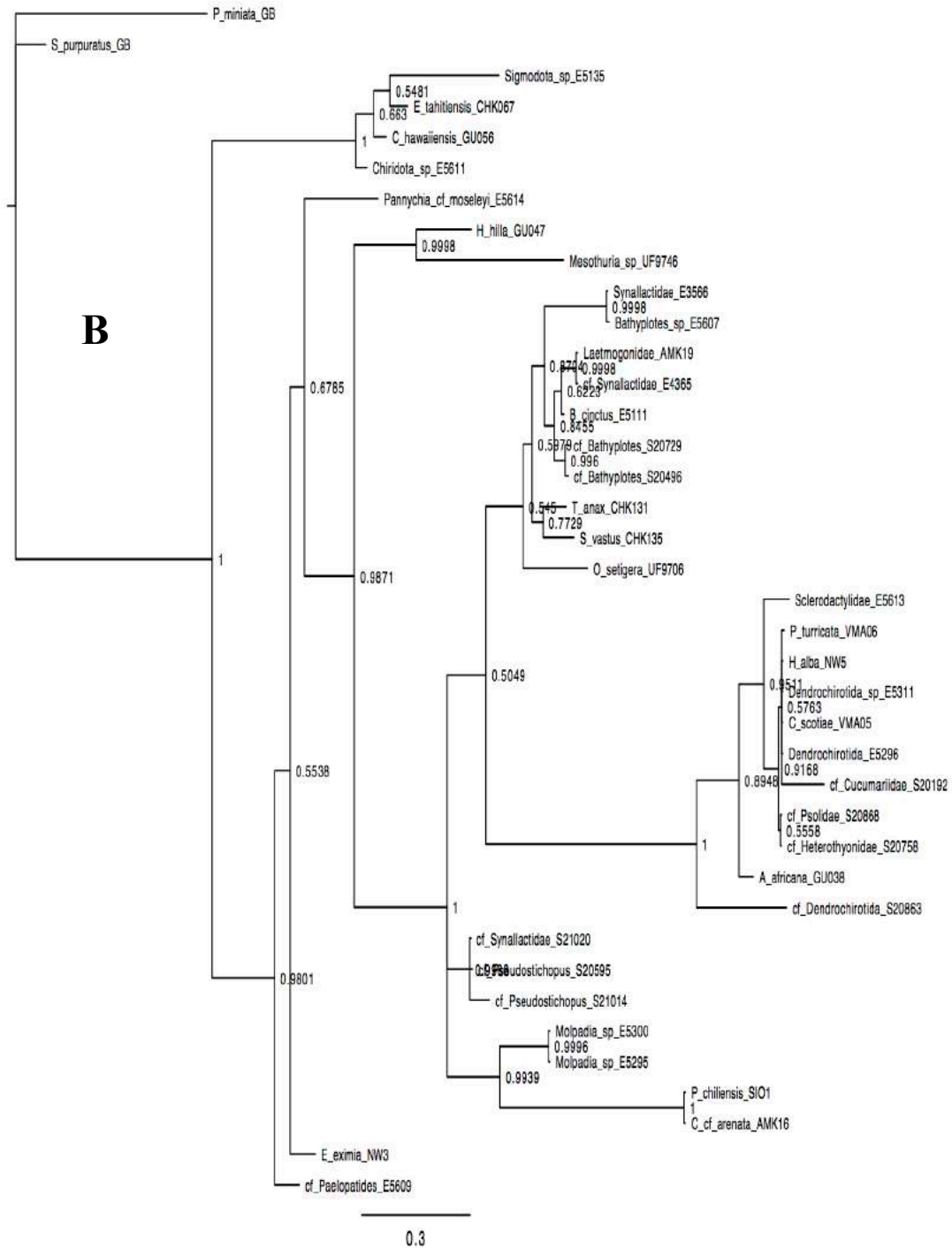

Appendix 1 continued.

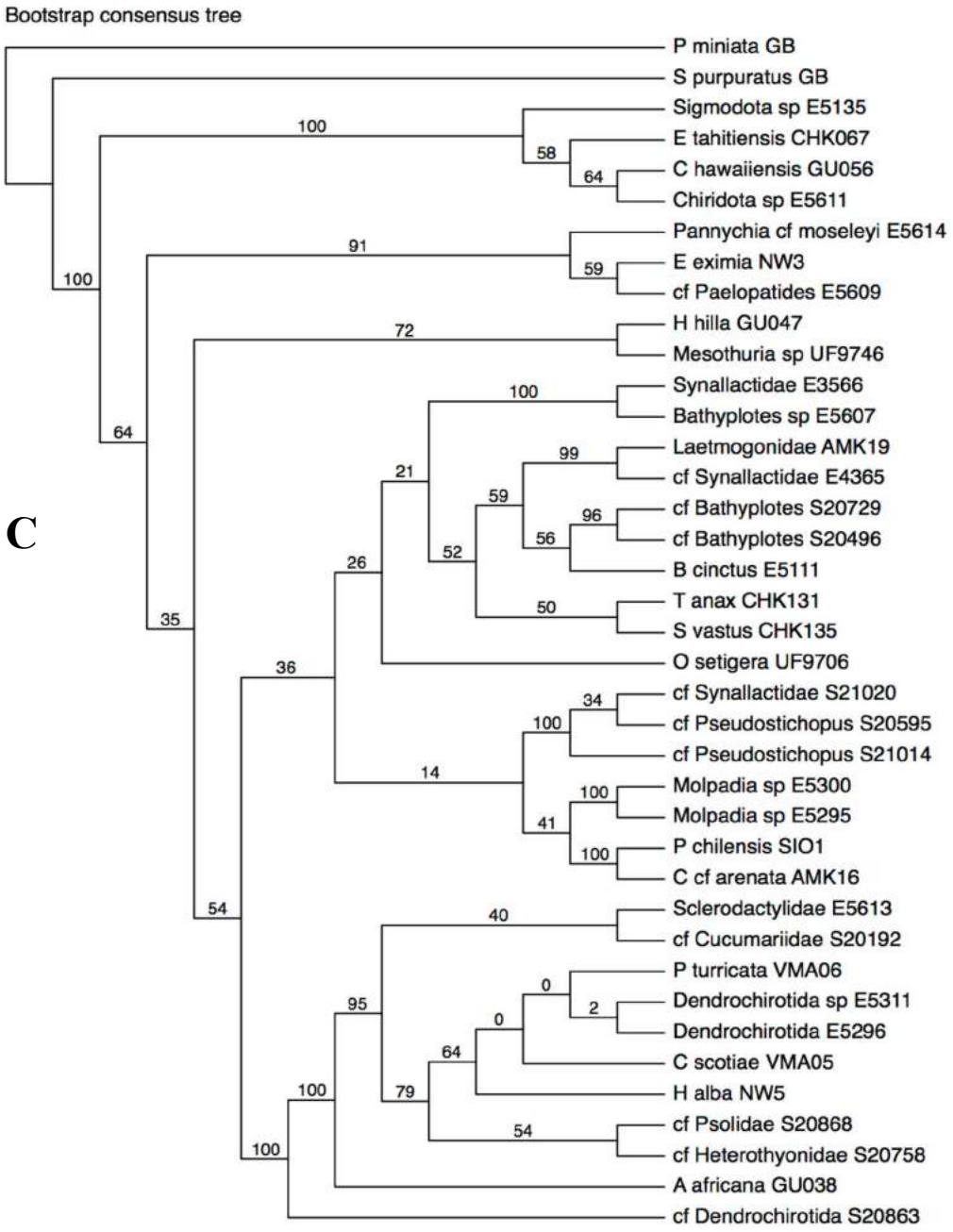

Appendix 1 continued.

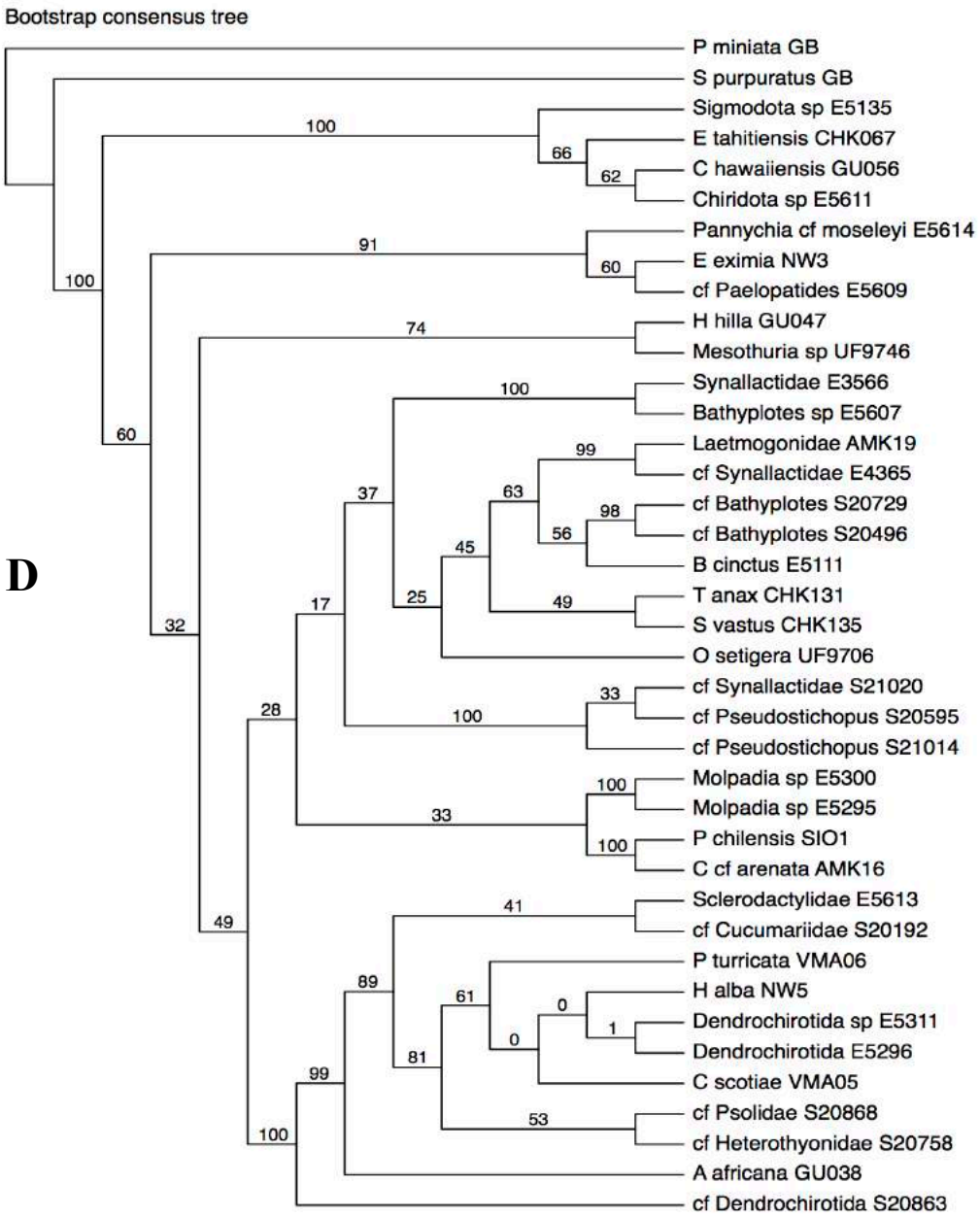

D

Figure 18. 28S ***A.*** ML, ***B.*** BI, ***C.*** MP (bootstrap) and, ***D.*** MP (jackknife) trees. The numbers at or adjacent to the nodes represent the bootstrap support values (***A.*** and ***C.***), Bayesian posterior probabilities values (***B.***), and jackknife support values (***D.***)

Appendix 1 continued.

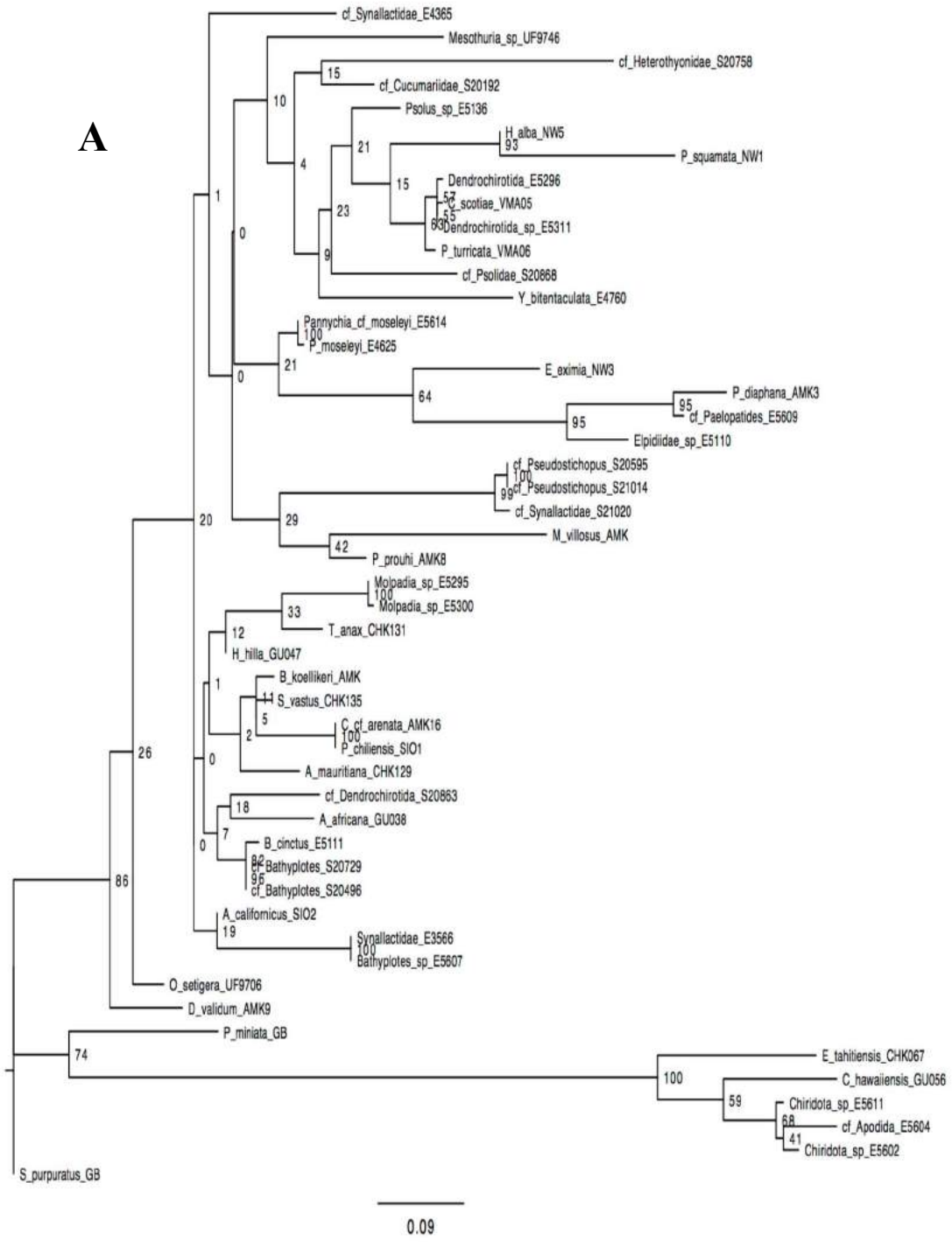

Appendix 1 continued.

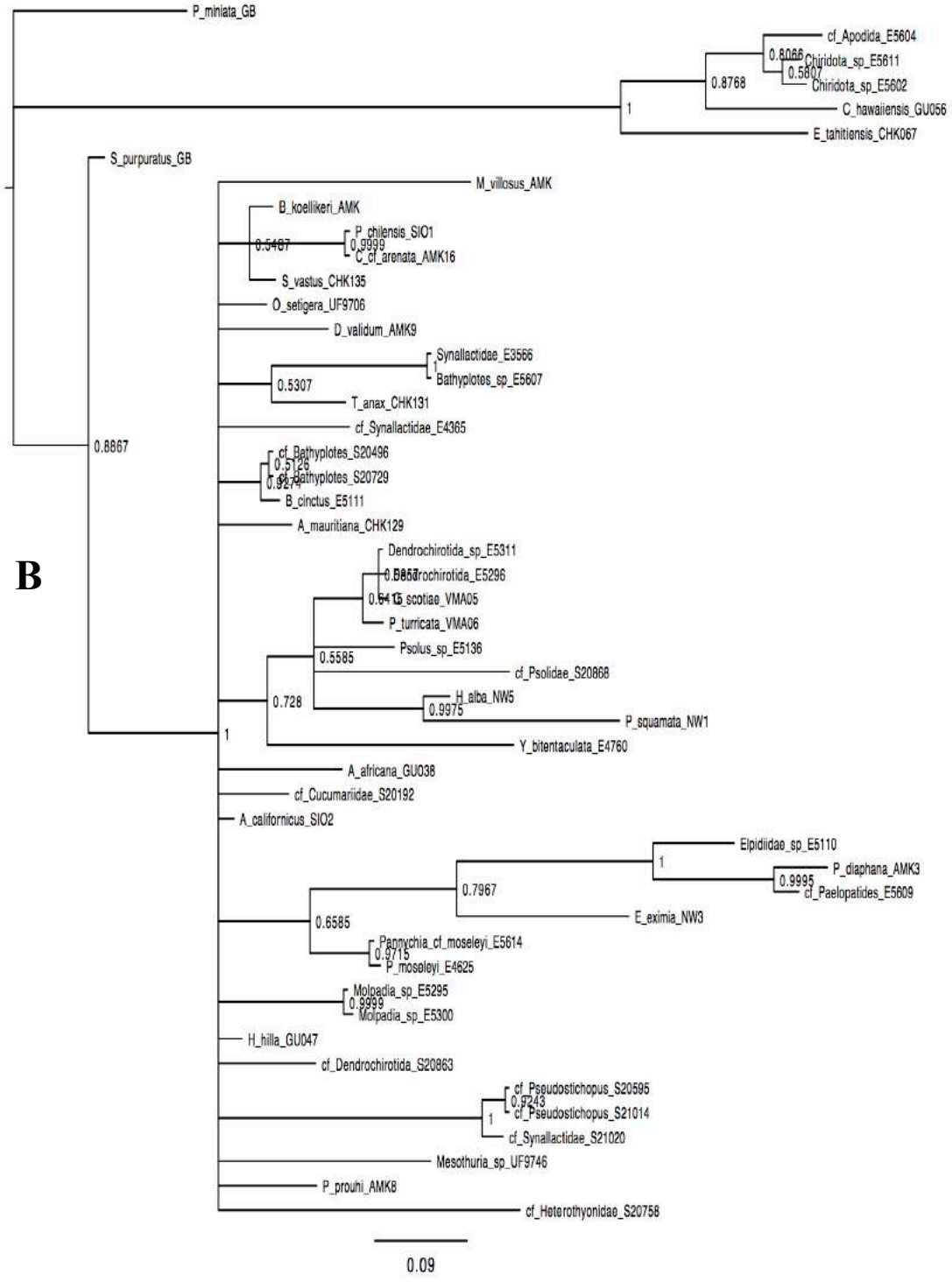

Appendix 1 continued.

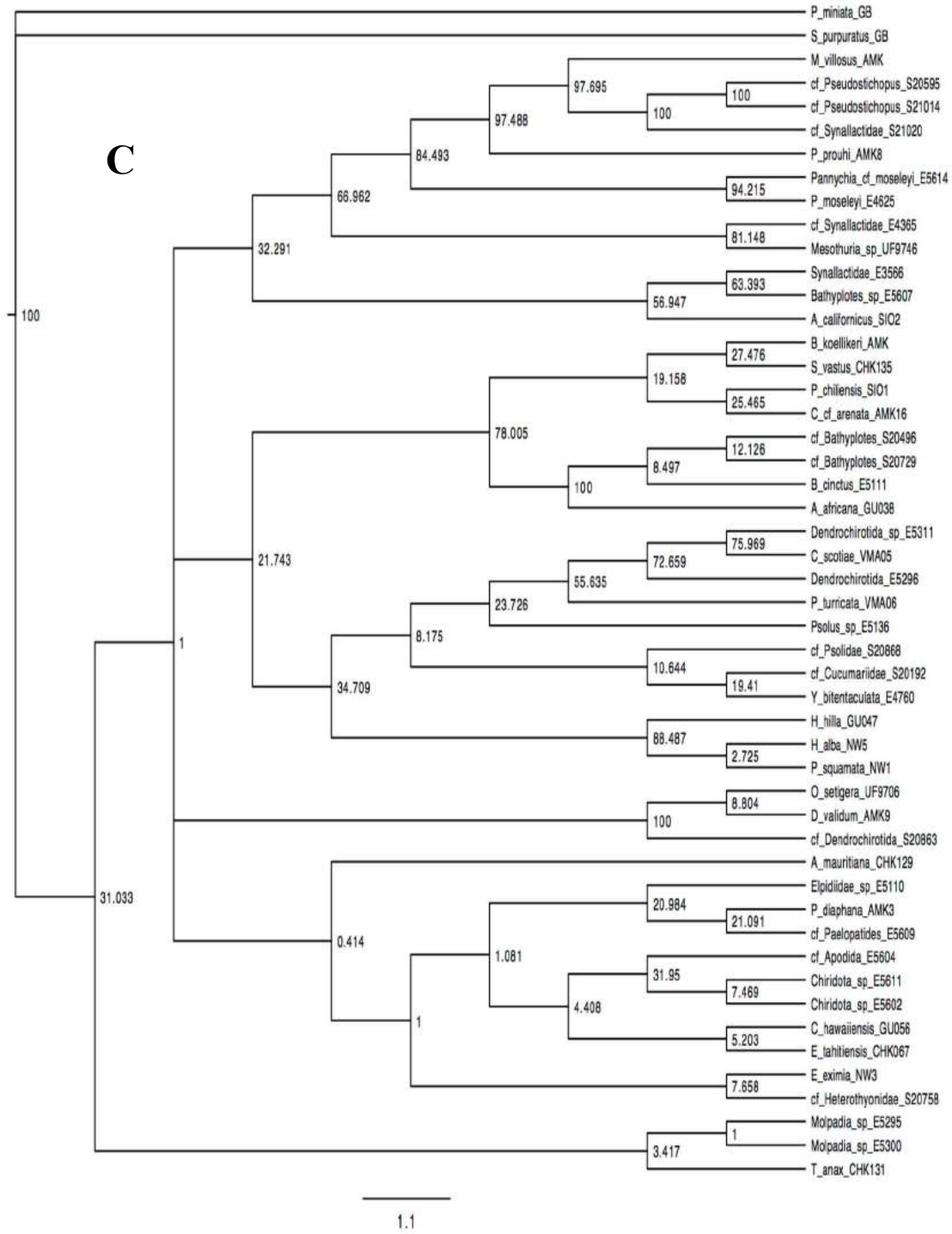

Appendix 1 continued.

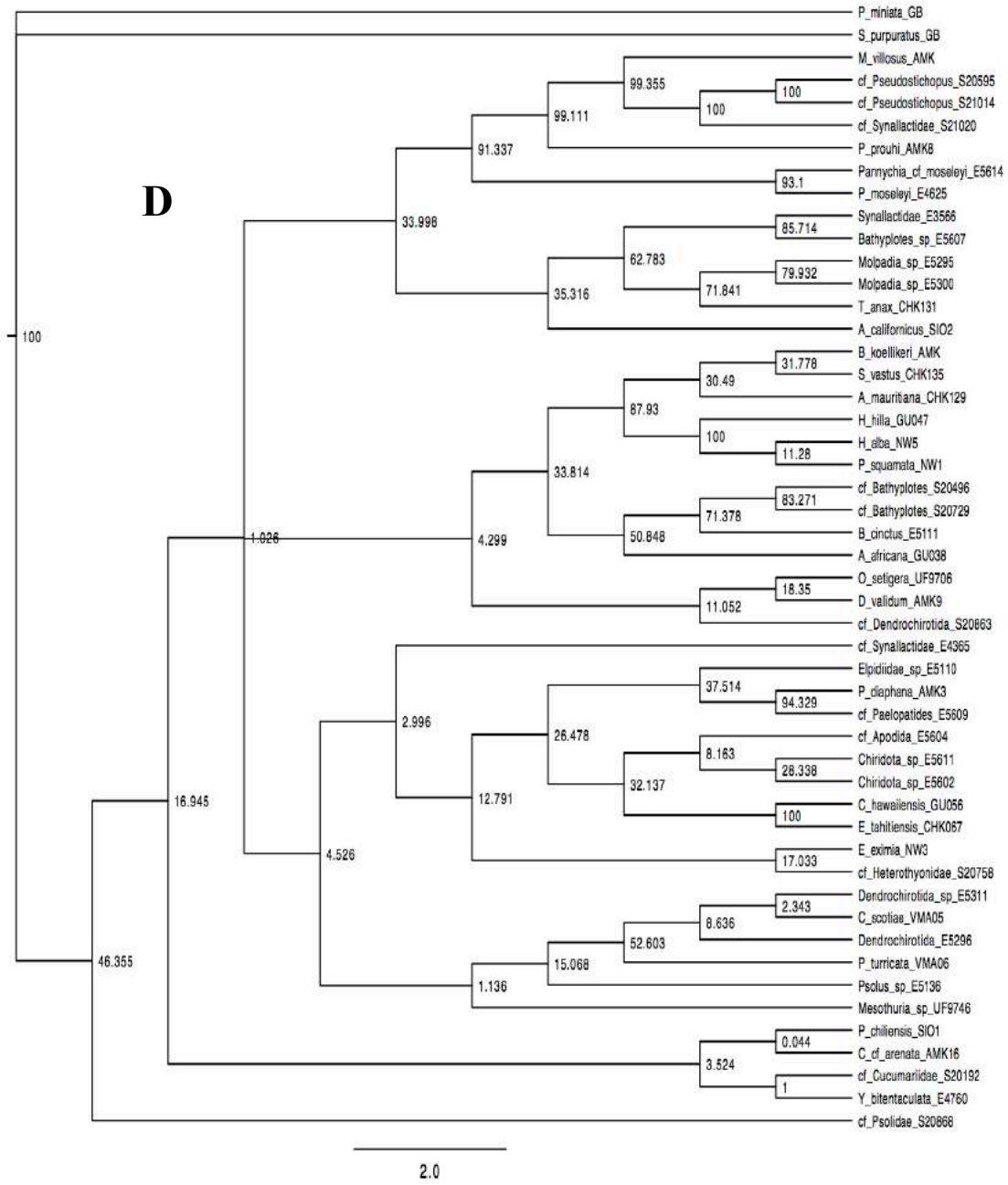

Figure 19. COI (1&2) ***A.*** ML, ***B.*** BI, ***C.*** MP (bootstrap) and, ***D.*** MP (jackknife) trees. The numbers at or adjacent to the nodes represent the bootstrap support values (***A.*** and ***C.***), Bayesian posterior probabilities values (***B.***), and jackknife support values (***D.***)

Appendix 1 continued.

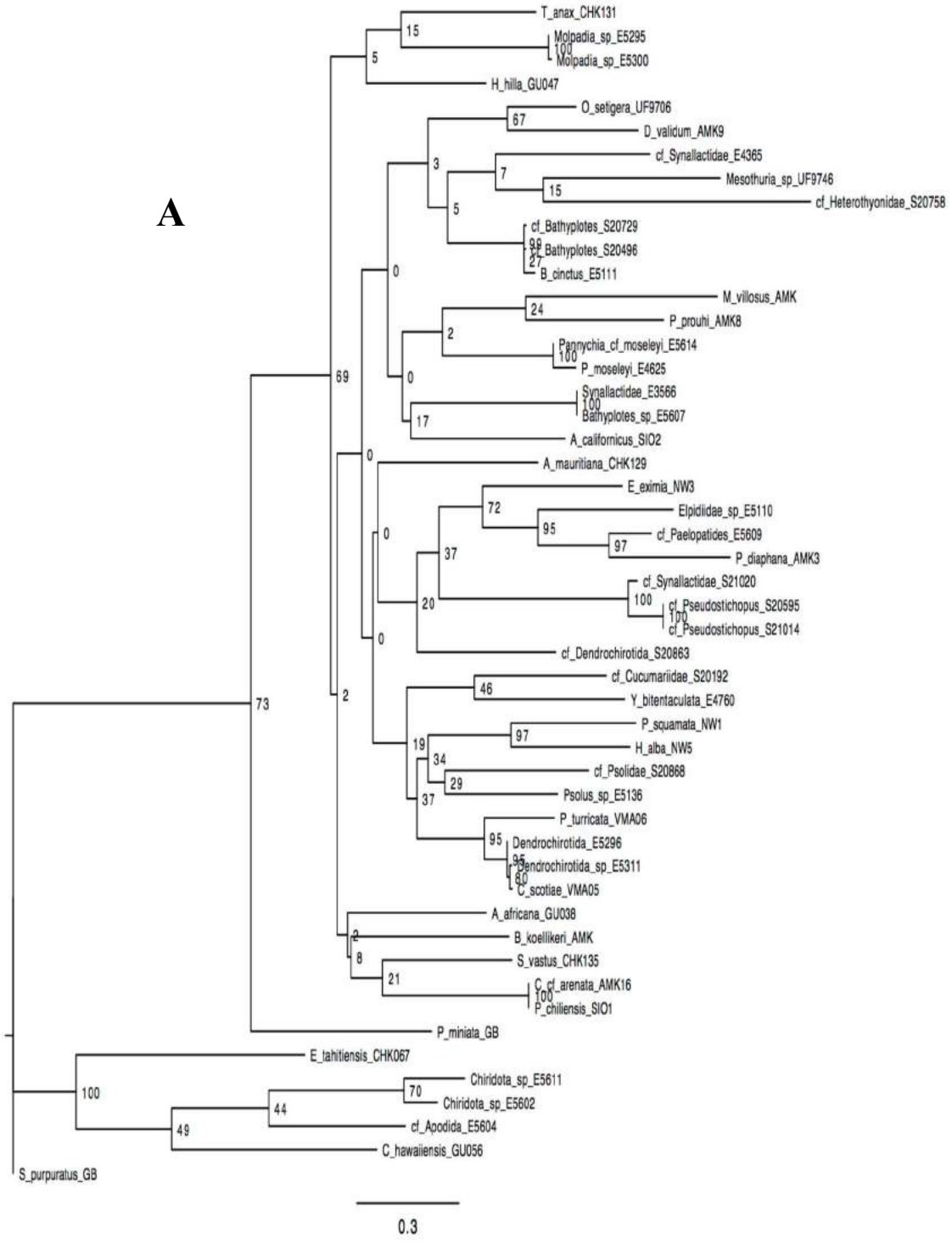

Appendix 1 continued.

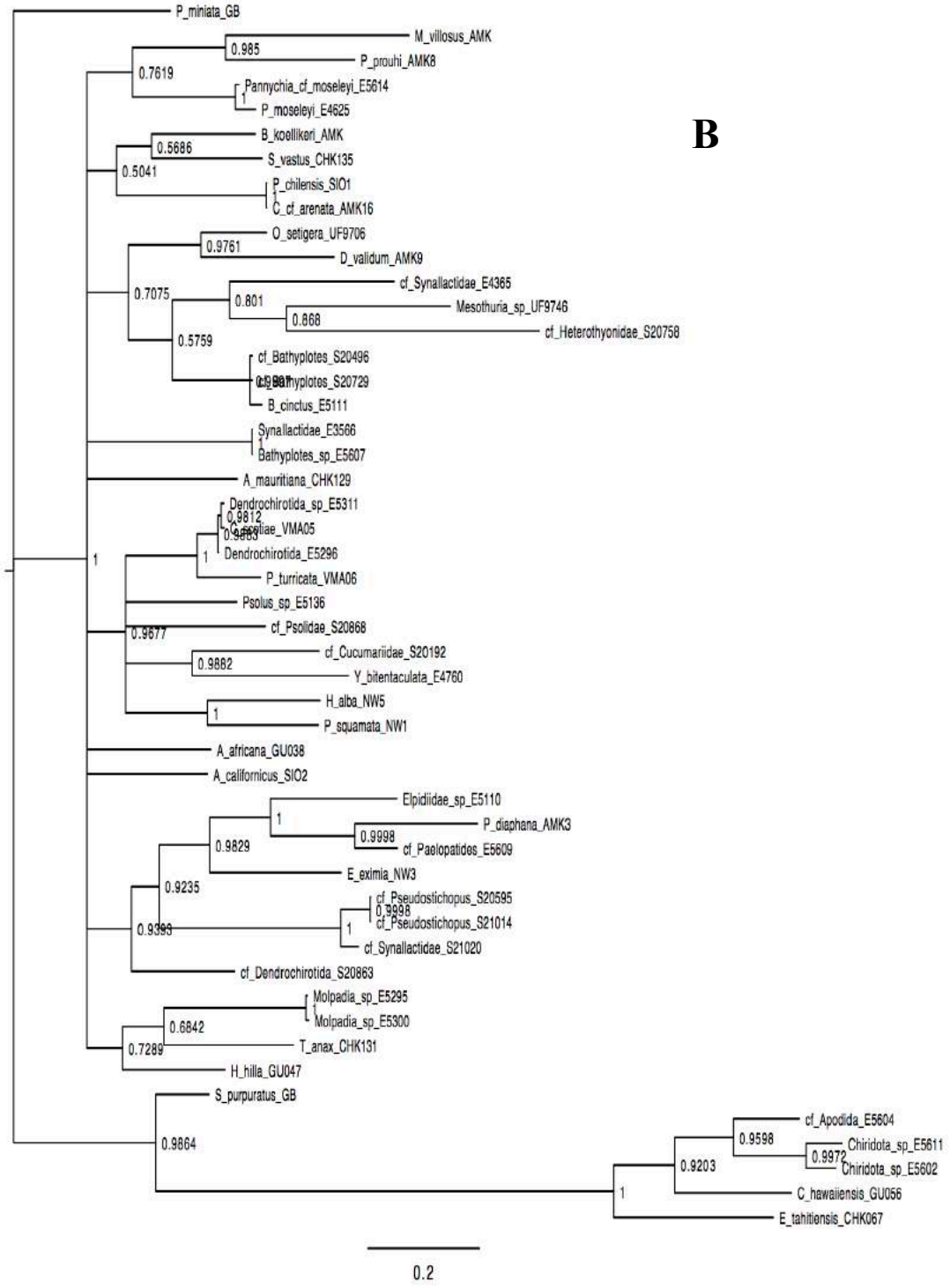

Appendix 1 continued.

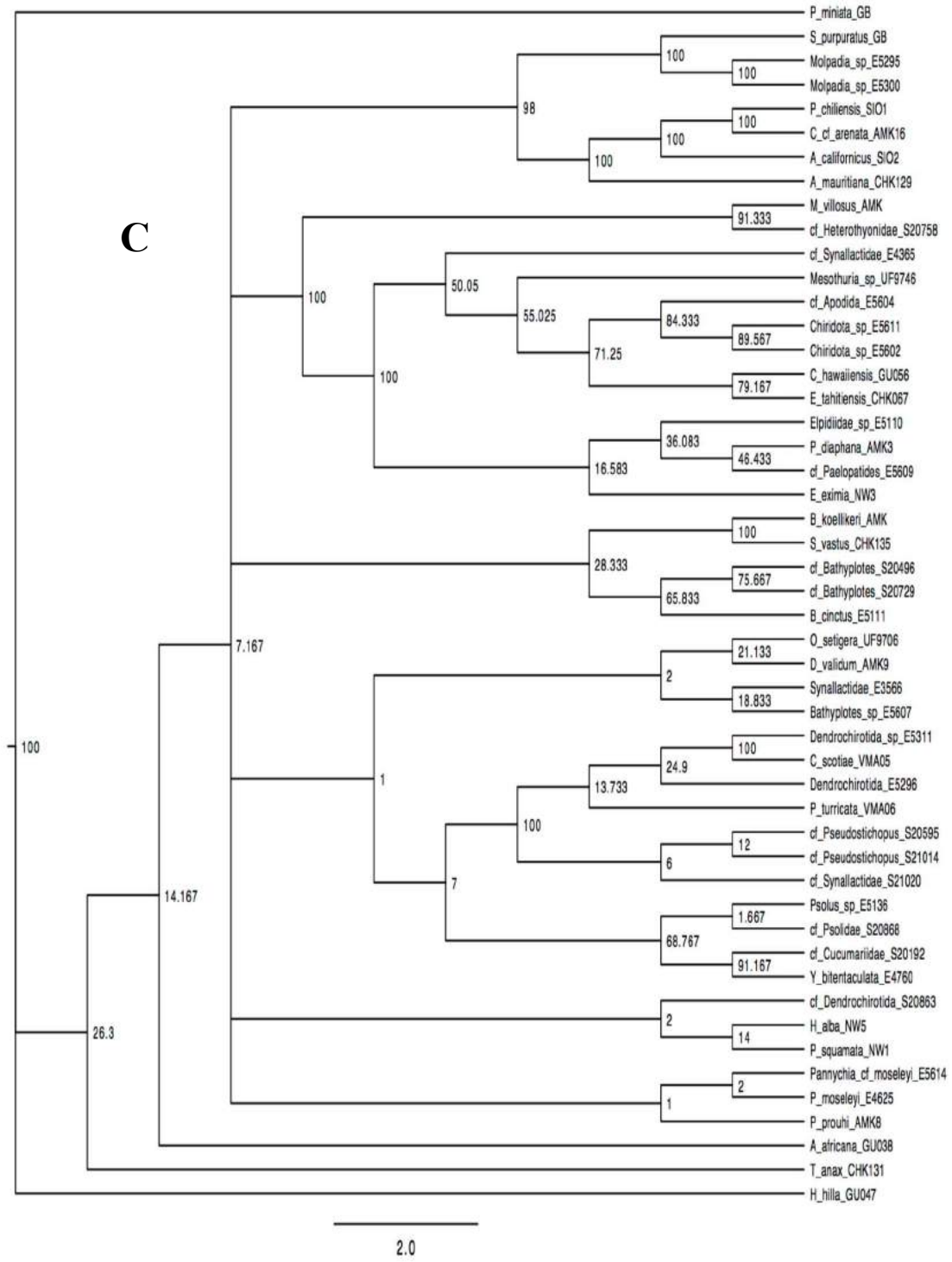

Appendix 1 continued.

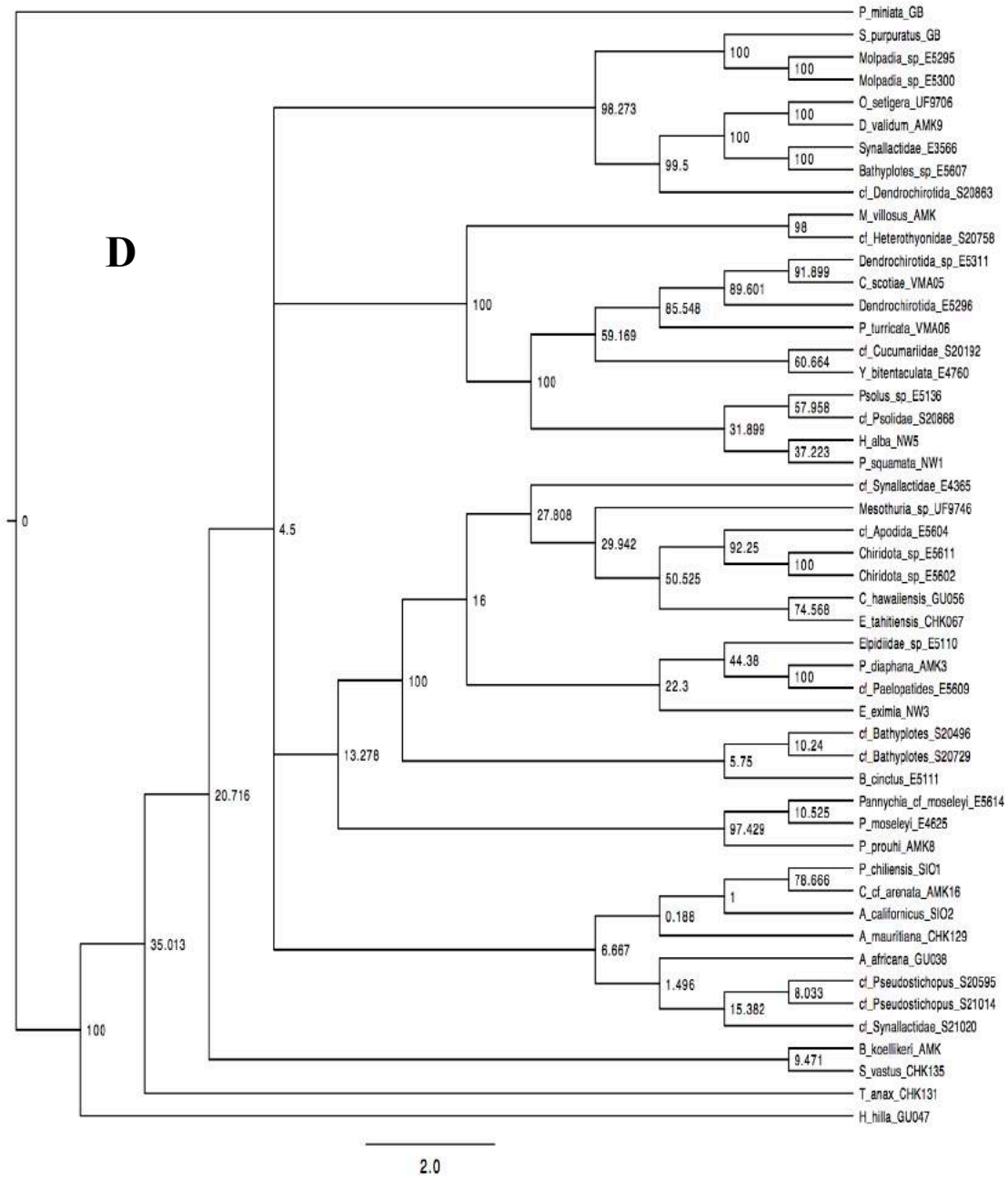

Figure 20. COI ***A.*** ML, ***B.*** BI, ***C.*** MP (bootstrap) and, ***D.*** MP (jackknife) trees. The numbers at or adjacent to the nodes represent the bootstrap support values (***A.*** and ***C.***), Bayesian posterior probabilities values (***B.***), and jackknife support values (***D.***)

Appendix 1 continued.

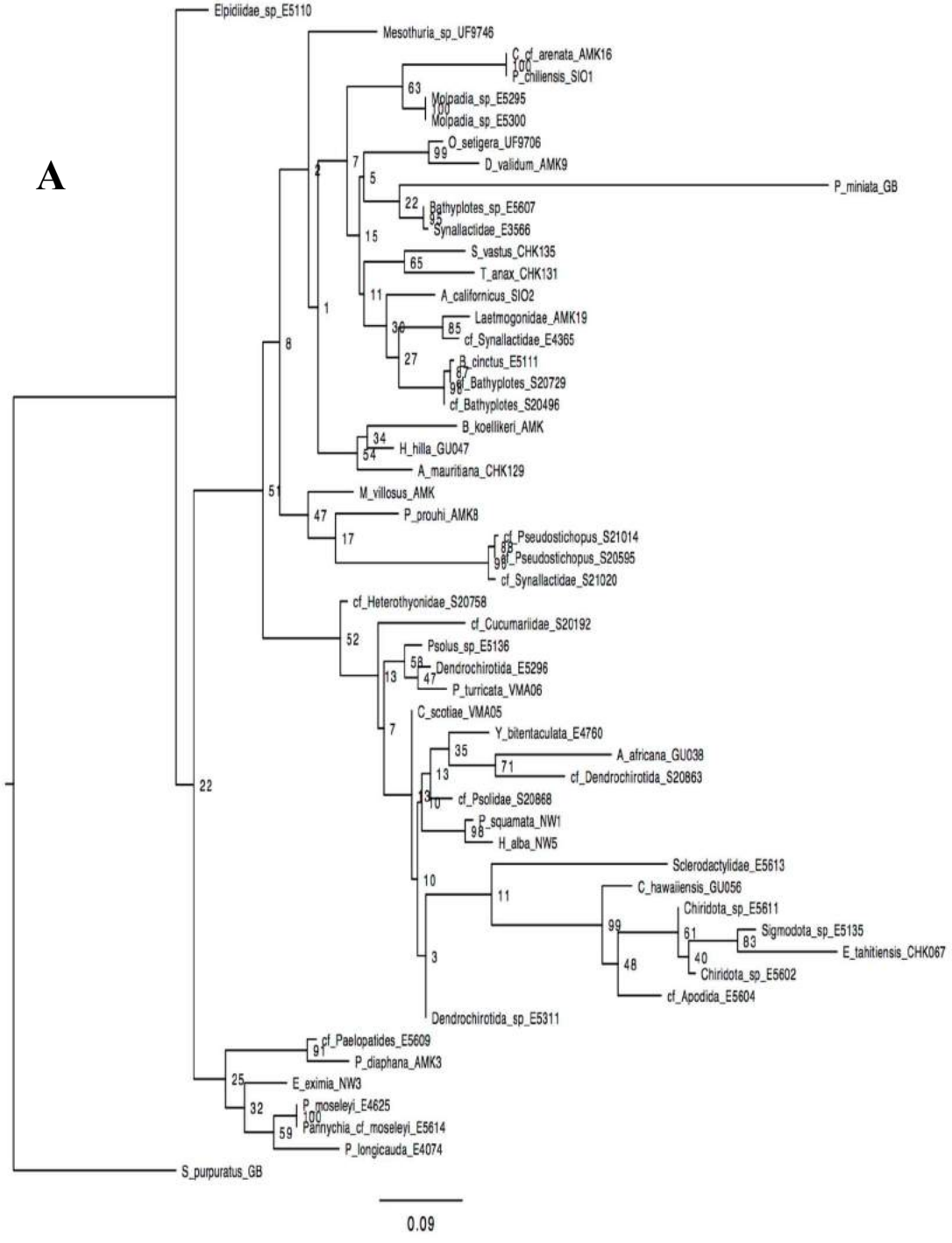

Appendix 1 continued.

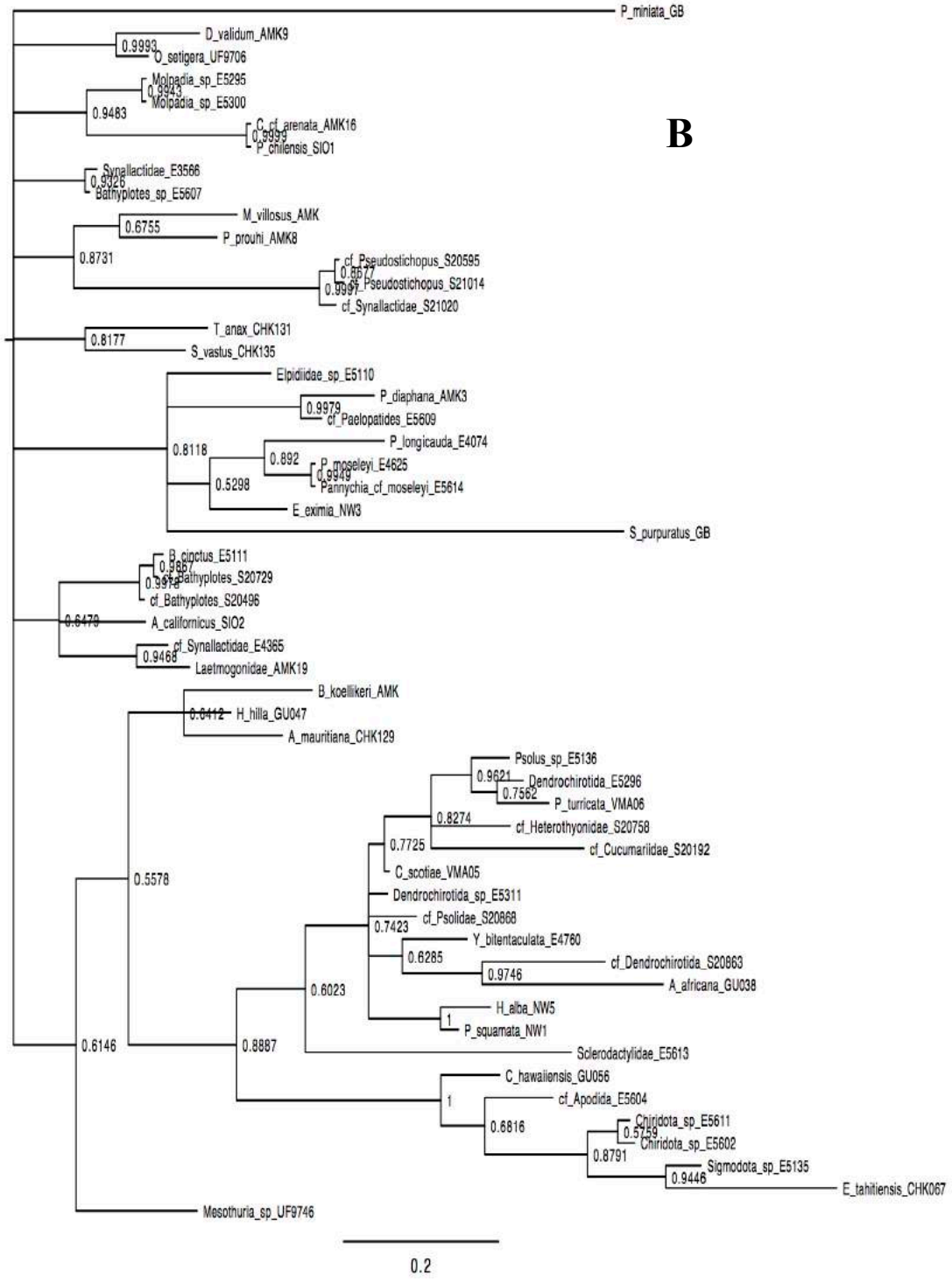

Appendix 1 continued.

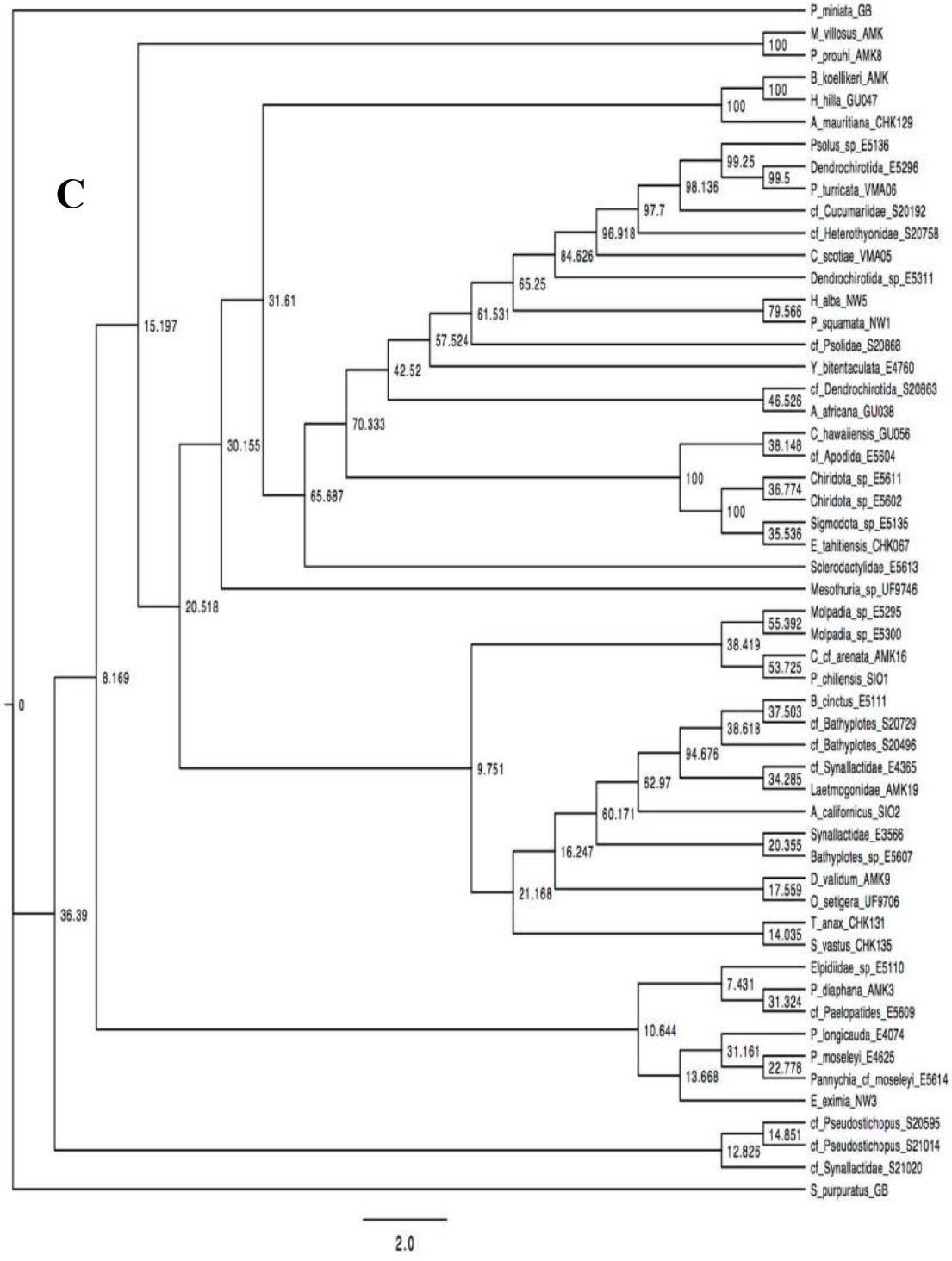

Appendix 1 continued.

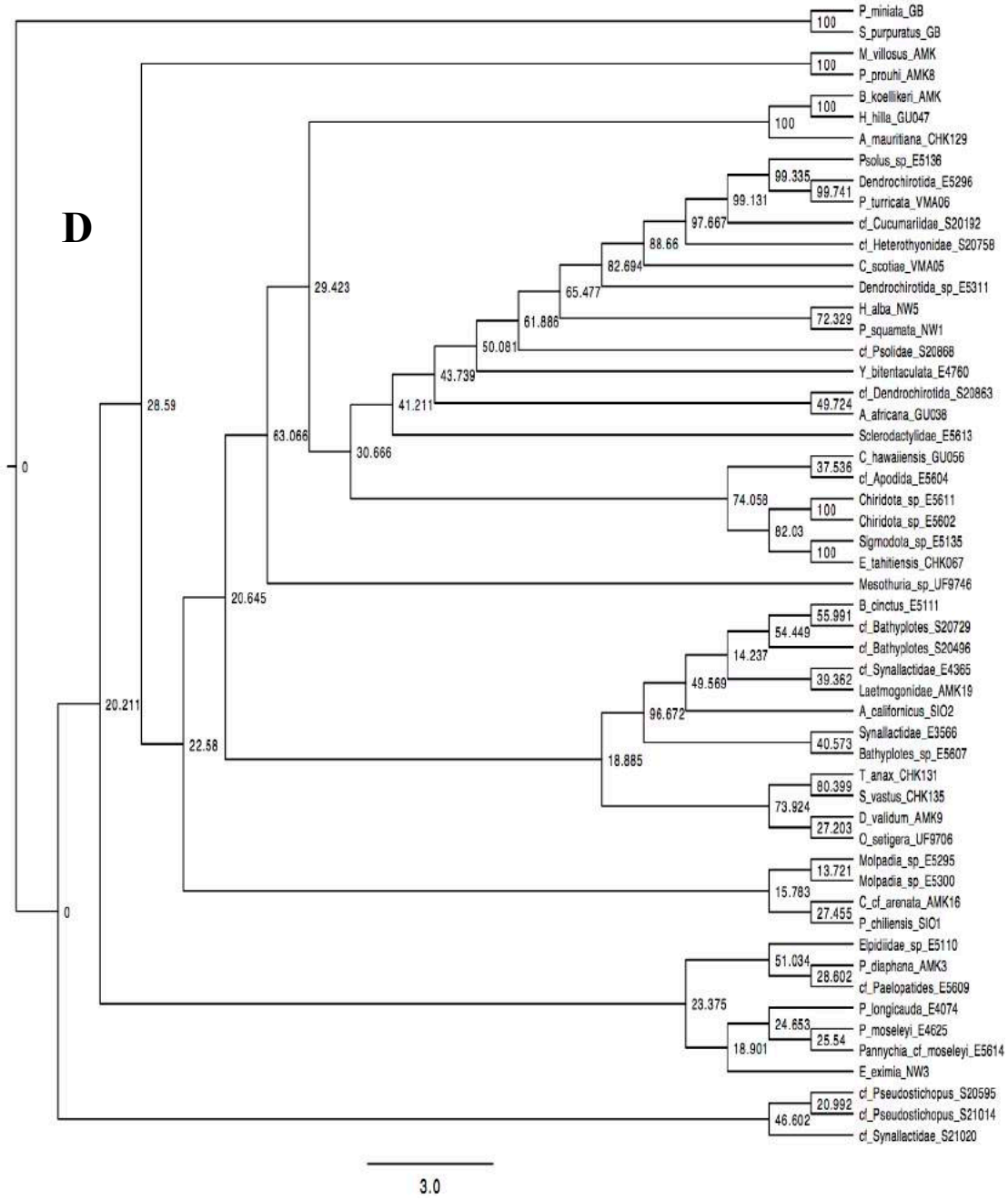

Figure 21. H3 ***A.*** ML, ***B.*** BI, ***C.*** MP (bootstrap) and, ***D.*** MP (jackknife) trees. The numbers at or adjacent to the nodes represent the bootstrap support values (***A.*** and ***C.***), Bayesian posterior probabilities values (***B.***), and jackknife support values (***D.***)

Appendix 2. Maximum likelihood (ML), Bayesian inference (BI), and maximum parsimony (MP) trees for the four concatenated datasets. *HVRR*: "highly variable regions removed" dataset. *COI (1&2)*: COI dataset with the 3rd codon position removed. *Note: the following taxon names were changed (names following "->" are the most recent identification). E5311 -> *Crucella scotiae,* E5296 – *Crucella scotiae,* AMK19 – *Paelopatides* sp, E4365 – Synallactidae, E5607 – *Synallactes* sp, E3566 – *Synallactes* cf *chuni,* AMK16 – *Molpadia arenicola*, SIO1 – *Molpadia arenicola*, E5295 – *Molpadia musculus*, E5300 – *Molpadia musculus*, E5609 – cf Elasipodida, and E5604 – *Chiridota* sp.

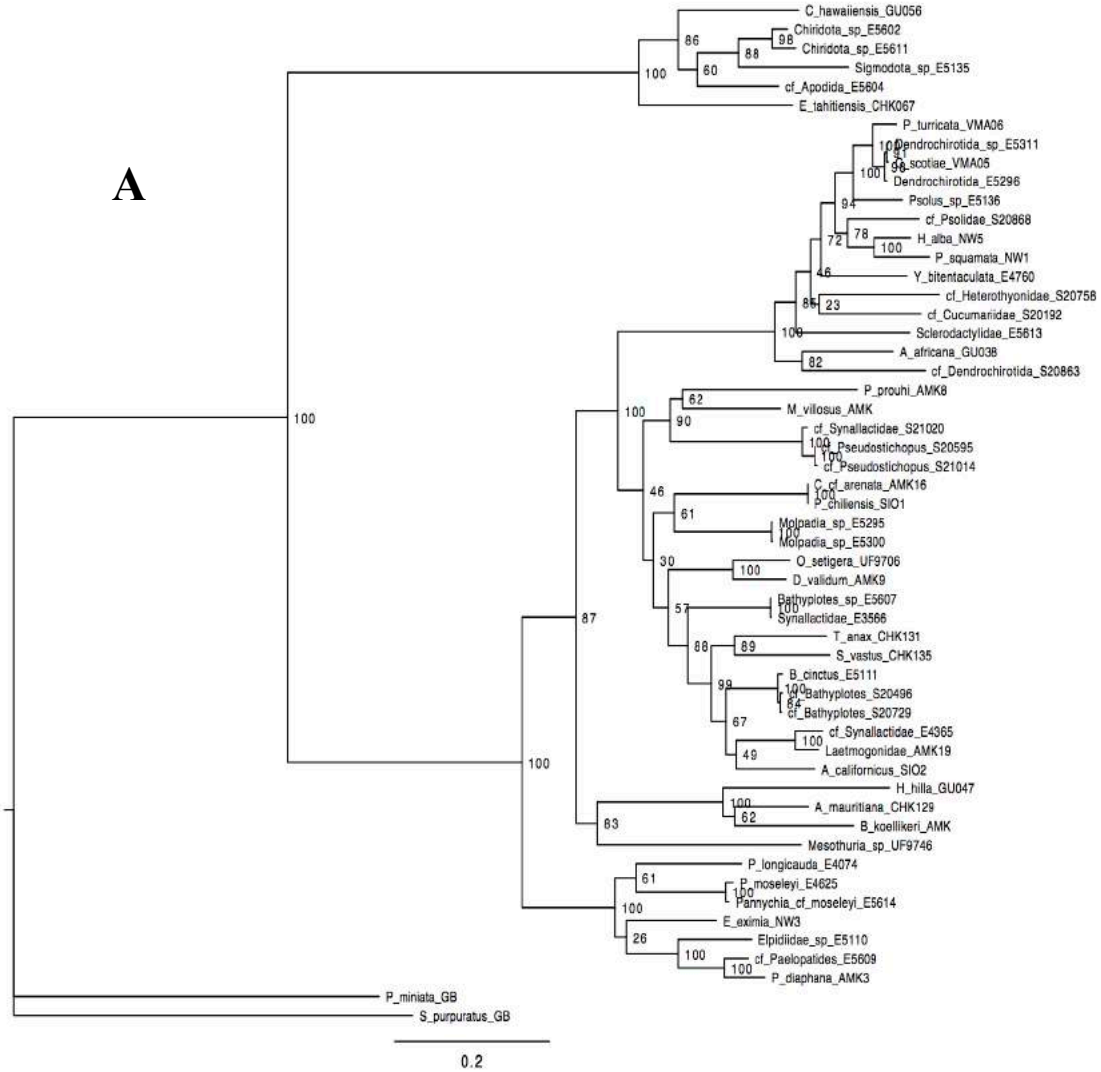

Appendix 2 continued.

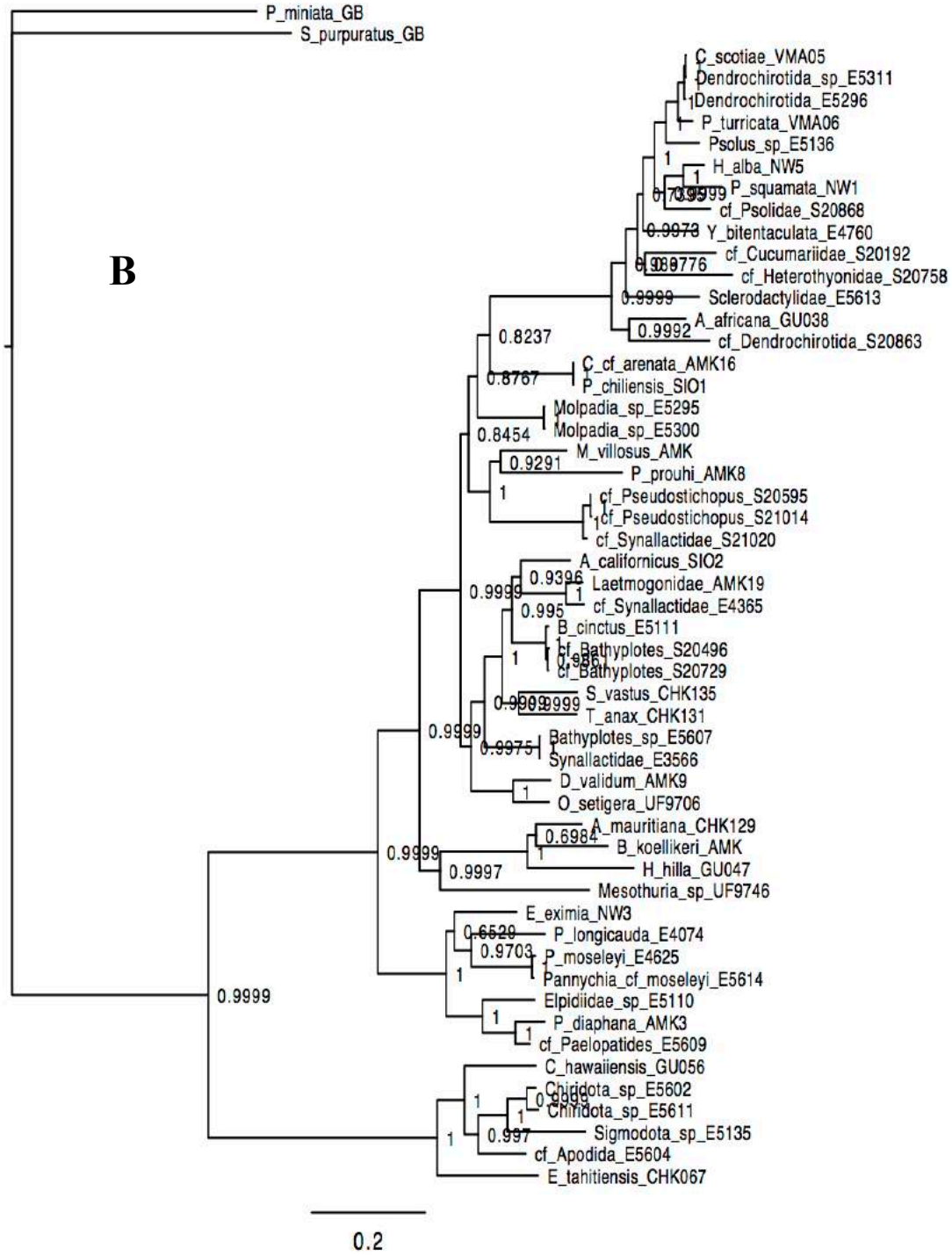

Appendix 2 continued.

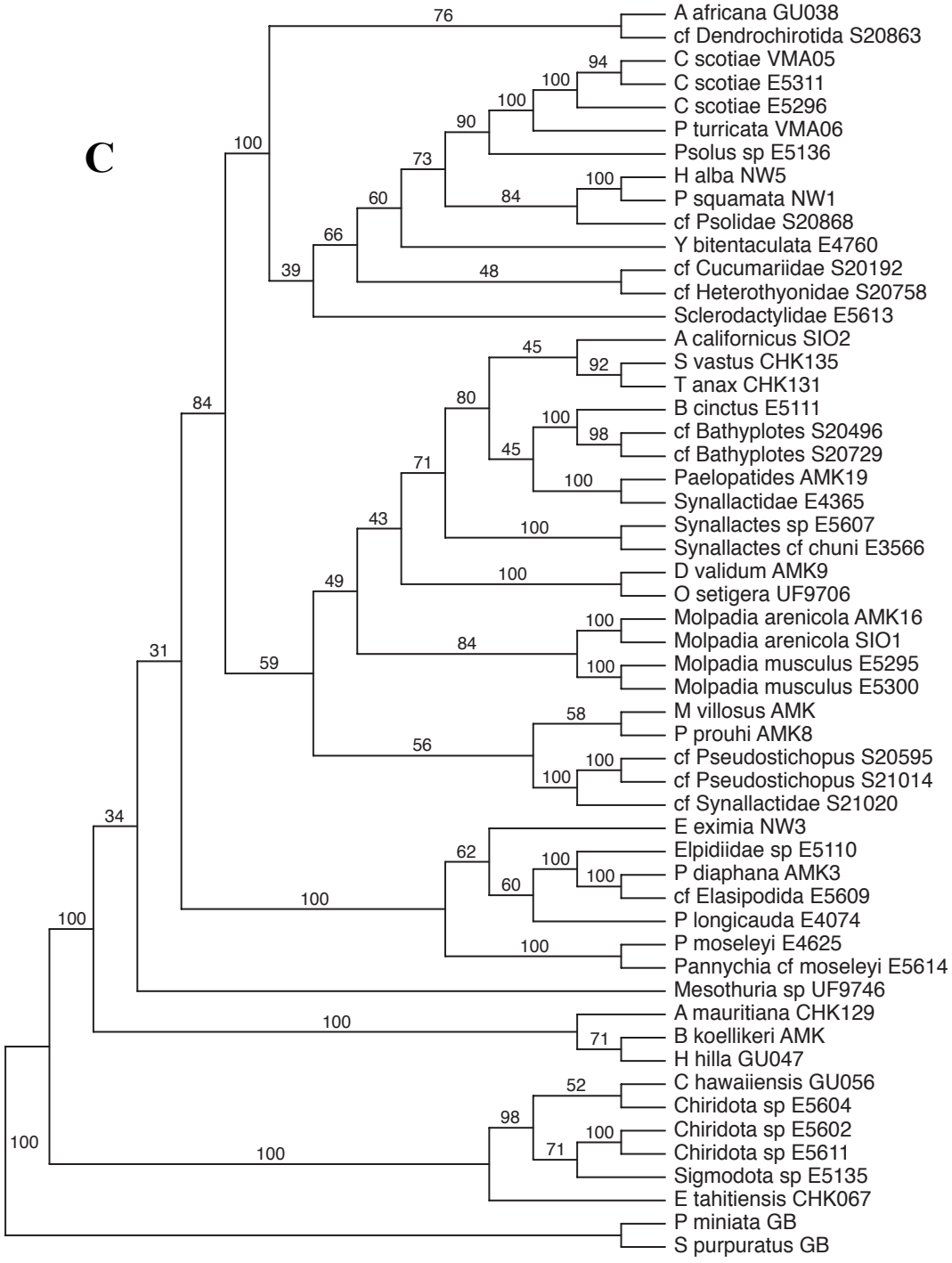

Appendix 2 continued.

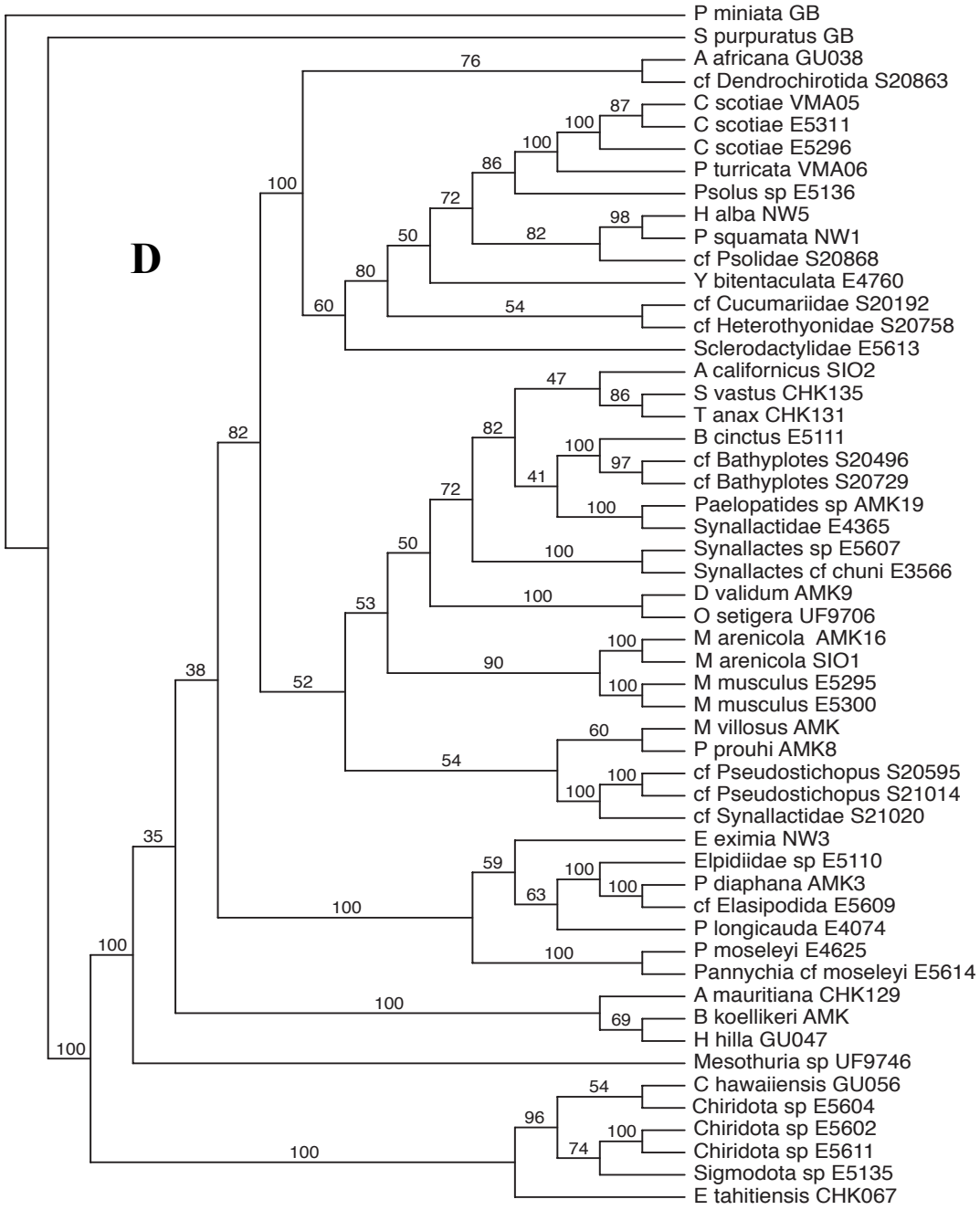

Figure 22. Concatenated dataset ***A.*** ML, ***B.*** BI, ***C.*** MP (bootstrap) and, ***D.*** MP (jackknife) trees. The numbers at or adjacent to the nodes represent the bootstrap support values (***A.*** and ***C.***), Bayesian posterior probabilities values (***B.***), and jackknife support values (***D.***)

Appendix 2 continued.

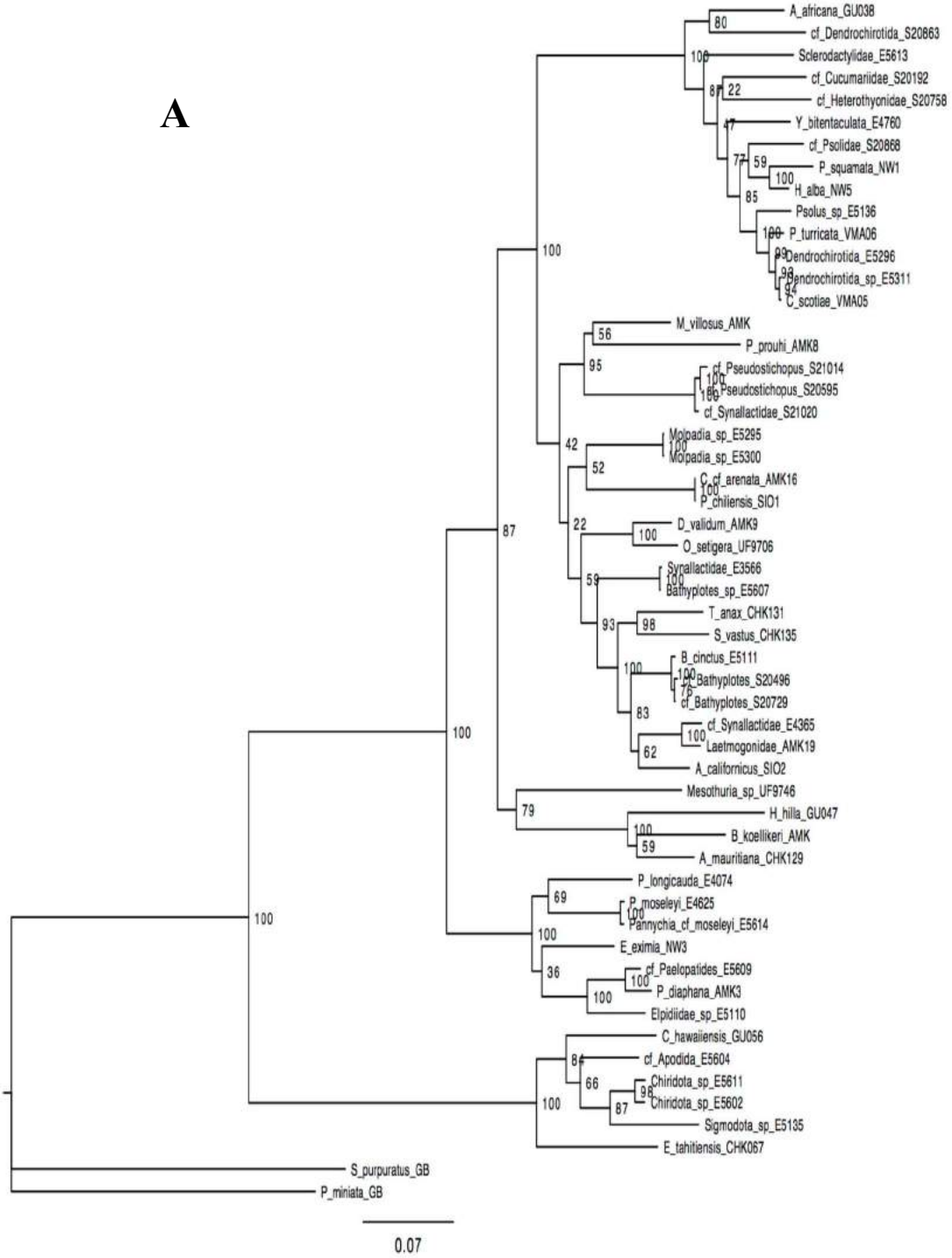

Appendix 2 continued.

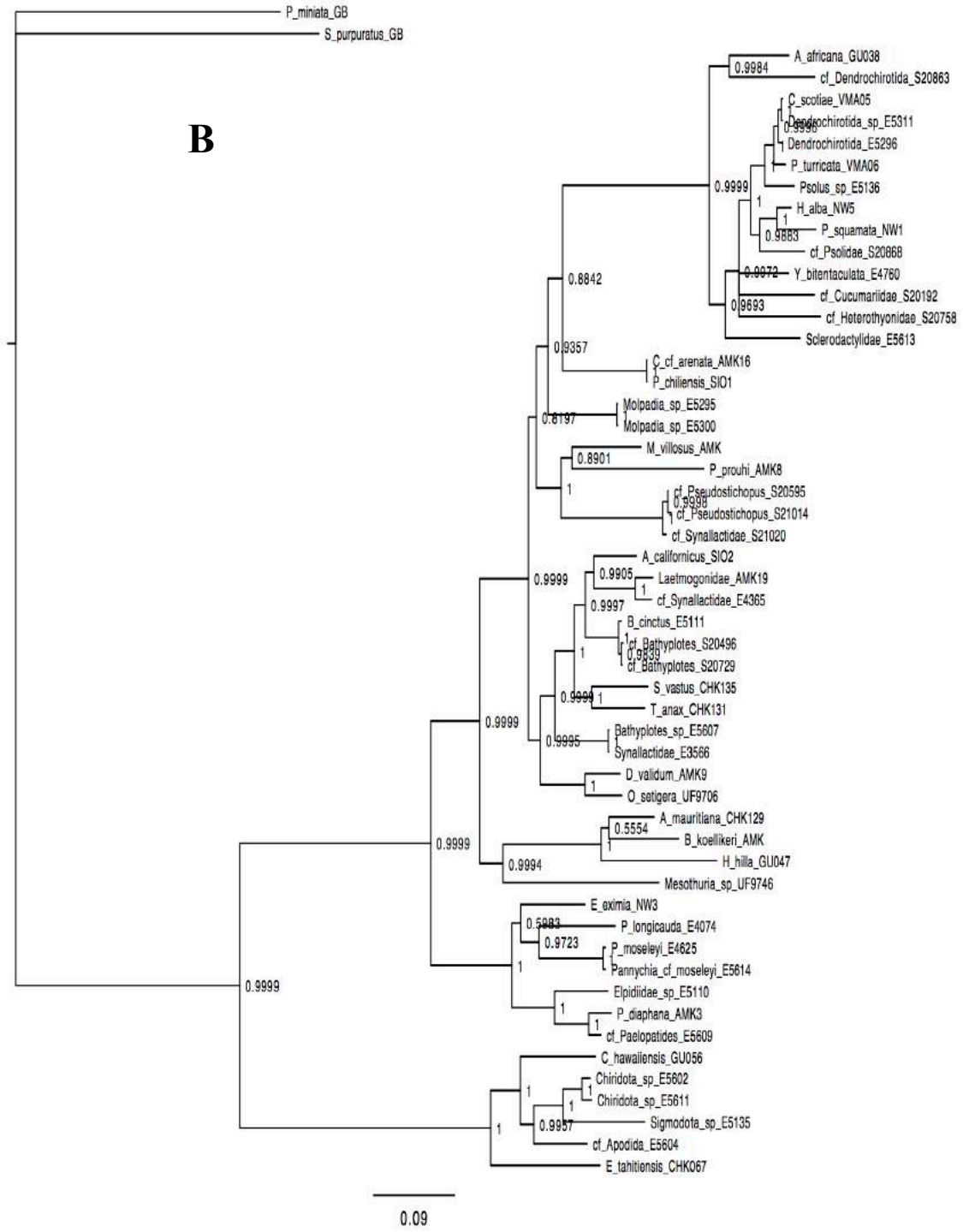

Appendix 2 continued.

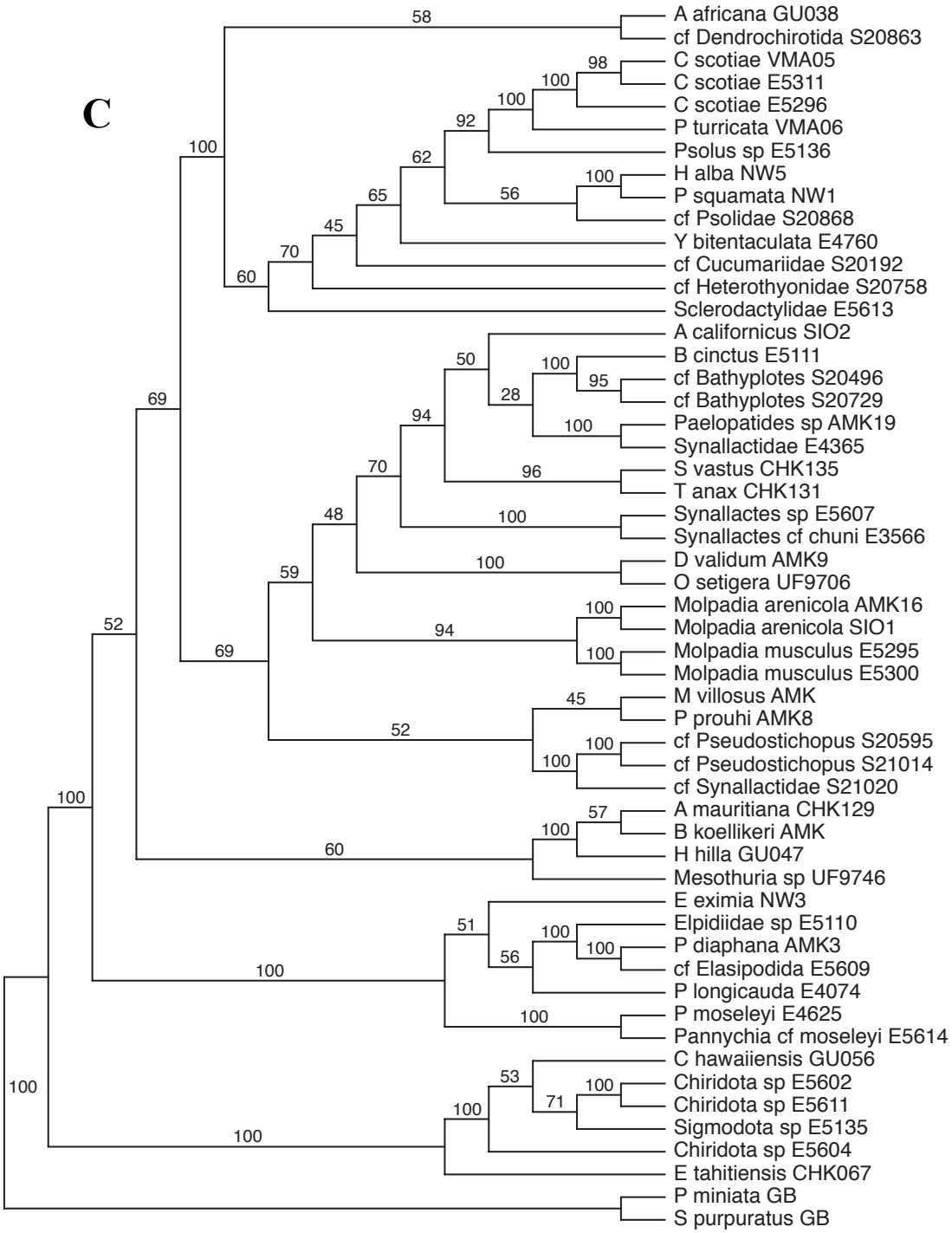

Appendix 2 continued.

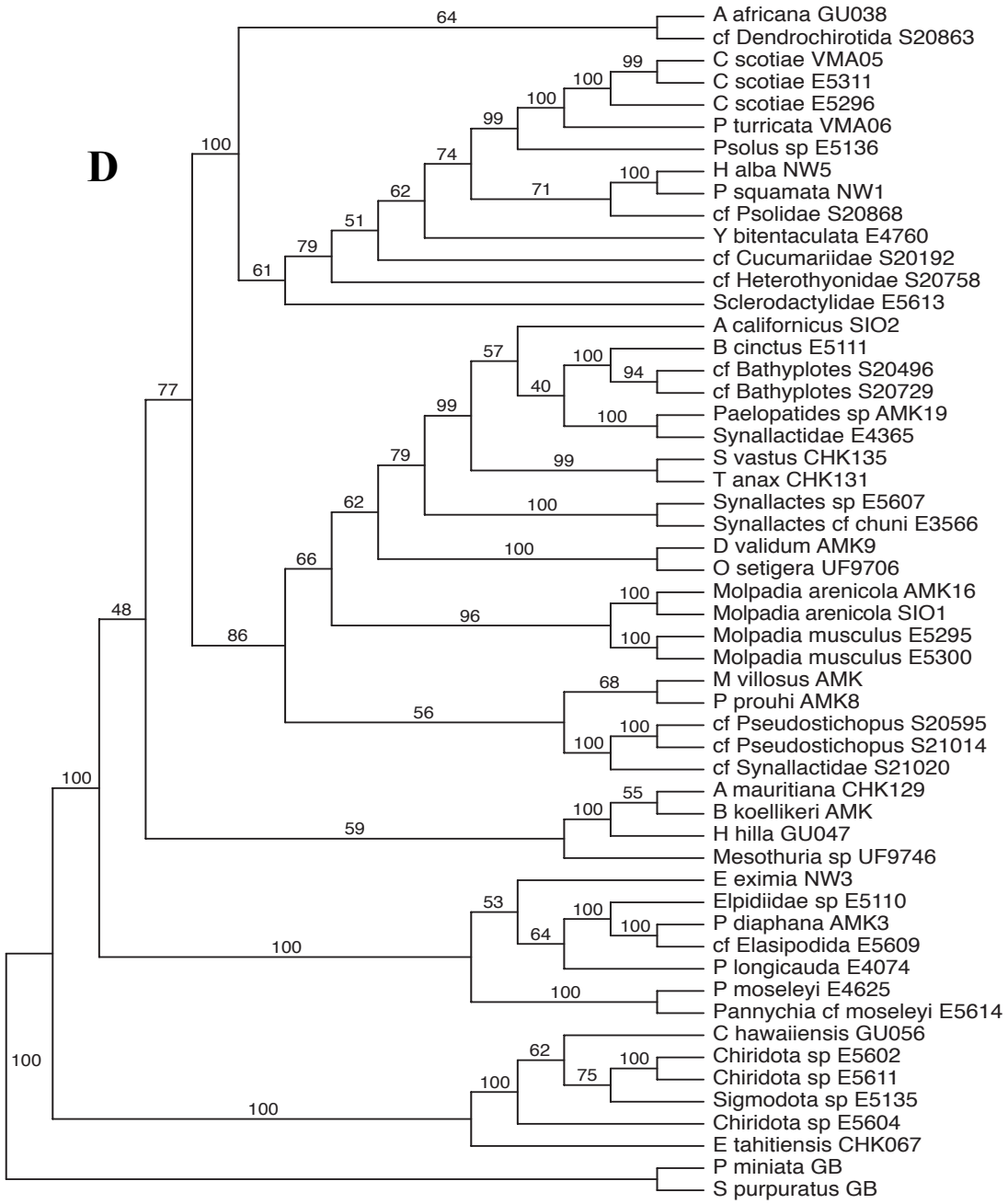

Figure 23. Concatenated COI (1&2) dataset ***A.*** ML, ***B.*** BI, ***C.*** MP (bootstrap) and, ***D.*** MP (jackknife) trees. The numbers at or adjacent to the nodes represent the bootstrap support values (***A.*** and ***C.***), Bayesian posterior probabilities values (***B.***), and jackknife support values (***D.***)

Appendix 2 continued.

A

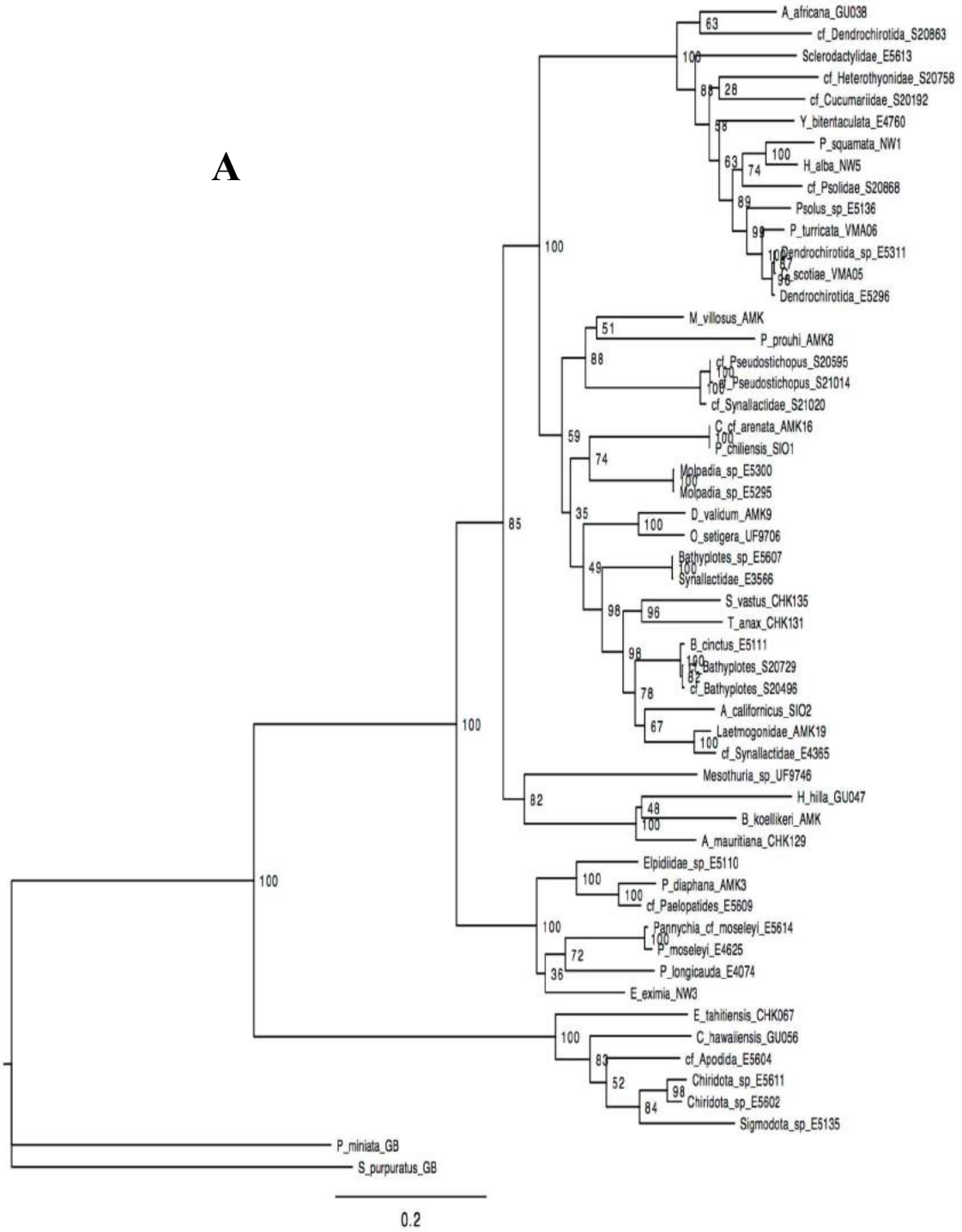

Appendix 2 continued.

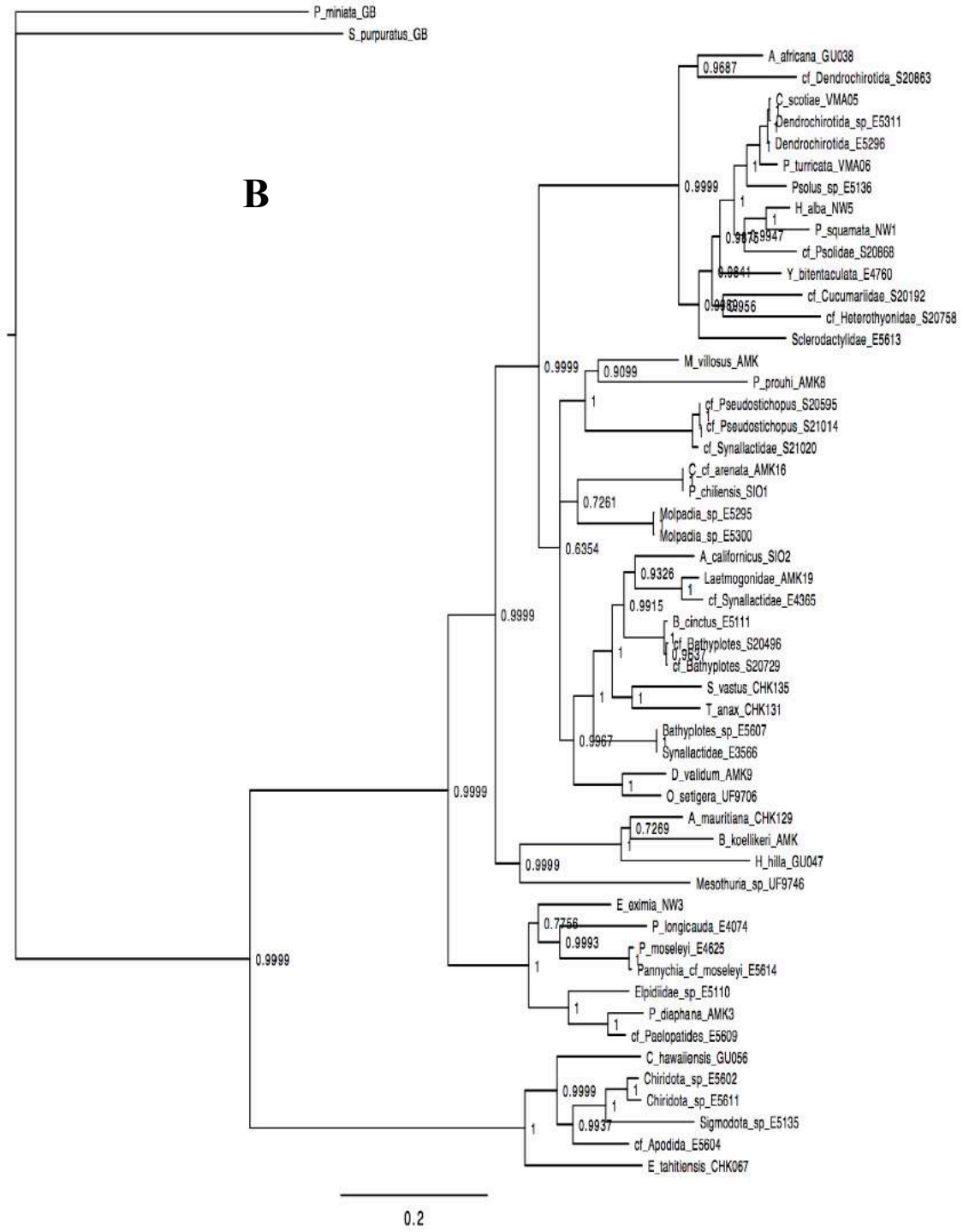

Appendix 2 continued.

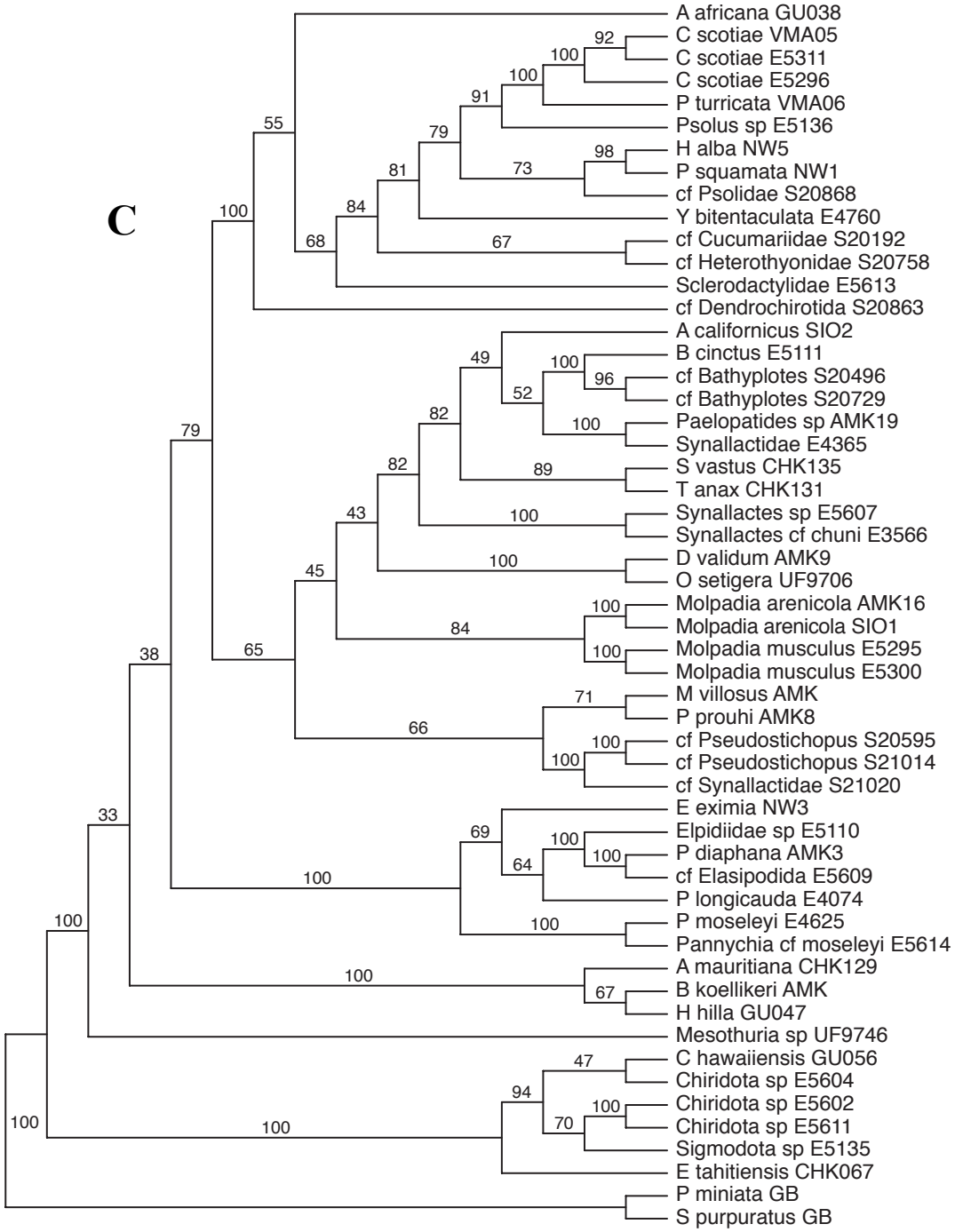

Appendix 2 continued.

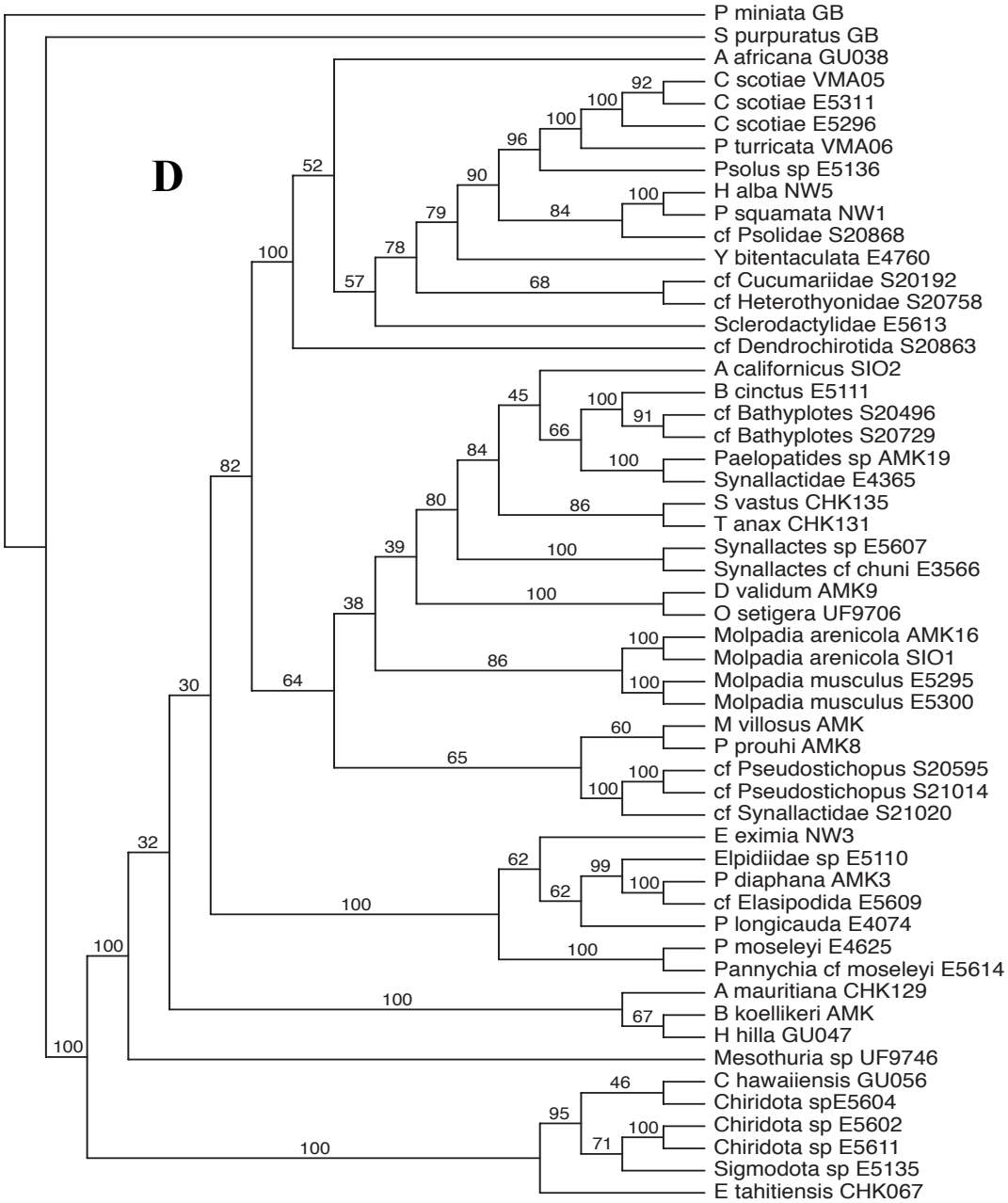

Figure 24. Concatenated HVRR dataset ***A.*** ML, ***B.*** BI, ***C.*** MP (bootstrap) and, ***D.*** MP (jackknife) trees. The numbers at or adjacent to the nodes represent the bootstrap support values (***A.*** and ***C.***), Bayesian posterior probabilities values (***B.***), and jackknife support values (***D.***)

Appendix 2 continued.

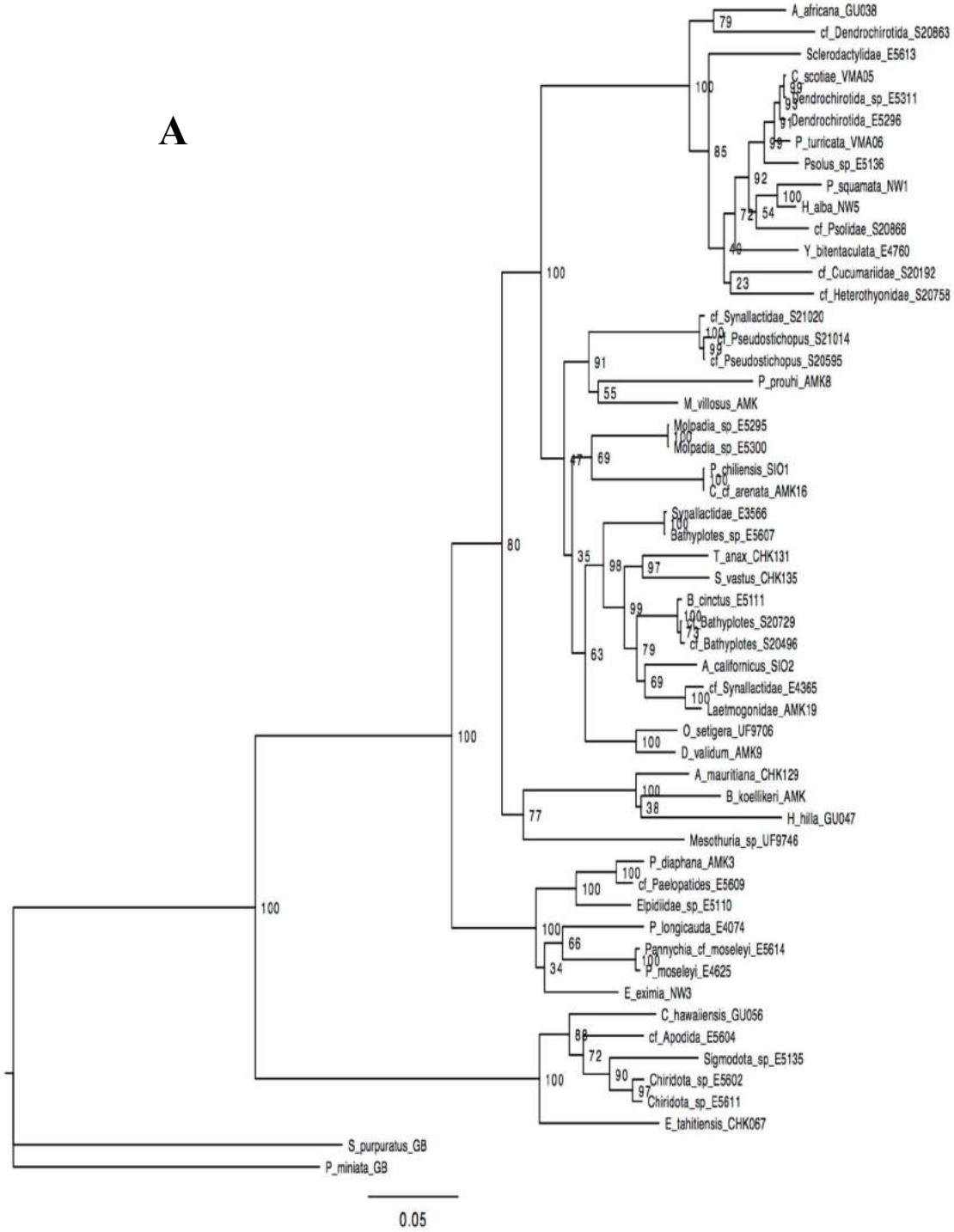

Appendix 2 continued.

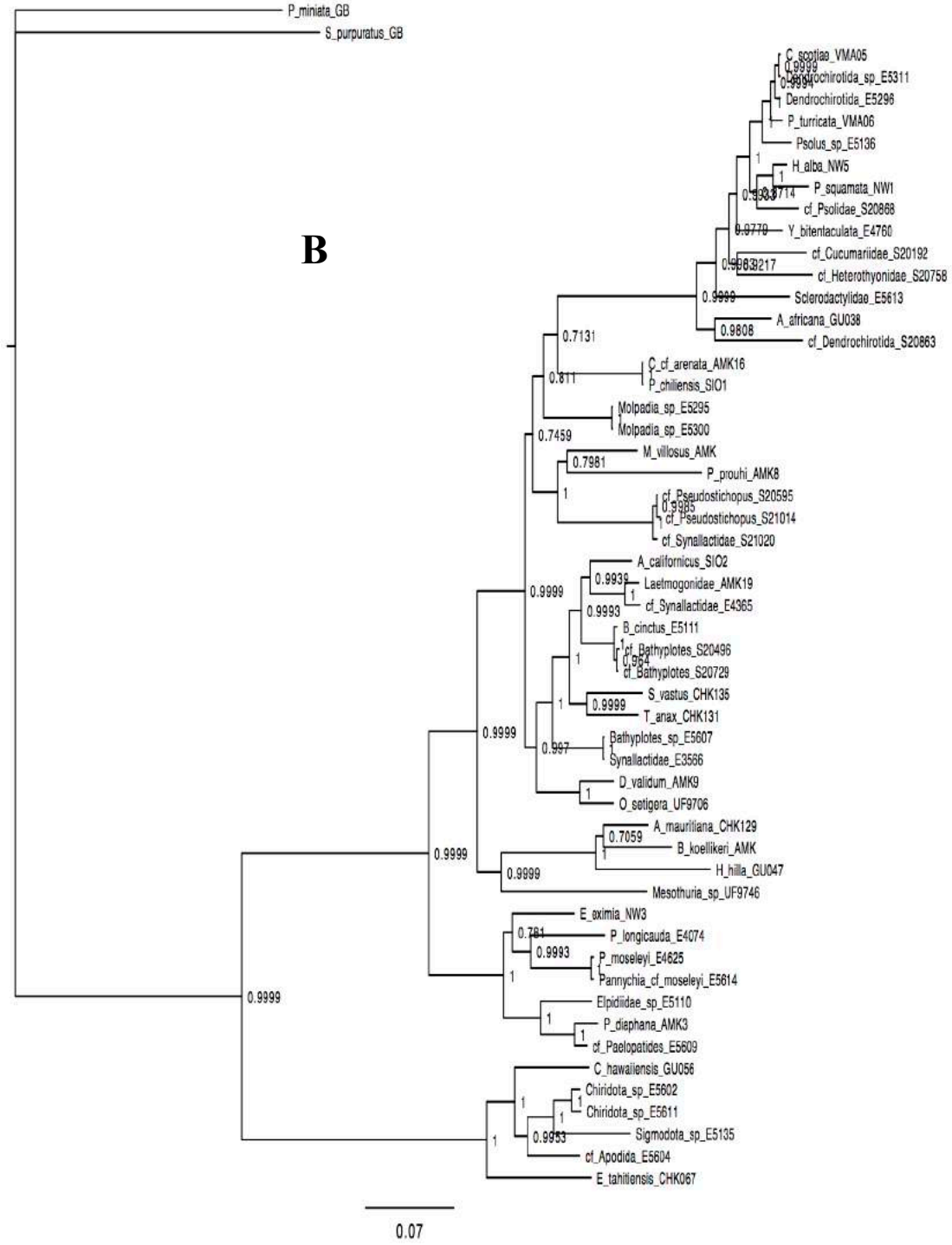

Appendix 2 continued.

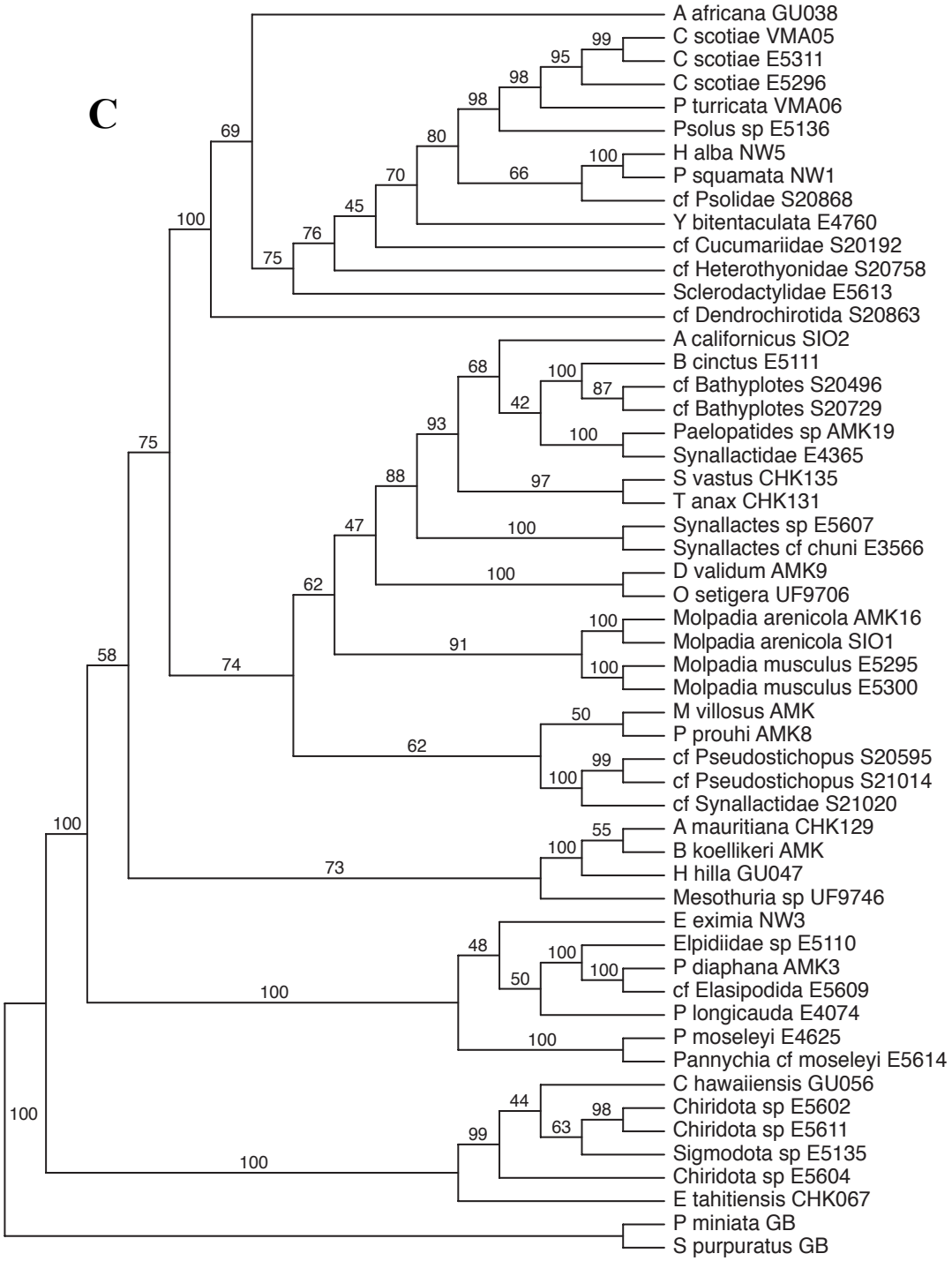

Appendix 2 continued.

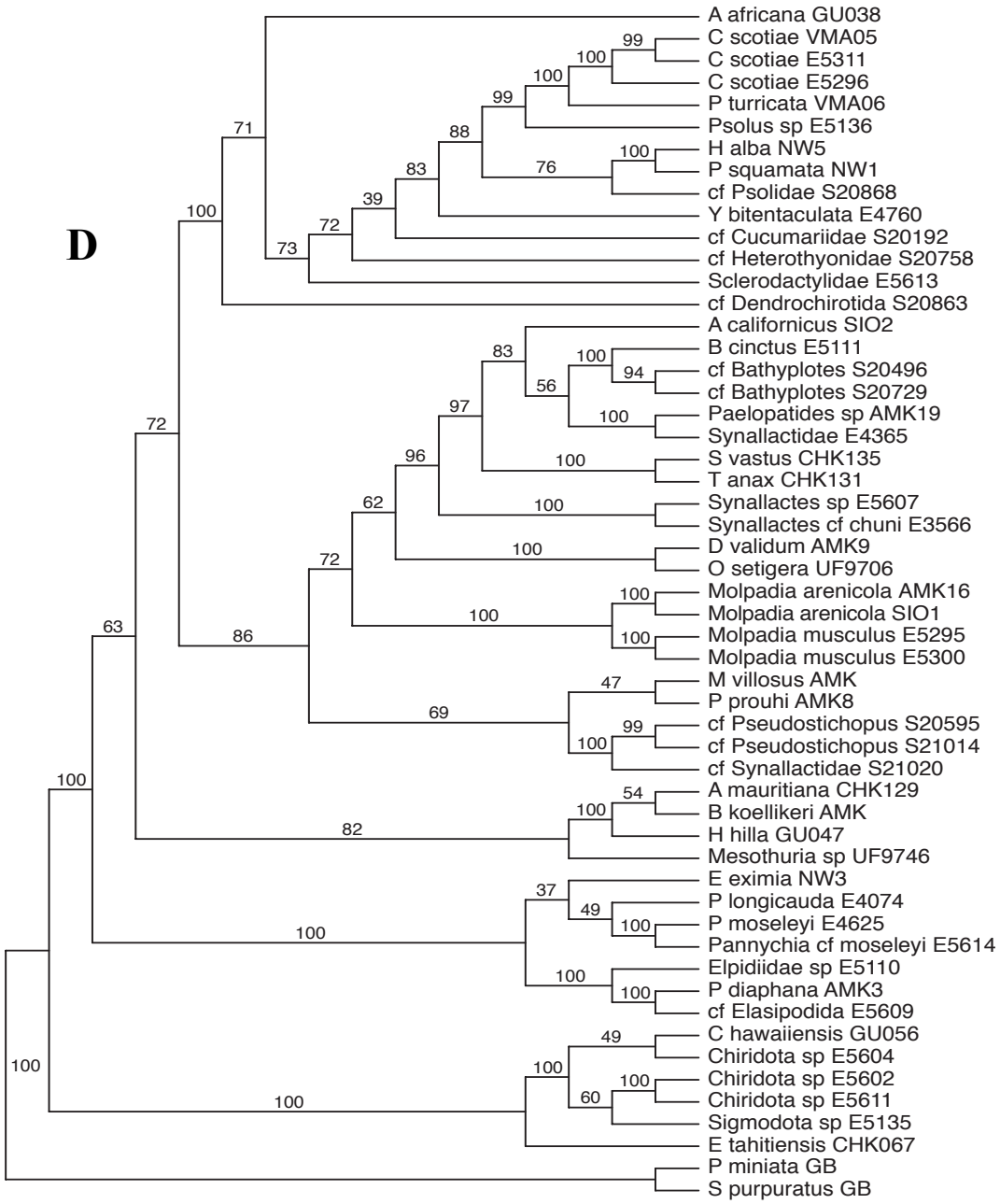

Figure 25. Concatenated HVRR COI (1&2) dataset ***A.*** ML, ***B.*** BI, ***C.*** MP (bootstrap) and, ***D.*** MP (jackknife) trees. The numbers at or adjacent to the nodes represent the bootstrap support values (***A.*** and ***C.***), Bayesian posterior probabilities values (***B.***), and jackknife support values (***D.***)